CAPITAL UNIVERSITY OF SCIENCE AND
TECHNOLOGY, ISLAMABAD

Control Oriented Dosage Design for p53 Revival

by

Muhammad Rizwan Azam

A thesis submitted in partial fulfillment for the
degree of Doctor of Philosophy

in the

Faculty of Engineering
Department of Electrical Engineering

2020

Control Oriented Dosage Design for p53 Revival

By

Muhammad Rizwan Azam

(PE 131007)

Dr. Rini Akmeliawati, Professor

The University of Adelaide, Australia

(Foreign Evaluator 1)

Dr. Saif Siddique Butt, Research Engineer

IAV Development GmbH, Gifhorn, Germany

(Foreign Evaluator 2)

Dr. Sahar Fazal

(Thesis Co-Supervisor)

Dr. Amer Iqbal Bhatti

(Thesis Supervisor)

Dr. Noor Muhammad Khan

(Head, Department of Electrical Engineering)

Dr. Imtiaz Ahmed Taj

(Dean, Faculty of Engineering)

DEPARTMENT OF ELECTRICAL ENGINEERING

CAPITAL UNIVERSITY OF SCIENCE AND TECHNOLOGY

ISLAMABAD

2020

DEDICATED TO MY FAMILY

CAPITAL UNIVERSITY OF SCIENCE & TECHNOLOGY ISLAMABAD

Expressway, Kahuta Road, Zone-V, Islamabad
Phone:+92-51-111-555-666 Fax: +92-51-4486705
Email: info@cust.edu.pk Website: https://www.cust.edu.pk

CERTIFICATE OF APPROVAL

This is to certify that the research work presented in the thesis, entitled "**Control Oriented Dosage Design for P53 Revival**" was conducted under the supervision of **Dr. Aamer Iqbal Bhatti**. No part of this thesis has been submitted anywhere else for any other degree. This thesis is submitted to the **Department of Electrical Engineering, Capital University of Science and Technology** in partial fulfillment of the requirements for the degree of Doctor in Philosophy in the field of **Electrical Engineering**. The open defence of the thesis was conducted on **December 26, 2019.**

Student Name: Mr. Muhammad Rizwan Azam (PE131007)

The Examining Committee unanimously agrees to award PhD degree in the mentioned field.

Examination Committee :

(a) External Examiner 1: Dr. Muhammad Abid,
Professor
PIEAS, Islamabad

(b) External Examiner 2: Dr. Iftikhar Ahmad Rana,
Assistant Professor,
SEECS, NUST, Islamabad

(c) Internal Examiner : Dr. Fazal ur Rehman
Professor
CUST, Islamabad

Supervisor Name : Dr. Aamer Iqbal Bhatti
Professor
CUST, Islamabad

Name of HoD : Dr. Noor Muhammad Khan
Professor
CUST, Islamabad

Name of Dean : Dr. Imtiaz Ahmad Taj
Professor
CUST, Islamabad

AUTHOR'S DECLARATION

I, **Mr. Muhammad Rizwan Azam (Registration No. PE-131007)**, hereby state that my PhD thesis titled, '**Control Oriented Dosage Design for P53 Revival**' is my own work and has not been submitted previously by me for taking any degree from Capital University of Science and Technology, Islamabad or anywhere else in the country/ world.

At any time, if my statement is found to be incorrect even after my graduation, the University has the right to withdraw my PhD Degree.

(**Mr. Muhammad Rizwan Azam**)

Dated: 26 December, 2019

Registration No : PE-131007

PLAGIARISM UNDERTAKING

I solemnly declare that research work presented in the thesis titled "**Control Oriented Dosage Design for P53 Revival**" is solely my research work with no significant contribution from any other person. Small contribution/ help wherever taken has been duly acknowledged and that complete thesis has been written by me.

I understand the zero tolerance policy of the HEC and Capital University of Science and Technology towards plagiarism. Therefore, I as an author of the above titled thesis declare that no portion of my thesis has been plagiarized and any material used as reference is properly referred/ cited.

I undertake that if I am found guilty of any formal plagiarism in the above titled thesis even after award of PhD Degree, the University reserves the right to withdraw/ revoke my PhD degree and that HEC and the University have the right to publish my name on the HEC/ University Website on which names of students are placed who submitted plagiarized thesis.

(**Mr. Muhammad Rizwan Azam**)

Dated: 26 December, 2019

Registration No : PE-131007

List of Publications

It is certified that following publication(s) have been made out of the research work that has been carried out for this thesis:-

Journal Publications

1. **M. R. Azam**, Vadim I. Utkin, Ali Arshad Uppal, A. I. Bhatti, "Sliding mode controller-observer pair for p53 pathway", *IET systems biology*, vol. 13, no. 4, pp. 204-211, 2019.

2. **M. R. Azam**, S. Fazal, M. Ullah, and A. I. Bhatti, "System-based strategies for p53 recovery", *IET systems biology*, vol. 12, no. 3, pp. 101-107, 2017.

3. M. Haseeb, S. Azam, A. Bhatti, **M. R. Azam**, M. Ullah, and S. Fazal, "On p53 revival using system oriented drug dosage design", *Journal of theoretical biology*, vol. 415, pp. 53-57, 2017.

Conference Publications

1. Haseeb, M., Azam, S., Bhatti, A. I., **Azam, M. R.**., Ullah, M., Fazal, S., "On p53 Revival using System Oriented Drug Dosage Design". *Drug Discovery & Therapy World Congress*, DDTWC, Boston, USA, (August 21-26), 2016.

2. Haseeb, M., Azam, S., Bhatti, A. I., **Azam, R. M.**, Ullah, M., Fazal, S., "System oriented dosage design for p53 revival and pulsation", *Workshop on Control and Observability of Network Dynamics*. Mathematical Biosciences Institute Ohio State University, USA, April 11-15, 2016.

Muhammad Rizwan Azam
(PE131007)

Acknowledgements

In the name of Allah, The Most Gracious, The Dispenser of Grace. All praise is due to Allah alone, Who granted me with the opportunity and abilities to pursue my postgraduate research and study. All respect is due to the Holy Prophet Muhammad (P.B.U.H), the last messenger of Allah, whose life is the perfect model for all humans and whose teachings are the source of guidance in all disciplines of life.

I am indebted to all my teachers whose teaching has brought me to this stage. In particular, I am highly grateful to my mentor and research advisor Dr. Amer Iqbal Bhatti for his valuable guidance, strong encouragement and kind support towards my research and study. His strong mathematical background and clear concepts of systems and control theory have always been the foremost source of motivation and inspiration for my research. I also like to express my gratitude to Prof. Vadim Ivanovich Utkin for his kind supervision, which enabled me to develop a Sliding Mode based control system for the p53 pathway. I am highly obliged to Dr. Ali Arshad, for his constructive comments and suggestions throughout my research phase.

I would also like to thank the whole CASPR group for their continuous and timely support, valuable suggestions and comments. Especially, I recognize the suggestions from Dr. Qudrat Khan, Dr. Yasir Awais Butt, Dr. Qadeer Ahmed, Mr. Raheel Anjum, Dr. Imran Khan, and Dr. Zeeshan Babar. Moreover, I would like to thank Dr. Sahar Fazal and all the members of the "Systems Biology" group at CUST, due to them I was able to conduct multidisciplinary research.

Above all, I am highly grateful to my parents for their prayers, my wife and daughter for their cooperation and patience, and siblings for their support.

Last but not least, I acknowledge the support provided by the international research support initiative program (IRSIP), HEC, Pakistan and the Ohio State University (OSU), OH, USA.

Abstract

In the last few decades, cancer has become one of the leading causes of death in the human race. A significant loss of the p53 protein, an anti-tumor agent, is observed in early cancerous cells (in around 50% of cancer cases). The p53 protein is being studied widely due to its pivotal role as a potential drug target. The induction of small molecules based drug Nutlin is by far the most prominent technique to revive and maintain wild-type p53 to the desired levels. The current research work proposes a systems theory-based novel drug dosage design for the p53 pathway. The pathway is taken as a dynamic system represented by ordinary differential equations (ODEs). Using control engineering practices, the system analysis and subsequent controller design are performed for the re-activation of wild-type p53.

For this purpose, two control strategies are adopted. In the first strategy, the attractor point analysis is carried out to select a suitable domain of attraction. A two-loop negative feedback control strategy is devised to drag the system trajectories to the attractor point. An integrated framework is constituted to incorporate the pharmacokinetic effects of Nutlin in the cancerous cells. In the second control strategy, a sliding mode control (SMC) based robust non-linear technique is presented for the drug dosage design of a control-oriented p53 model. The control input generated by the conventional SMC is discontinuous, however, depending on the physical nature of the system, the drug infusion needs to be continuous. Therefore, to obtain a smooth control signal, a dynamic SMC (DSMC) is designed. To make the model-based control design possible, the unknown states of the system are estimated using equivalent control based, reduced-order sliding mode observer (SMO). The robustness of the proposed technique is assessed by introducing input disturbance measurement noise, and parametric uncertainty in the system. The effectiveness of the proposed control scheme is witnessed by performing *in silico* trials, revealing that the sustained level of p53 can be achieved by controlled drug administration. Moreover, a comparative quantitative analysis shows that both controllers yield similar performance. However, DSMC consumes less control energy.

Contents

List of Figures

List of Tables

Abbreviations

ATM	Ataxia telangiectasia mutated
ATR	Ataxia telangiectasia and Rad3
CLF	Control Lyapunov function
DNA	Deoxyribonucleic acid
DSB	Double-strand break
DSMC	Dynamic Sliding Mode Control
G-Phase	Gap Phase
IR	Ionizing radiation
MDM2	Murine double minute 2
M-Phase	Mitotic Phase
mRNA	Messenger RNA
ODE	Ordinary Differential Equation
p53	Protein 53
PID	Proportional Integral Derivative Control
RMSE	Root-mean-square error
RNA	Ribo Nucleic Acid
SMC	Sliding Mode Control
SMO	Sliding Mode Observer
S-Phase	Synthesis Phase
SSB	Single-strand break
UV	Ultra-violet
VSC	Variable Structure Control
WIP1	Wild-type p53-Induced Phosphatase 1

Symbols

x	States
u	Input
y	Output
ζ	Disturbance
σ_p	Production rate of p53
α	MDM2 independent deactivation/degradation of p53
δ	MDM2 dependent deactivation/ degradation of p53
k_t	Transcription of MDM2
k_{tl}	Translation of MDM2
β	Degradation rate of MDM2 mRNA
γ	MDM2 degradation/deactivation
k_b	Dissociation of MDM2-p53
k_m	Nutlin rate constant
k_D	Dissociation constant of MDM2-p53
n_{ref}	Recommended dosage of Nutlin in the cell
σ	Dynamic sliding surface
t_s	Finite time interval
s	Conventional sliding surface
v	Dynamic control law
ζ	Input Disturbance for p53 model
V	Lyapunov function
u_{eq}	Equivalent control
u_d	Discontinuous control

$sign$	Signum function
k_p	Proportional gain
k_i	Integral gain
k_d	Derivative gain
B_{max}	concentration of plasma protein binding sites
K_a	equilibrium association constant in plasma
p_{oral}	dose conversion factor for oral delivery
δ_1	Production rate of p53
δ_2	elimination rate constant
i_1	rate of Nutlin intracellular import
k_{d3}	Nutlin-MDM2 dissociation rate
e_1	rate of Nutlin cell export

Chapter 1

Introduction

In the last few decades, cancer has become one of the leading causes of death in the human race. According to the American Cancer Society, "cancer is the second most common cause of death in USA [1]". Cancer is mainly developed as a consequence of oncogenes activation and inactivation of tumor suppressors. It has been observed that around 50% cancer cases contain either mutations or inactivation of the tumor suppressor protein: p53. In recent years p53 has become a mainstream target in anti-tumor drug development [2].

After the discovery of the p53 protein in 1979 by Arnold J. Levine, scientists have invested a considerable amount of effort in exploring the protein. The p53 protein attains the significance due to its role in cancer suppression and its ability to respond to various stresses which are toxic for the genome. In its wild-type state, p53 induces responses like DNA repair mechanism, senescence, cell cycle arrest, and cell death [3]. Whenever the cell gets endangered by stresses (e.g., radioactivity or DNA damage), p53 activates multiple downstream targets to ensure the healthy functioning of the cell. In fact, whenever the genome's integrity is questioned, p53 plays its role to preserve it, hence named "guardian of the genome" [4].

Owing to the contradicting role p53 plays in the progression of cancer, i.e., guardian and killer, scientists faced difficulties in understanding the true functionality and potential of this protein. The first three decades of research on p53 revealed its

realization as tumor suppressor protein, its function as a transcription factor and metabolic pathway regulator. In the fourth decade of its discovery, it is established that this tumor suppressor protein is non-functional in various cancers and hence the researchers are exploring p53 signaling pathway based drugs to fight cancer [5]. The subsequent sections investigate the role of p53 in cancer suppression and explore target-able interactions, which can become the basis for chemotherapy drug development.

1.1 The Fight Against Cancer

"Cancer" is a disease, in which cells are able to divide uncontrollably. Environmental, as well as genetic factors, are responsible for causing cancer. The incidence of cancer has been extensively increased since the birth of the industrial revolution. The prominent cause of cancer is DNA damage, which enables cells to bypass the cell cycle checkpoints and proliferate. The DNA can be damaged due to various reasons including, but not limited to, tobacco smoke, alcohol consumption, X-rays and ultraviolet radiation exposure, radiotherapy and to some extent infections [6]. Most commonly, cancer is treated with surgery, by removing cancerous tissues from the effective area of the patient. However, this procedure is only plausible in easily target-able areas and can cause severe discomfort or further implications. Furthermore, during surgery, unintended loss of healthy cells is inevitable.

The second most common treatment method is radiotherapy, in which X-rays are used to destroy cancerous cells. Although radiotherapy removes the need for surgery, sometimes the emitted radiations itself lead to cancer development. Chemotherapy is another such treatment strategies (usually used as adjunctive therapy), in which anti-tumor agents target rapidly growing cells. However, rapidly growing normal cells such as hair follicles are also neutralized as a consequence. Apart from that it also causes fatigue, nausea, hair loss, and vomiting. Furthermore, pertaining to the inherent resistance in the cancerous cells against these agents, cancer can return at a later stage.

The side effects associated with current treatment methods demand a change in the perspective towards cancer therapy. Recently, the focus in therapeutic drug development is shifting towards agents targeting the pathways involved in cancer development. There is vast research being carried out in investigating the protein-protein interactions (PPIs) for the treatment of cancers. The medicinal chemistry and drug-discovery communities have grown interest in studying PPIs, as they provide greater control in modulating cellular response in comparison with the conventional drug targets. The difficulty arises due to the dynamic nature of protein interactions. Furthermore, the interaction sites are usually large, flat and sometimes hydrophobic, complicating the access of binding pockets. In the subsequent sections, protein-protein interactions in the p53 pathway (one of the most important pathways related to cancer) are explored and the drug-able targets are looked into.

1.2 Role of p53 in Cancer Suppression

p53 is a tumor suppressor protein that plays an important role in preserving the integrity of the genome. In normal cells with no mutations, p53 is missing or suppressed, hence maintains a low-level [7]. However, it becomes activated in response to stresses or DNA damage, hence expressed in high levels. These stresses can alter the normal functionality of the cell cycle, or make a normal cell cancerous by introducing mutations in the genome [8]. Besides this, p53 acts as a transcription factor for more than 30 known genes involved in DNA repair, cell cycle control, differentiation, senescence, and apoptosis.

The cell progression of damaged cells is stopped at G_1-S phase and G_2-M phase checkpoints of the cell cycle. p53 along with CDK pathway controls the cell progression at G_1 to S phase and controls the G_2 to M phase progression with help of CDK protein pathway [9]. Normally p53 resides inside the nucleus to scan the DNA for any damage. If any DNA damage is detected, the p53 level rises. Depending upon the severity of the damage, p53 can initiate one of the

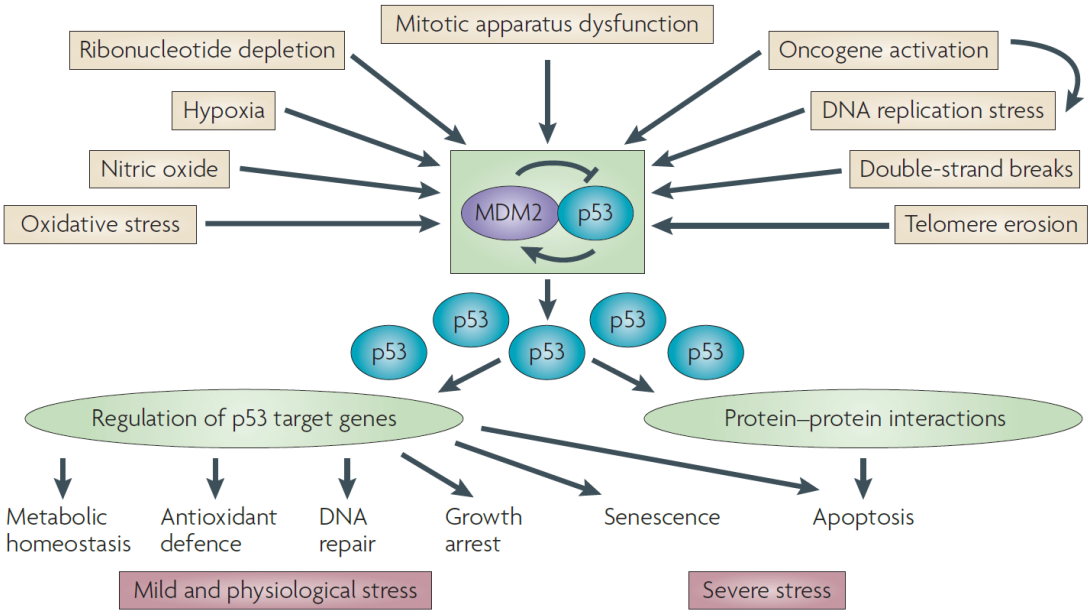

FIGURE 1.1: Diverse cellular outcomes mediated by p53 in response to multiple stresses. [5]

three responses i.e DNA repair, senescence, and apoptosis. In the subsequent subsection, we explore the mechanisms to repair the cell by p53.

1.2.1 p53 Repair Mechanisms

At every passing moment, a cell is facing multiple stresses or mutagens of different kinds, e.g, chemicals, and radiations, etc, having a greater impact on disrupting the homeostasis of a normal cell. These stresses act as activating agents for p53. The DNA damage is one of the prominent stresses, inducing active cellular p53. Figure 1.1 identifies some of the responses mediated by p53. It is evident that p53 acts as a single common node, which acts upon multiple stresses to generate various responses accordingly. There is a consensus upon the fact that the nature of p53 response is proportionate to the stress signal. Mild stresses attempt to repair the damage caused by it, while severe stresses induce extreme responses, i.e., senescence and apoptosis. Hence, whenever DNA damage is detected, the p53 protein gets activated and its concentration is increased accordingly. p53 responds in following three ways in response to stresses, by activating several hundred genes involved in DAN repair, senescence, and apoptosis.

1.2.1.1 DNA Repair

The DNA is damaged due to multiple intrinsic and extrinsic stresses. The most common reason is the radiation exposure of normal cells due to radiotherapy, Ultraviolet (UV) radiations and gamma (γ) radiations. The stress causes damage to DNA in the form of single-strand breaks (SSBs) and double-strand breaks (DSBs). Hence, whenever DNA is slightly damaged, various downstream repairing proteins get activated, which repair the DNA and cell cycle process continues.

1.2.1.2 Cell Cycle Arrest

If DNA is beyond repair then the cell remains at the G_1-S phase checkpoint and the p53 ensures that the cell does not divide. These cells exit to a quiescent stage, known as G_0 phase, where they are metabolically active but cannot proliferate any further. The cell cycle does not allow the cell to go to the next phase, hence cell growth is stopped unless the damage is repaired at any stage, then the cell cycle resumes its normal course.

1.2.1.3 Apoptosis

If DNA damage is severe then the self-destructing proteins are activated, which destroy the damaged cells. p53 induced apoptosis is a result of the transcription of genes, inducing pro-apoptotic proteins (PUMA and NOXA), which inhibit the function of anti-apoptotic proteins of the Bcl family [10]. It is worth mentioning that chemotherapy is the same process only done manually.

1.2.2 p53 as a Target Gene

The most frequent cause in sustained tumor cell division is the inactivation of tumor suppressor protein p53. Multiple factors induce inactivation of p53 protein, including a mutation in genes and interaction with an over-expressed p53 inhibitor:

Murine double minute 2 (MDM2) [11]. Overexpression of MDM2 leads to rapid degradation in the level of p53 and it limits the tumor suppressor functionality of p53. Therefore, compounds which attempt to revive the p53 protein, or inhibit the MDM2 protein are being investigated to act as therapeutic agents against cancer [5]. In the subsequent section, we first investigate the protein-protein interactions of p53 and MDM2 and then explore possible ways to revive p53.

1.3 Regulation of p53

In the cells, for the conservation of energy and materials, the proteins are produced whenever necessary, and eliminated after performing their functions. This process is called regulation. The under activation of p53 may lead to cancer while the overexpression of p53 can accelerate the aging process by excessive apoptosis. The critical role of p53 in regulating numerous cellular processes demands precise control of its level and activity. It has been conclusively demonstrated that the function of p53 is determined by the cellular level of the p53 protein. Under normal unstressed conditions, the p53 is very unstable, having a half-life of around 5 to 30 minutes [12]. Hence, under normal circumstances, the concentration of p53 is maintained at a low steady-state level. The level of p53 protein is undetectable due to continuous degradation by the proteasome. Conversely, p53 is sensitive to different stresses such as mutations in DNA caused by UV or γ irradiations. p53 is activated at a very early stage of DNA breaks through ATM (Ataxia-telangiectasia-mutated) or ATR (ataxia telangiectasia and Rad3-related) pathways, depending upon the type of DNA damage. Double strand break activates p53 through the ATM pathway and the single-strand break initiates regulation of p53 by the ATR pathway.

Activated p53 acts as a transcription factor. It expresses hundreds of genes depending upon the type and intensity of stress [13]. These transcribed genes are involved in cell cycle arrest (by inhibiting CDK-cyclin complex) and inactivation of p53 by a feedback loop (through transcription of MDM2 and MDMX) [14]. MDM2 and MDMX have similar structure and function, hence from now on only

the MDM2 will be considered. In most of the cancers, an over-expression of protein MDM2 is observed, which acts as a cellular antagonist for p53, reducing its level and limiting the anti-tumor function. In human cancers, the over-expression of MDM2 is attributed to the gene amplification. On average, 7% of human cancers contained MDM2 gene amplification, however in a certain type of tumors more than 80% cases contained MDM2 gene amplification [11]. Some other causes of MDM2 over-expression can be increased transcription, or translation and single-nucleotide polymorphism. In the next subsection, we further investigate the interactions between p53 and MDM2 proteins.

1.3.1 p53-MDM2 Interaction

It is required to tightly regulate and stabilize the cellular levels of p53 protein under unstressed conditions. The MDM2 protein is the primary negative regulator of p53 [15]. The MDM2 inhibits the functionality of p53 in three ways;

- MDM2 binds to p53, acts as its E3 ligase and initiates proteasomal degradation
- MDM2 inhibits the binding of p53 to the targeted DNA, blocking the p53 transcriptional activity.
- MDM2 initiates the p53 export out of the nucleus, limiting the access to its targeted DNA, further minimizing its role as a transcriptional factor.

p53 and MDM2 constitute an auto-regulatory feedback loop for mutual regulation. While activation of p53 causes transcription of MDM2 mRNA, which in turn, increases the level of MDM2 protein [15]. The MDM2 protein serves as an E3 ligase, which is responsible for the destruction of p53 through the ubiquitination process [16]. Moreover, MDM2 limits the severe implications due to p53-mediated physiological activity in response to non-lethal stresses. The p53-MDM2 interactions to regulate the level of p53 are depicted in Figure 1.2.

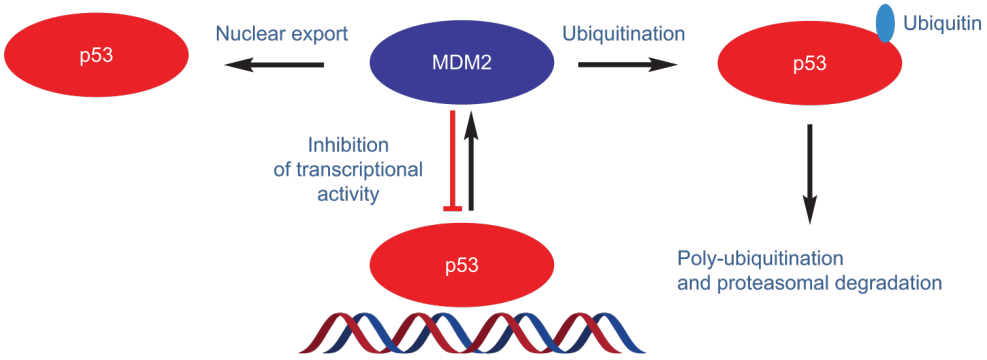

FIGURE 1.2: The auto-regulatory loop of MDM2 and p53 [15], the ↓ symbol represents activation and ⊥ symbol shows inhibition of a protein.

p53 is attached to MDM2 at its designated binding site, where MDM2 attaches a phosphate ion along with p53 to initiate its degradation by proteasome [17]. MDM2 is transcribed and up-regulated by p53, forming a feedback loop. The negative feedback loop ensures a lower concentration of p53 in normal cells [18]. The MDM2 blocks the transcriptional activity of p53 and stimulates inhibition in the nucleus and cytoplasm. MDM2 is also auto-regulated through ubiquitination and proteasomal degradation [17].

1.3.2 Revival of p53

In many tumors, overexpression of MDM2 is the reason for reduced levels of p53, which prevents DNA damage repair, cell cycle arrest, and apoptosis. Thus, inhibiting the protein-protein interaction between p53 and MDM2 can activate and restore the levels of wild-type p53, which in turn, can restore the normal cell functionality through p53 mediated responses [19]. Hence, due to the same reason, MDM2 is becoming a mainstream therapeutic target in the cancerous cells [18, 20]. A continuous search is ongoing to find some agents that directly target MDM2, and re-activate wild-type p53.

MDM2 inhibits p53 functionality through different mechanisms by directly interacting with it. The p53 protein binds with MDM2 through hydrophobic residues at designated binding pockets [15]. It is revealed from the structure of p53 that

some small non-peptide molecules can mimic the binding pattern between p53 and MDM2. These molecules can prevent the protein-protein interaction amongst p53 and MDM2 leading to increased accumulation of p53. Blocking the protein-protein interaction through such molecule inhibitors is emerging as a promising therapeutic strategy for human cancer retaining wild-type p53 [21].

1.3.3 Small Molecular Inhibitors of MDM2-p53

Efficient development for such small molecules depends on our understanding of the structural biology of p53-MDM2 interactions. The search for highly potent, non-toxic and non-peptide molecules has been proven to be far more complicated than originally anticipated. The discovery of p53 binding pocket structure on the surface of MDM2 served as the basis towards the development of such molecules. Kussie, et. al. observed that only three amino acid residues i.e Phe19, Trp23, and Leu26 are vital for the p53 to bind firmly in the binding pocket of MDM2 [22].

After an intense effort by the scientific communities, numerous small molecule inhibitors have been reported in recent years. The most widely studied MDM2 inhibitors are Nutlins (Nutlin-2, Nutlin-3a, RG7112), spiro-oxindoles (Mi-773) and pyrrolidines (RO5503781). Many of these inhibitors have already completed successful preclinical and clinical trials, either as monotherapy or in conjunction with classical chemotherapeutic agents i.e. cytarabine and doxorubicin. All of these small molecule inhibitors disrupt the interaction of MDM2 and p53, by binding at Phe19, Trp23, and Leu26 residues [15].

Amongst these inhibitors, Nutlins were the first small molecule inhibitors discovered by Vassilev et al. in 2004 [23] by a structure-based screening of the available libraries of the chemical compounds. Nutlin family is the first MDM2 inhibitor to be synthesized and advanced into human clinical trials. It binds to the N-terminal pocket of MDM2, precisely where p53 binds, with a higher affinity, without creating genotoxicity [18]. The cocrystal structure of the interaction of Nutlin and MDM2 are depicted in Figure 1.3. Nutlin-3a is highly potent and is reported to

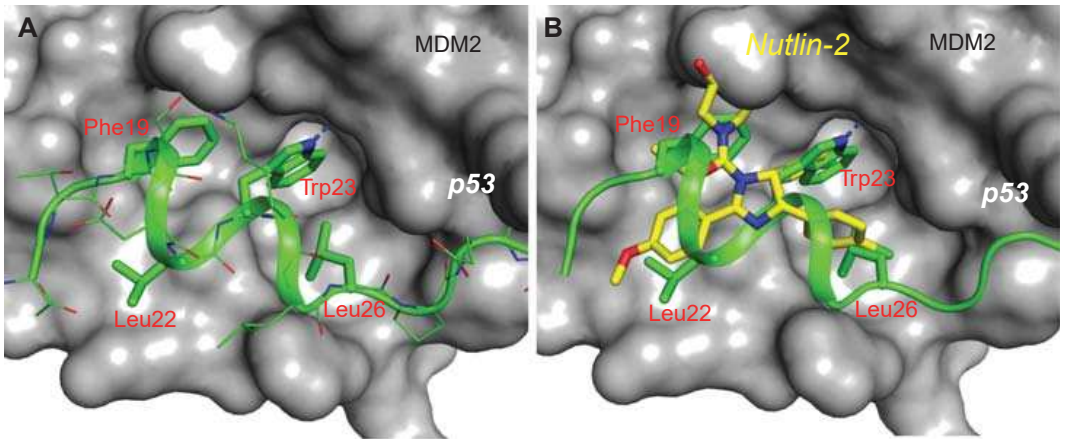

FIGURE 1.3: Crystal structure of protein-protein interactions. (A) Interaction of MDM2 with p53, p53 utilizes mainly three residues i.e Phe19, Trp23, and Leu26 to interact with the hydrophobic pocket in MDM2. (B) Superposition of both the complexes i.e. p53-MDM2 complex and Nutlin-MDM2 complex. [15]

have restored wild-type p53 functionality, and also inhibit cell growth in a dose-dependent manner, while some other variants of Nutlin have effectively treated tumors with dysfunctional or mutant p53 [24]. Nutlin-3a is orally bio-available, and the preclinical data shows that at 100 to 200 mg/kg oral administration twice a day in some tumor cell lines containing MDM2 gene amplification, inhibits tumor growth without any toxicity. An improved version of Nutlin-3a named RG7112 was developed as a result of optimizing original Nutlin-3a, to improve the potency and MDM2 binding. Henceforth, we will only describe these variants as Nutlin.

One of the advantages associated with Nutlin is its independence of p53 and auto-ubiquitination of MDM2, leaving no room for p53 to bind. These molecules were subjected to different experiments and the results confirm the accumulation of p53. Experimental results on mice ensure suppression of tumor growth in nearly 90% of cases. The available preclinical data confirms that Nutlin has a therapeutic potential to treat human cancer [15]. In the current study, Nutlin will be used as the inhibiting agent for the p53-MDM2 complex and henceforth, will be referred to as the drug.

The drug development is a costly process ranging from hundreds of thousand dollars to billions of dollars for every new drug [25]. Fortunately, with improved computational powers, the research community is able to accelerate and improve

the accuracy of the drug development process. It is now practical to use the *in silico* mathematical models in improving the process [26], wherein, the models characterize the dynamics and the control principles are applied to better understand the biological network and hence, aid the drug dosage design.

1.4 Research Objectives

Keeping in view the importance of a sustained cellular level of p53, it is desired to suppress the MDM2 interaction with p53. The current study aims to develop a therapeutic strategy to disrupt this interaction in cancerous cells. Based on this conviction, we aim to:

- Develop a control-oriented mathematical model to represent the complex interactions of the p53 pathway.
- Design a model-based robust control system to revive the p53 concentration level by proper drug dosage administration.
- Design an estimator to recover the unmeasurable state variables, which are required to achieve the above objective.

1.5 Thesis Contributions

The major contribution of the thesis is the development of a model-based nonlinear control system design for the p53 pathway system. The following are the individual contributions that lead to this objective.

- Development of a control-oriented mathematical model, based on the two generic models from literature [24, 27]. The developed model has the capability to incorporate the design of the drug intervention in the control systems paradigm.

- Model-based controller development for the drug dosage design in order to reactivate p53:

  (a) Application of Lyapunov based control design to drag the system trajectories to an attractor point, representing a healthy state of the cell.

  (b) Design of the sliding mode control (SMC) based robust nonlinear control technique to achieve the desired cellular level of p53.

  (c) Design of a modified control based on dynamic sliding mode control (DSMC), in order to obtain a smooth and continuous control signal.

- Estimation of the unknown system states by employing an equivalent control based, reduced-order sliding mode observer (SMO). Unknown system states are required in the development of a model-based control system, discussed above.

1.6 Thesis Organization

In this chapter, an introduction to the cancer disease along with the importance of the p53 pathway as an anti-tumor agent is presented. The protein-protein interaction of p53/MDM2 is investigated, and it is established that the overexpression of MDM2 is the main hurdle in the normal functionality of p53 in cancerous cells. It is shown that small molecule-based drugs are the foremost therapeutic agents to inhibit their interaction. Hence, there is a strong need to use computational frameworks to regulate drug dose administration.

Chapter 2 accounts for the literature review relating to the mathematical modeling and control of biological systems. Numerous mathematical models of the p53 pathway are reviewed to select a feasible control-oriented model. It has been observed that there is always a trade-off between computational complexity and accuracy of the mathematical model. Some earlier research carried out in the field of systems biology and feedback controller design for biological systems, in general, and specifically for the cancer control is discussed. The complexities involved in

the implementation of the biological feedback control systems are discussed along with the discussion of the two most popular implementation strategies.

Chapter 3 is dedicated to explaining the non-linear, control-oriented mathematical model of the p53 pathway. The Physiological Based Kinetic (PBK) model for the drug Nutlin is also presented. The chapter also describes the controllability analysis of the p53 pathway model.

Chapter 4 presents a Lyapunov based controller design for the p53 revival. In this chapter, a two-loop negative feedback control strategy is devised to drag the system trajectories to the desired attractor point and to regulate the cellular concentration of Nutlin, respectively. The simulation results are presented to assess the efficacy of the proposed control scheme.

In Chapter 5 a sliding mode control (SMC) based robust non-linear technique is presented for the drug design of the control-oriented p53 model. Another variant of SMC i.e. dynamic sliding mode control (DSMC) is also designed to reduce the chattering and obtain a smooth control signal. In order to ensure the overall stability of the system, the boundedness of the zero-dynamics is also proved. To make the model-based control design possible, the unknown states of the system are estimated using equivalent control based, reduced-order sliding mode observer (SMO). The robustness of the proposed technique is assessed by introducing input disturbance, measurement noise and parametric uncertainty in the system. The effectiveness of the proposed control scheme is witnessed by performing *in-silico* trials.

Finally, the thesis is summarized in Chapter 6. This chapter presents the conclusive remarks and set the direction for future work emanating from the course of current research work.

Chapter 2

Literature Review

Anti-tumor drug development is proving to be an important component of therapeutic interventions, along with classical techniques, i.e surgery, and radiation therapy. Effective drug development is only possible through a better understanding of complex nonlinear interactions in the biological networks, mediating the drug actions. The computational frameworks provide useful tools to better understand the network topology, create a new hypothesis and explore the areas for which we lack complete understanding. Both the mathematical modeling and consecutive simulation studies act as the basis for studying the nonlinear dynamics in-depth and to define effective control mechanisms.

"Systems Biology" provides tools to understand the underlying principles governing the dynamics of a biological system. It allows us to investigate the dynamic features of a specific protein regulatory network or a signaling pathway. The approaches based on mathematical modeling provide a significant insight on the operation of a regulatory network. Generally, the networks are represented by a diagram, which depicts the static behavior of the system. However, these diagrams lack the capability to express the dynamic behavior of the system along with the working logic. Hence, merely drawing interconnections of genes and proteins is not sufficient, systems biology requires a system-level understanding, acquired in the following steps [28]:

- An essential first step is to recognize the structure of the system (represented as gene regulatory network or cell signaling pathways etc.) and transform the interconnections in the form of a static picture.
- The system dynamics (behavior of a system over time) are understood and modeled with some valid approximations.
- The control method of the system along with the potential drug targets are identified.
- Lastly, the system is evaluated and redesigned to attain the required features.

In summary, the main objective of systems biology is to handle these pathways as a system, model and simulate the underlying biochemical interactions in order to better characterize the cell function and disease mechanisms. Hence, mathematical modeling proves to be a significant asset in characterizing the range of dynamic behaviors expressed by the known components.

This chapter is mainly focused upon a comprehensive review of computational modeling methods and control system design for biological systems. Numerous mathematical models of the p53 pathway are reviewed to select a feasible control-oriented model. The literature survey is carried out to learn about the existing control design techniques for the cancer suppression, followed up with the discussion on the implementation strategies for the biological feedback control systems. Lastly, based on the literature survey, a gap analysis is presented.

2.1 Mathematical Modeling of p53 Pathway

In general, cellular dynamics are categorized as inter-cellular and intra-cellular. The inter-cellular dynamics represent the interactions of genes and proteins within the context of a cell, and the intracellular dynamics examines the interactions of cell in the context of tissues, organs and the organism as a whole. This text investigates the mathematical modeling in the context of cell signaling, where the

molecular interactions affect the concentration of proteins etc. The underlying mechanism includes nonlinear dynamic interactions, positive and negative feedback loops, time delays and crosstalk between different pathways. The dynamic nature of these pathways and the feedback regulation strategies, enable us to use the same tools that have been in practice by engineers to develop control systems for years.

A more detailed discussion on modeling preliminaries for biological systems is presented in Appendix A.1, which lays down the basic laws and principals on which the development of mathematical models, presented in the upcoming sections is based upon. The dynamic behavior of a regulatory network is determined by, whether it is constituted of positive or negative feedback loops or the combination of both. The study of feedback loops in biological systems leads us to investigate the feedback loops involved in defining the dynamic behavior of the p53 pathway. A detailed discussion on the feedback loops in the biological system and their role in producing diverse dynamic behaviors is provided in Appendix A.2. The subsequent sections focus upon the dynamic response patterns generated by the p53 pathway, and the efforts to model the pathway in order to achieve the desired response patterns.

2.1.1 p53 Dynamic Response

The cells have a complete molecular signaling mechanism which receives stimuli (signal) from the environment or from other cells, interprets the signal and responds to it accordingly. The information contained in the cellular structure is insufficient to characterize the complete behavior of the p53 pathway. The dynamics of the pathway are to be incorporated as well. The true function of a pathway can be determined by systematically varying the input, to study the response. For the p53 pathway, there have been multiple studies, which provide an artificial dose to observe the p53 response. It has been observed that p53 has rather complex dynamic behavior in response to similar or different signals. The DNA damage causes p53 concentration to fluctuate regularly within a cell, which shows that

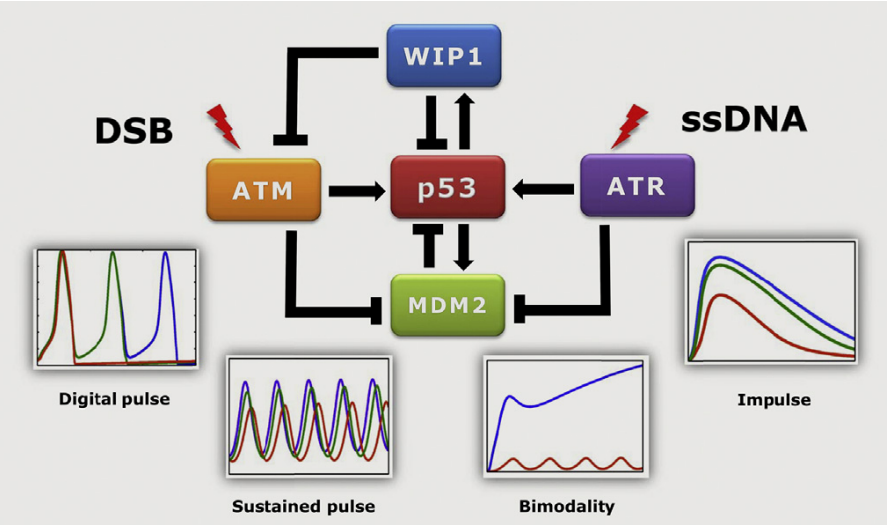

FIGURE 2.1: Multiple dynamic responses displayed by p53 [29].

appropriate p53 dynamic response is mandatory to restrict tumor development [29].

The complex feedback interactions of the p53 pathway govern its dynamic response. Initial studies were aimed at measuring the dynamics at the cell population level [30]. However, later on, it was realized that measuring the dynamics in the population may hide the actual behavior expressed by single cells. Hence analyzing the fluorescence-tagged protein reveals the hidden dynamics of an individual cell [31]. Microscopic advancements reveal complex nonlinear dynamics expressed by p53 [32]. The Negative feedback loop among p53 and MDM2 opens the possibility for oscillatory behavior [33].

Variation in the parameters of the MDM2-p53 loop can elicit multiple dynamic patterns such as damped oscillations, sustained oscillations, impulses, digital pulses, and bio-modality [13]. Figure 2.1 shows all possible outcomes of p53 for multiple types of DNA damage. ATM, ATR, and WIP1 pathways are not discussed further to avoid unnecessary complexities. Depending on the stimulus, the p53-MDM2 loop can exhibit multiple dynamic response patterns. Broadly, these patterns are either oscillatory or sustained [13]. For less extensive DNA damage, the p53 pathway is reported to go into oscillations. The oscillations in the p53 pathway initiate further downstream targets that repair the cell by DNA repair, cell cycle arrest or senescence [24, 31].

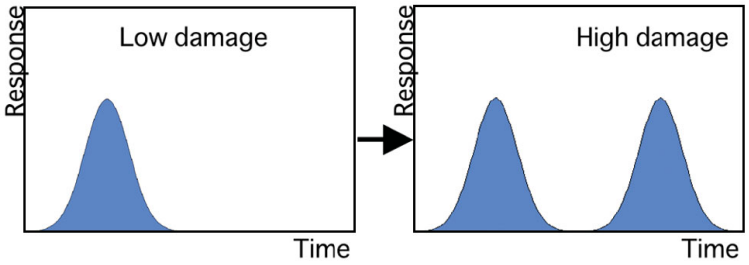

FIGURE 2.2: Pulses increase with increased intensity of DNA damage [31].

2.1.1.1 p53 Oscillatory Response

p53 invokes different dynamic patterns in response to diverse stress signals. The amplitude, frequency and pulse width of p53 may alter gene expression or control differentiation. Lahav et al. [32], demonstrated through experiments that the DNA damage in the case of γ irradiation forces p53 to express constant frequency and amplitude pulses. This, in turn, leads to cell cycle arrest. The status of the DNA is verified after each pulse of approximately six hours. In case the DNA is repaired, the oscillatory p53 dies out and resumes the blocked cell cycle process [31].

The oscillatory response by p53 induces proteins involved in responses like cell cycle arrest and DNA repair [31]. The number of pulses increases with the increased intensity of DNA damage, as depicted in Figure 2.2. The greater number of continuous pulses of p53 activates genes that cause senescence [32]. Generally, the oscillatory behavior delays gene expression, so that after recovery, cells can again undergo division.

2.1.1.2 Sustained p53 Response

The sustained p53 response is initiated due to extensive DNA damage. The amplitude and width of the response are directly dependent upon the extent of the damage. UV radiations produce a single pulse of p53, whose amplitude and width are dependent upon dose. Sustained p53 response expresses genes that induce senescence and leads to irreversible cell fate i.e. cell death [32]. Figure 2.3 depicts

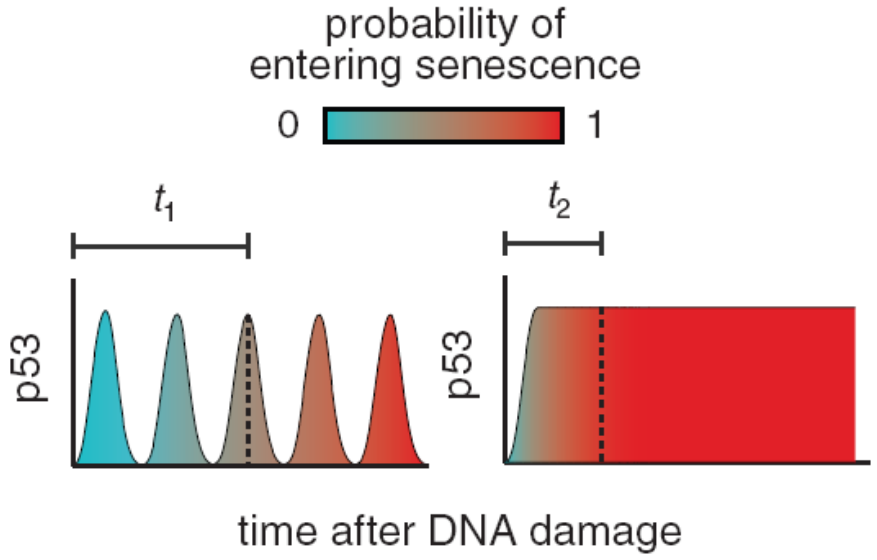

FIGURE 2.3: Probability of entering senescence for the pulsed and sustained p53 [32].

the probability of entering senescence for pulsating as well as sustained p53. It can be seen that pulsed p53 provides extra time for DNA recovery. On the other hand, it is evident that sustained p53 does not provide adequate time for DNA to repair, and kills the cell immediately. Hence, in summary, γ-irradiations produce an oscillatory response, which leads to DNA repair mechanism or cell cycle arrest, and the UV radiations produce a single prolonged pulse, which leads to apoptosis.

2.1.2 Effect of Nutlin on p53 Dynamics

The effect of Nutlin on p53 dynamics is evaluated, first through a computational model and then by the experimental results by Purvis et al. in [34]. First, the cell is exposed to γ-irradiations, which cause DNA breaks and in response p53 expresses a series of pulses having fixed amplitude and frequency. In the second step, a specific pattern of Nutlin dose is introduced, which results in the transformation of p53 pulses to a sustained response (a single pulse) having the same amplitude a as the peak amplitude of original pulses, as shown by Figure 2.4. Although both the responses have the same peak amplitude, the accumulative content of p53 will be much higher in the case of sustained response, which in turn leads to senescence or apoptosis.

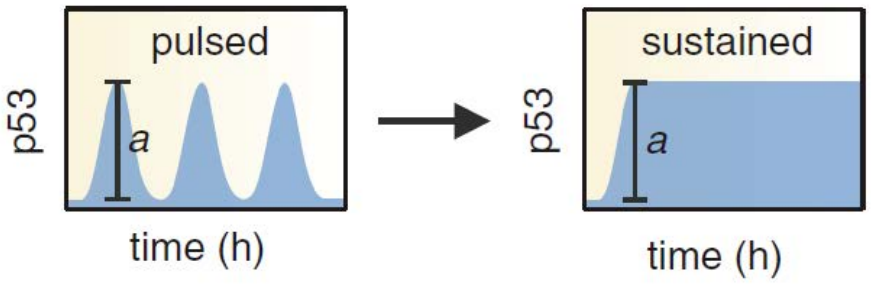

FIGURE 2.4: Nutlin perturbed pulsating p53 to produce a sustained response [34].

The main findings from the above studies are that the p53 function is directly dependent upon its pattern of cellular dynamics. Secondly, we can alter the p53 dynamics through controlled drug administration of Nutlin. Various computational models are developed in literature with respect to achieving the above discussed dynamic patterns. These models can be then used to design a system that optimizes the drug administration to achieve the desired response. In the subsequent section, a literature review of previously developed mathematical models is presented, in order to search for a feasible, control-oriented and computationally less expensive model.

2.1.3 Existing Mathematical models of p53 pathway

The efforts to model the p53 pathway are mainly focused upon the interactions between P53 and MDM2 governing its responses [35]. To investigate the construction and deconstruction mechanism of p53, numerous mathematical models have been developed in literature including continuous-time differential equations, discrete-time differential equations, delayed differential equations, and stochastic models [36]. Every modeling approach has been devised by keeping certain aspects in view. For example, the time delay models focus on the time taken by the production of protein in response to a promoter in real cells. The stochastic models consider quantized protein levels, the probability of instantaneous effects is taken almost zero. Some of the previous mathematical models are discussed in the next section.

Early models were built on the assumption that the p53 pathway undergoes damped oscillations in response to IR. An ordinary differential equation (ODE) based model was built by Lev Bar-Or et al. [30], this model considers negative feedback between p53 and MDM2 which is responsible for oscillations. This model considers coupled differential equations to emulate time delay between a promoter and the production of proteins. Many other researchers also explored the origin of the oscillations in the MDM2 and p53 level in response to IR [36–39]. The papers in [40], [41] and [42] introduced large time delays to model sustained oscillations. These models do not incorporate damped oscillation. Tyson et. al. in [33] used the time delay model with negative feedback to generate damped oscillations.

The effect of DNA damage on p53 pulses has been modeled by multiple researchers. Various mathematical models use different scenarios to create pulsating behavior. The model by Ciliberto et al. [39] displayed digital pulses in response to irradiation levels. The parameter set chosen in this model express limit cycles. The time in which the response stays in limit cycles is controlled by the extent of DNA damage. Tyson et al. [33] used the time delay model with negative feedback to generate damped oscillations.

Ma et al. [38] proposed a stochastic model to focus on stochastic effects on cell fate due to ionizing radiation (IR). The model proposes a three-module structure to investigate the p53 pulse generation due to a double-strand break (DSB). The DSBs stimulate DNA repair mechanism, ATM activation, and a p53-MDM2 feedback loop. The model uses implicit time delays by considering MDM2 mRNA and intermediate forms of MDM2.

Lipniacki et al. [43] proposed a hybrid model, which quantitatively analyzed the experimental data. They explored thethe p53-MDM2 negative loop and positive feedback loop involving PTEN, PIP3 and Akt. The DNA repair mechanism is built by considering variable duration in limit cycles with the help of Hopf bifurcation. Later on, they extended their work in [24] to incorporate pharmacokinetics of drug Nutlin. They demonstrated *in-silico* that at a lower level the dose-splitting

is ineffective, however at a higher dose level the p53 threshold is exceeded, which can induce apoptosis.

The model proposed by Hunziker et al. [27] investigated the negative feedback loop of p53 and MDM2. The effect of various stresses is modeled, and it is demonstrated that the p53 acts as a single node, capable to produce multiple oscillatory responses and transcribes various genes. This model offers a simplistic approach that allows control-oriented analysis and drug dosage design, yet it includes all the major characteristics of the p53 pathway. Hence, we have chosen this model in order to implement a control strategy to regulate p53 through drug Nutlin. In the subsequent section, some evidence of the recent application of control for the cancer is presented.

2.2 Application of Control Theory in the Cancer Control

"Systems biology" has long been used to understand, and to predict the behavior of biological systems through computational models. Recently, systems biology along with the control theory have been considered as a great tool for a more precise therapeutic intervention in complex biological networks. Nevertheless, some noteworthy developments have been made in drug delivery of cardiovascular systems [44–46], blood pressure control [47, 48], anesthesia drug delivery [49, 50], diabetes control [51], Parkinson's Tremor [52] and HIV/AIDS control [53, 54]. The current advancements in control of biological systems also explore the possibility of controller design for cancer treatment.

The application of control theory in cancer treatment is a fairly new subject. The main objective in the cancer treatment is remission of cancerous cells within minimum time while maintaining the health profile of a patient. The traditional treatment techniques, such as chemotherapy, radiotherapy, and surgical procedures are one way around, but these procedures may reduce the quality of life of the

patient [55]. The current research trend is shifting towards the in-silico methods for analysis and control. There is a strong need to use these in-silico models to implement drug design using control theory.

In the traditional techniques, the amount of administered drug is of utmost importance for the survival of patients, because the therapy does not only kill cancerous cells but also affects healthy human tissues. Hence, to improve the efficacy of the above-mentioned techniques, the dosage of cancer therapy is carefully controlled in order to kill a maximum number of tumor cells, whilst causing minimum damage to healthy tissues. In literature, multiple control strategies are implemented (mostly upon the tumor growth models) to optimize drug therapy. The most notable work in this regard is by de Pillis et al. [56], in which they constructed an ODE based tumor growth model, containing the number of the tumor, healthy and immune cells as state variables. They later included a time-varying drug term and applied bang-bang type optimal control to adjust the amount of drug that minimizes the tumor cells, while maintaining healthy and immune cells above a required level [57]. This work is later extended by [58], in which they applied a linear time-varying (LTV) approximations based optimal control strategy, which simplifies the controller design and also provides globally valid results.

A state-dependent Riccati equation (SDRE) based optimal control is applied to the above-mentioned model in [59], with the aim to reduce the administrated drug. SDRE permits to consider the specific conditions of the patients by assigning state-dependent weighting matrices in the cost function. Later on, [60] appended Kalman filter with SDRE to estimate the unknown state, associated with the population of tumor cells. In [61] a model reference adaptive control (MRAC) is compounded with the existing SDRE approach to preserve the benefits of both the techniques. The proposed algorithm handles the unmodeled dynamics and parametric uncertainties in the model. The scheme works in two steps: firstly, a reference patient (with known mathematical model) is stabilized by applying the SDRE approach, secondly, the proposed algorithm is applied on an unknown patient to adapt the drug administration of the reference patient.

The above-discussed control design techniques are mainly applied to the macroscopic level. However, after the discovery of small molecule chemotherapy drugs, that can directly target the protein-protein interactions, the current research trend is shifting towards utilizing control techniques in drug dosage design at the cellular level. In the literature, a couple of model-based control techniques are explored for the p53 pathway. In our previous work [62], we designed a simple proportional type control to obtain the desired normalized concentrations of p53 and MDM2 proteins. In [63], a mathematical model consisting of 11 states for the p53 and relating pathways is exploited to design flatness based control for maintaining the desired level of active p53.

From the drug-manipulation viewpoint, it is evident that a drug dose will be constructed by the contribution of the state variable. The controller action is based on different mathematical operations being performed on the variables, namely addition, subtraction, scalar multiplication, integration, and differentiation. The physical realization of these operations becomes important when implementing the proposed closed-loop control system for drug delivery in the human body. The following section discusses the possibilities regarding the implementation of the proposed feedback control schemes.

2.3 Feedback Control Implementation

The realization of a feedback control system demands high-quality sensing, adequate computational power, and accurate actuating components. This becomes more challenging when we are dealing with biological systems. Engineers and experimental biologists have tackled this challenge in two ways;

- *in silico* feedback control
- *in vivo* feedback control

illustrated in Figures 2.5(a) and 2.5(b) respectively. Each of the techniques are discussed in the subsequent sections.

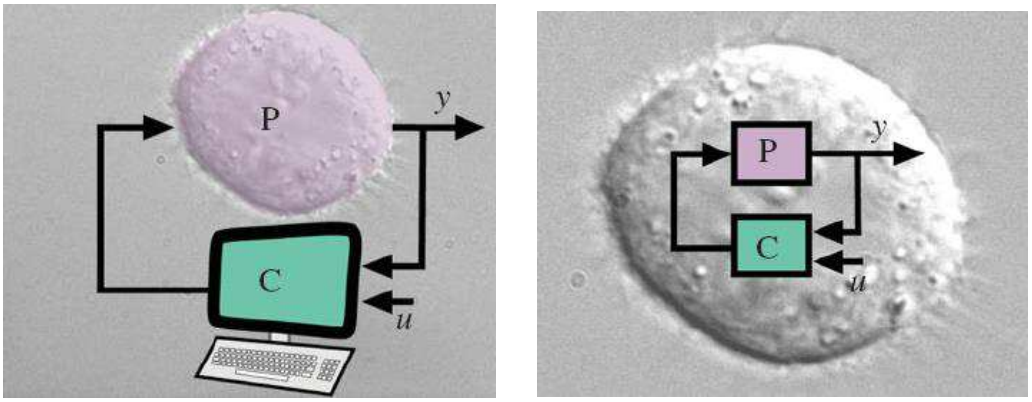

(a) In silico feedback control (b) In vivo feedback control

FIGURE 2.5: Feedback control implementation techniques

2.3.1 *in silico* Control Implementation

The *in silico* control implementation considers the molecular circuitry of a cell or population of cells as the process "P" to be controlled, and the controller "C" is implemented on a computer, outside the body, as depicted in Figure 2.5(a). For the real-time implementation, techniques like microscopy [64, 65] , flow cytometry [66] and rapid immunoassay [67] enable fast measurements of protein concentration in patients. Methods like immunomagnetic- electrochemiluminescent require seconds to collect samples from the patient's serum and minutes to complete the measurement process. The sampling period between intervals can be set according to the therapeutic requirements.

The measured data "y" is compared with the desired data "u" *in silico* and the control input computed by the controller serves as the dose for targeted cells. The interface between computer and cells is achieved by biological transducers that are capable of responding to input in either light or chemical form. The control scheme proposed in Section 4.1, for p53 protein revival, can be implemented in this manner, provided all the state measurements are available. The implementation becomes more challenging for the inner loop controller as it requires at every instant the measurement for the drug Nutlin inside the cell. A better way to tackle this problem is to implement the controller inside the cellular structure, discussed in the following section.

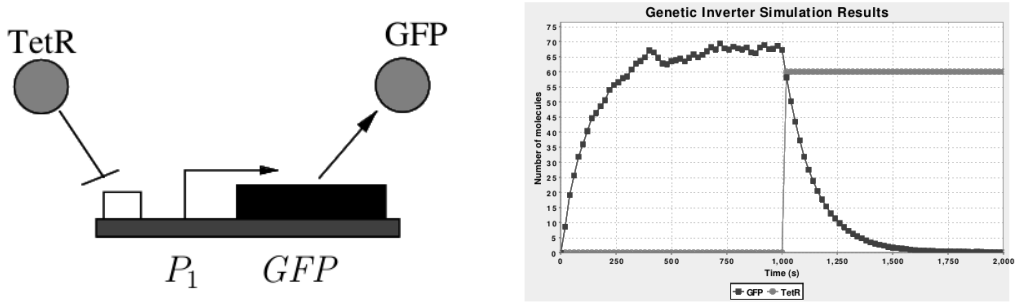

(a) Genetic implementation (b) Stochastic simulation

FIGURE 2.6: Genetic Implementation of a logic gate inverter

2.3.2 *in vivo* Control Implementation

Synthetic biology enables engineers to program living cells to serve as therapeutic agents to cure genetic disease. Engineered bio-systems are built with a bottom-up approach of synthesizing small parts that constitute functional modules, and composition of these modules build systems [68, 69]. The *in vivo* feedback control employs synthetic biology to control the cellular behavior by assembling molecular circuits in cells [70]. Both the process and controller are realized within cells with the help of biomolecular processes, as depicted in Figure 2.5(b).

With the help of genetic circuits and synthetic sensors, any feedback control system can be implemented into cells. The transcription of a gene is initiated and regulated by transcription factors (TF). The binding sites of TF can be used in designing synthetic systems [71]. For example, a basic logic gate inverter can be constructed from genetic material as shown in Figure 2.6(a). The genetic circuit is composed of a promoter and gene which transcribes green fluorescent protein (GFP). Cells containing this circuit glow green whenever input protein TetR is unavailable in the cell [72]. There are a number of regulators that control the rate of gene transcription by binding to separate gene promoter regions. Many logic gates have also been constructed with these DNA-binding proteins [73].

Genetic implementation of negative feedback has been achieved by either increased degradation of mRNA [74] or suppression of the translation process by making use of mRNA binding proteins [75]. Chemical reactions are employed to construct and

implement integral feedback control [76] and nonlinear quasi sliding mode (QSM) control [77]. However, all of these techniques require rigorous theoretical analysis to ensure stability, reliability, and robustness. We, therefore, propose a hybrid method for the biological implementation of the controller, proposed in Section 4.1. The nonlinear outer loop Lyapunov controller will be embedded inside a digital computer (*in silico*) and the inner loop PID controller will be synthesized by biological circuits (*in vivo*). The control scheme proposed in Section 5.2 can be implemented *in silico*, by employing the control inside a computer.

Based on the above discussion on modeling and control of p53 pathway, the found shortcomings (the current study aims to address) are presented in the subsequent section.

2.4 Gap Analysis

In the literature, there has been extensive work on p53 mathematical modeling, and a number of models have been developed based upon mainly either time-delay approach or differential equation approach. Most of the previous research is focused on the analysis of these mathematical models and lacks their utilization for drug design purposes. The use of these models in drug design can speed up the process by providing a better understanding of drug interactions with targets. From the control design perspective, there has not been much consideration for control-oriented modeling. Hence, it is required to obtain a model that would support the administration of the drug in a prescribed manner. Two factors should be considered while selecting a feasible mathematical model for the p53 pathway: model accuracy and ease of control design. The accuracy of the model increases the complexity, which can make the control design difficult. As the controller expressions are derived from the model, therefore, the model-based controller requires a computationally less expensive mathematical model. Furthermore, for more complicated mathematical models the parameter search is difficult. In this research, we have chosen the model proposed in [27] which offers a simplistic

approach that allows control-oriented analysis and drug dosage design. We will develop a control-oriented mathematical model based upon this existing model.

The complex dynamics, multiple interactions, nonlinear behavior and the nature of uncertainty in biological systems make the control design challenging. Usually, the process for measurement of the parameters is either very cumbersome or expensive, hence the mathematical models of bio-systems are not always precise. Another issue with the most biological models is that they are not defined in any formal mechanism, which further complicates the control design. Hence, there is a strong need to design a sophisticated control system, which accounts for all the physical issues, that could arise in a biological feedback control system i.e., parametric uncertainties, external disturbances, unmeasurable state variables, and measurement noise. The control techniques presented in [62, 63] are not inherently robust and are based upon certain assumptions, which may not be the case in actual scenarios. In this research, we aim to design such a control system that is neither too complicated nor is operating under such assumptions that limit the practicality of the feedback control in real systems.

2.5 Summary

This chapter accounts for the literature review related to the mathematical modeling and control of the p53 pathway. Numerous mathematical models are developed in the literature, trying to capture the dynamics of the p53 pathway. Here, a comprehensive literature review of the existing mathematical models is presented, in the search for a feasible control-oriented model. In the biological systems, it is of importance that all the parameter values are available. Secondly, it has been observed that there is always a trade-off between computational complexity and accuracy of the mathematical model. Therefore, a compromise is made between both the requirements and a model by Hunziker et al. [27] is selected. This model is relatively simple and at the same time captures all the fundamental dynamical properties of the p53 pathway.

The suitability of the controller design for biological processes is motivated through a review of the existing biological feedback controller design. Lastly, the complexities involved in the implementation of the biological feedback control systems are discussed. The next chapter describes the selected mathematical model and the associated parameters in detail, accompanied by the controllability analysis.

Chapter 3

Mathematical Model of p53 Pathway

Before designing a control system, it is desired to choose a feasible, computationally less expensive and control-oriented model. The mathematical model presented in [27] allows a control-oriented drug dosage design. The model offers a simplistic approach yet adequately preserves the fundamental dynamical properties of the p53-MDM loop. The subsequent section describes the mathematical model of the p53 pathway.

3.1 Hunziker et al. Mathematical Model

The ordinary differential equation (ODE) based model, presented by Hunziker et al. in [27] investigated a positive feedback loop of p53-Mdm2 mRNA and negative feedback loop between p53 and Mdm2, to produce oscillations in the response. The effect of different stresses on the p53 response is also investigated. The model offers a simplistic approach yet adequately preserves the fundamental dynamical properties of the p53-MDM loop, and allows control-oriented drug dosage design. The interactions between Mdm2 and p53 protein are represented by a schematic diagram shown in Figure 3.1.

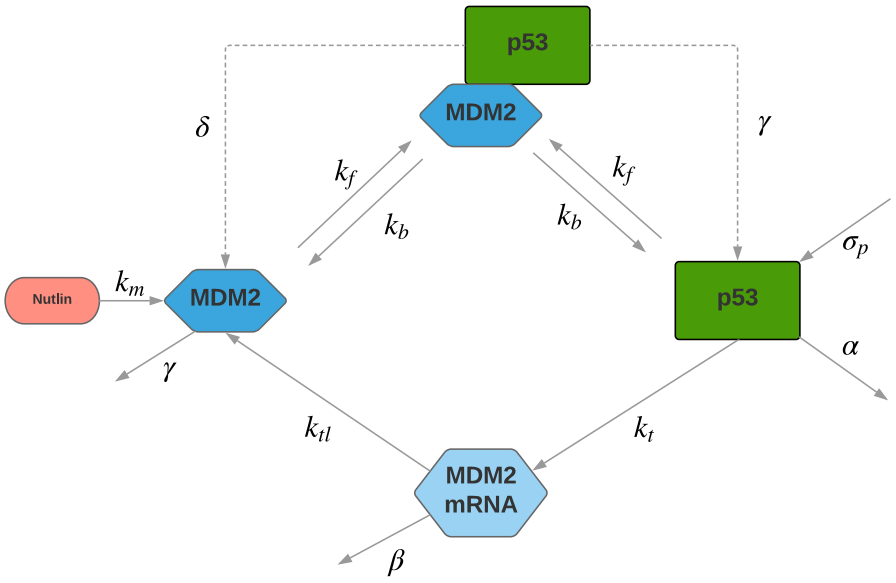

FIGURE 3.1: Schematic model of p53 pathway dynamics, representing the components and interactions that correspond to each of the state in the mathematical model (3.1)

In the current research work, we provide a modified version of the Hunziker's model, in which we incorporate a new term for the clinical trial drug Nutlin 3a in order to investigate its proper dosage and p53 response. The Mdm2 and Nutlin complex is introduced in the dynamic equation of Mdm2. The single cellular dynamics of the p53 pathway is characterized by an ODE-based mathematical model, presented in state space form by

$$\begin{aligned}
\dot{x_1} &= \sigma_p - \alpha x_1 - k_f x_1 x_3 + k_b x_4 + \gamma x_4, \\
\dot{x_2} &= k_t x_1^2 - \beta x_2, \\
\dot{x_3} &= k_{tl} x_2 - k_f x_1 x_3 + k_b x_4 + \delta x_4 - \gamma x_3 - k_m (u - \zeta) x_3, \\
\dot{x_4} &= k_f x_1 x_3 - k_b x_4 - \delta x_4 - \gamma x_4.
\end{aligned} \tag{3.1}$$

Where x_1 is concentration of p53 protein, x_2 is Mdm2 mRNA, x_3 is concentration of Mdm2 protein and x_4 is the concentration of Mdm2-p53 protein complex. All of these concentrations are measured in nM. The control input u to the system is the concentration of the anti-tumor drug "Nutlin", measured in mg/kg (Note: x_3 is positive by physical nature, and takes part as control gain) and the concerned output is x_1 (concentration of p53 protein).

The parameters and rate constants being used in the p53 model are listed and described in Table 3.1. Here, the Greek letters (α, β, γ and δ) represent the degradation rates. The parameter α models all the processes that result in Mdm2 independent deactivation of the p53 protein, leading to a reduced active p53 concentration in the nucleus. Whereas, the parameter δ represents the Mdm2 dependent p53 deactivation. The parameter β is the degradation rate of Mdm2 mRNA and γ is the Mdm2 protein degradation, due to the auto-ubiquitination process.

TABLE 3.1: Definition of model parameters and kinetic rate constants [27]

Parameter	**Definition**	**Value**
σ_p	Production rate of p53	1000 $nM.hr^{-1}$
α	Mdm2 independent deactivation/ degradation of p53	0.1 hr^{-1}
δ	Mdm2 dependent deactivation/ degradation of p53	11 hr^{-1}
k_t	Transcription of Mdm2	0.03 $nM^{-1}.hr^{-1}$
k_{tl}	Translation of Mdm2	1.4 hr^{-1}
β	Degradation rate of Mdm2 mRNA	0.6 hr^{-1}
γ	Mdm2 degradation/deactivation	0.2 hr^{-1}
k_b	Dissociation of Mdm2-p53	7.2 hr^{-1}
k_m	Nutlin rate constant	200 hr^{-1}
$k_D = k_b/k_f$	Dissociation constant of Mdm2-p53	1.44 nM

The subscripted letters represent the production rates, such as the parameter σ_p models the synthesis of p53 protein, which is assumed to be produced at a constant rate. The rate constant k_t describes the transcription of Mdm2 mRNA, whereas the subsequent translation to Mdm2 protein is described by the rate constant k_{tl}. The rate constants k_f and k_b describe the Mdm2-p53 complex formation and breakup, respectively.

Many of these parameters are fixed using data from the literature, e.g., the Mdm2 independent degradation rate of p53 α is taken as 0.1 hr^{-1}. The degradation rate is taken small as p53 does not degrade in 120 min in the absence of Mdm2 [78],

the value $\alpha = 0.1\ hr^{-1}$ corresponds to a half life of 7.5 hrs. The Mdm2 dependent half life of p53 is measured to be less than 15 minutes [78]. Therefore, γ is taken in the range of $1-20\ hr^{-1}$, corresponding to a half life of $2-40$ minutes. The half life of the Mdm2 mRNA is measured to be one to two hours [79]. Therefore, the degradation rate of Mdm2 mRNA is fixed as $\beta = 0.6\ hr^{-1}$, which corresponds to a half life of around one hour. The dissociation constant of Mdm2-p53 is reported to be in between $0.2 - 700nM$ [80, 81], the dissociation of Mdm2-p53 is taken as $k_b = 7.2\ hr^{-1}$ and from the relation $k_D = k_b/k_f$, the Mdm2-p53 association is taken as $k_f = 5.1428\ nM^{-1}\ hr^{-1}$, which implies that $k_D = 1.44\ nM$. The levels of p53 and Mdm2 in the cells are used to constrain the values of σ_p, γ, k_t and k_{tl} as presented in Table 3.1.

The nonlinear model presented in (3.1) can be written in control affine form i.e.

$$\dot{x} = f(x) + g(x)(u + \zeta), \tag{3.2}$$

where $x \in \mathbb{R}^4$ is the state vector, $f, g \in \mathbb{R}^4$ are smooth vector fields. The vector fields $f(x)$ and $g(x)$ are given as

$$f(x) = \begin{pmatrix} \sigma_p - \alpha x_1 - k_f x_1 x_3 + k_b x_4 + \gamma x_4 \\ k_t x_1^2 - \beta x_2 \\ k_{tl} x_2 - k_f x_1 x_3 + k_b x_4 + \delta x_4 - \gamma x_3 \\ k_f x_1 x_3 - k_b x_4 - \delta x_4 - \gamma x_4 \end{pmatrix},$$

$$g(x) = \begin{pmatrix} 0 \\ 0 \\ -k_m x_3 \\ 0 \end{pmatrix}.$$

Here, ζ is the input disturbance, faced by cellular structure due to intrinsic noise, unwanted interference from neighboring pathways and environmental stresses. It appears with the same vector g as the input u, hence ζ is assumed to be a matched disturbance. The disturbance satisfies the following assumption:

Assumption 1. Consider ζ to be a matched disturbance (bounded by $||\zeta|| \leq \zeta_0$ and $\zeta_0 \in \mathbb{R}^+$), which is sufficiently smooth i.e. $\dot{\zeta}$ is continuous and bounded i.e. $\dot{\zeta}(t) \leq \psi(t), ||\psi(t)|| \leq \psi_0$ where $\psi(t)$ is a smooth function and $\psi_0 \in \mathbb{R}^+$.

Recent techniques, such as microscopy, flow cytometry, rapid immunoassay and immunomagnetic-electrochemiluminescent (ECL) are used for the rapid measurements of p53 and Mdm2 concentrations using patient's serum [64, 66, 67]. Accordingly, the measurement vector y_m is given by

$$y_m = [x_1 \quad x_3]^T. \tag{3.3}$$

3.2 Nutlin PBK Dynamics

To investigate the *in vivo* treatments of Nutlin, the extra-cellular dosage concentration and dynamics are defined by [24] with the help of Physiological Based Kinetic (PBK) model. Puszyński et al., explored the pharmacokinetics data in mice to investigate the effect of Nutlin oral delivery. They considered a uni compartmental model, which includes the extra-cellular and intra-cellular portions of a cell. The total extra-cellular concentration of Nutlin, denoted by N_{tot} is defined by;

$$N_{tot} = N_b + N_e, \tag{3.4}$$

where N_b is the concentration of the blood plasma bound Nutlin. The Nutlin-plasma binding data is fitted to the following equilibrium equation,

$$N_b = B_{max} \frac{K_a N_e}{1 + K_a N_e}, \tag{3.5}$$

where B_{max} represents the concentration of total plasma protein binding sites, and the constant K_a denotes the equilibrium association constant [82]. The second portion of N_{tot} is the extra-cellular concentration of free Nutlin, denoted by N_e. The concentration of N_e is relatively small due to substantial binding of Nutlin

with plasma. The extra-cellular free Nutlin concentration can be articulated in terms of N_{tot} as;

$$N_e = \frac{-(1 + K_a B_{max} - K_a N_{tot}) + \sqrt{(1 + K_a B_{max} - K_a N_{tot})^2 + 4K_a N_{tot}}}{2K_a}. \quad (3.6)$$

"N_e'' is the available concentration, to be imported inside the cell. The concentration of the intra-cellular Nutlin, denoted by N_{UT} is described by the following equation;

$$\frac{d}{dt}N_{UT} = i_1 N_e + k_{d_3}\, MDM_i - k_m N_{UT}\, MDM_a - e_1 N_{UT} \quad (3.7)$$

where MDM_i represents the inactive form of MDM (due to binding with Nutlin), $N_{UT}\, MDM_a$ represents the active MDM present in MDM-Nutlin complex. The constants k_{d_3} and k_m are the dissociation and association rate constants of Nutlin and MDM, respectively. The pharmacokinetic effects for Nutlin are incorporated in the following equation

$$\frac{d}{dt}N_{tot} = p_{oral}\, D\, \delta_1 e^{-\delta_1(t-t_0)} - \delta_2\, N_e, \quad N_{tot}(t_0) = 0, \quad (3.8)$$

where p_{oral} describes conversion from mg Kg^{-1} to moles per distribution volume, D is the drug dosage (in mg Kg^{-1}) and t_0 is the initial time for drug delivery [24].

In the current research, the effect of Nutlin dose on the p53 pathway is simulated by integrating Hunziker et al., and Puszyński et al. models. The p53 dynamics are taken from Hunziker et al., and Nutlin PBK dynamics from Puszyński et al., reintegrated into Mdm2 rate equation in (3.1), where Nutlin is added as a sink term $k_m u$. The model parameters used in the PBK model are presented in Table 3.2 with the associated units and their meaning. It is worth mentioning that to integrate both models, the units are kept consistent. Hence, the parameters derived from [24] are converted from *sec* to *hr* and from M to nM.

To achieve the required performance characteristics discussed earlier, we will need to design a controller. Before the application of control to complex bio-systems, like one we are dealing with, investigation for applicability of control design is

TABLE 3.2: Definition of kinetic rate constants for Nutlin PBK model [24]

Name	**Definition**	**Value**
B_{max}	concentration of plasma protein binding sites	$286 \times 10^{-3}\, nM$
K_a	equilibrium association constant in plasma	$0.085 \times 10^{-3}\, nM$
p_{oral}	dose conversion factor for oral delivery	$7.5\, nM/mg/Kg$
δ_1	Production rate of p53	$0.719\ hr^{-1}$
δ_2	elimination rate constant	$19.44\ hr^{-1}$
i_1	rate of Nutlin intracellular import	$457.2\ molec\,(hr\, nM)^{-1}$
k_{d3}	Nutlin-Mdm2 dissociation rate	$720\ hr^{-1}$
e_1	rate of Nutlin cell export	$1.8\ hr^{-1}$

required. The test of a system for the ability to achieve desired control performance is called "controllability analysis". The next section highlights the controllability analysis for the p53 network model.

3.3 Controllability Analysis

Linear, as well as nonlinear approaches, are used to test controllability of a system. In most cases the linear test is sufficient. The nonlinear systems can be linearized for application of linear approaches. But in many cases, linear approaches are not conclusive as was in our case. Hence, a Lie algebra based nonlinear controllability analysis approach is applied.

Consider a nonlinear system of the form,

$$\dot{x} \;=\; f(x) + g(x)u, \tag{3.9}$$

with f and g some smooth vector fields on $\mathbb{R}^n$. The lie bracket of f and g is another vector field [83], written as

$$[f,\, g] \;=\; \nabla g\, f - \nabla f\, g, \tag{3.10}$$

where ∇g and ∇f are gradients of g and $f$respectively.

Generally the lie bracket of f and g is written as $ad_f g$ (where ad represents the "adjoint"), and the repeated Lie brackets are defined as

$$\begin{aligned} ad_f^0 g &= g, \\ ad_f^i g &= [f,\, ad_f^{i-1}\, g], \qquad i = 1, 2 \ldots n. \end{aligned} \tag{3.11}$$

A lie bracket of two vector fields f and g is defined as;

$$\begin{aligned} ad_f g(x) &= [f,\ g](x) \\ &= \frac{\partial g}{\partial x}(x) f(x) - \frac{\partial f}{\partial x}(x) g(x), \end{aligned} \tag{3.12}$$

where, $\partial g/\partial x$ and $\partial f/\partial x$ are Jacobian matrices of g and f respectively.

According to Lie algebra, the nonlinear system (3.9) is controllable, if for any x_0, the controllability Jacobian matrix

$$J_c = [g(x),\ ad_f g(x), \ldots\ldots\ldots\ldots,\ ad_f^{n-1} g(x)], \tag{3.13}$$

have linearly independent columns, or the matrix have full rank.

Application of Lie algebra based controllability analysis defined in (3.13) to the p53 model (3.2) with $n = 4$, the Jacobian controllability matrix J_c becomes;

$$J_c = [g(x) \quad ad_f^1 g(x) \quad ad_f^2 g(x) \quad ad_f^3 g(x)]. \tag{3.14}$$

By using f and g matrices from (3.2), the J_c can be found. For example, $ad_f^1 g$ can be computed as;

$$\frac{\partial\, g(x)}{\partial x} = \begin{pmatrix} 0 & 0 & 0 & 0 \\ 0 & 0 & 0 & 0 \\ 0 & 0 & -k_m & 0 \\ 0 & 0 & 0 & 0 \end{pmatrix},$$

$$\frac{\partial f(x)}{\partial x} = \begin{pmatrix} -k_f\, x_3 - \alpha & 0 & -k_f\, x_1 & k_b + \gamma \\ 2\, k_t\, x_1 & -\beta & 0 & 0 \\ -k_f\, x_3 & k_{tl} & -k_f\, x_1 - \gamma & k_b + \delta \\ k_f\, x_3 & 0 & k_f\, x_1 & -k_b - \delta - \gamma \end{pmatrix},$$

and

$$\frac{\partial\, g(x)}{\partial x} f = \begin{pmatrix} 0 \\ 0 \\ -k_m\,(-k_f\, x_1\, x_3 + \delta\, x_4 - \gamma\, x_3 + k_b\, x_4 + k_{tl}\, x_2) \\ 0 \end{pmatrix},$$

also,

$$\frac{\partial\, f(x)}{\partial x} g = \begin{pmatrix} k_f\, x_1\, k_m\, x_3 \\ 0 \\ -k_m\, x_3\,(-k_f\, x_1 - \gamma) \\ -k_f\, x_1\, k_m\, x_3 \end{pmatrix}.$$

Hence, the $ad_f^1 g = [f \quad g] = \partial g/\partial x\, f - \partial f/\partial x\, g$ turns out to be,

$$ad_f^1 g = \begin{pmatrix} -k_f\, x_1\, k_m\, x_3 \\ 0 \\ -k_m\,(-k_f\, x_1\, x_3 + \delta\, x_4 - \gamma\, x_3 + k_b\, x_4 + k_{tl}\, x_2) + (-k_f\, x_1 - \gamma)\, k_m\, x_3 \\ k_f\, x_1 k_m\, x_3 \end{pmatrix},$$

Similarly, $ad_f^2 g$ and $ad_f^3 g$ can be computed as;

$$ad_f^2 g = [f \quad ad_f^1 g], \tag{3.15}$$

$$ad_f^3 g = [f \quad ad_f^2 g]. \tag{3.16}$$

After substituting the parameter values from 3.1, the Lie Algebra based controllability matrix J_c becomes;

$$J_c = \begin{pmatrix} 0 & -1.34x_3x_1 & \begin{array}{c}-48.85x_4x_1 - \\ 3.75x_2x_1 + \\ x_3(-1342.27 - \\ 9.93x_4 + \\ x_1(-9.66+6.90x_1))\end{array} & \begin{array}{c}-542.3x_4^2 - 5637.5x_2 - 7.89x_2x_1 - \\ 0.16x_1^3 + x_3^2(-6903.03 + (-51.08 - \\ 71x_1)x_1) + x_4(-73288. - 41.7x_2 + \\ 806.168x_1 + x_3(38.7 - 51.08x_3 + \\ 153.2x_1)) + x_3(-19462.9 + \\ x_1(20531.2 + (-403.8 - 35.5x_1)x_1))\end{array} \\ 0 & 0 & 0.0805362x_3x_1^2 & \begin{array}{c}x_1(4.39728x_4x_1 - 0.828364x_3^2x_1 + \\ 0.338252x_2x_1 + x_3(241.609 + \\ 1.7879x_4 + (1.03086 - \\ 0.828364x_1)x_1))\end{array} \\ -200\,x_3 & \begin{array}{c}-4.75x_4- \\ 0.36x_2\end{array} & \begin{array}{c}2.11x_2 + x_4(86.45 - \\ 24.42x_1) + \\ ((-48.85 - \\ 6.90x_3)x_3 - \\ 1.87x_2 - 0.01x_1)x_1\end{array} & \begin{array}{c}-180.7c^2 - 73288.x_3 - 13806.1x_3^2 + \\ x_4(-26002.8 + (-542.3 - \\ 102.1x_3)x_3 - 13.9x_2) - 1891.4x_2 - \\ 21.9x_1 + (x_4(-886.9 - 376.9x_3) + \\ x_3(7.3 + x_3(203.6 + 35.5x_3) - \\ 28.9x_2) - 114.8x_2)x_1 + (0.06 - \\ 125.6x_4 + 71x_3^2 - 9.6x_2)x_1^2 - 0.1x_1^3\end{array} \\ 0 & 1.3x_3x_1 & \begin{array}{c}48.8x_4x_1 + \\ 3.7x_2x_1 + \\ x_3(1342.2 + 9.9x_4 + \\ (24.2 - 6.9x_1)x_1)\end{array} & \begin{array}{c}542.3c^2 + 5637.5x_2 + x_4(73288. + \\ 41.7x_2 + x_3(177.7 + 51x_3 - \\ 153.2x_1) - 7.3x_1) + 69.3x_2x_1 + \\ 0.1x_1^3 + x_3^2(6903.03 + x_1(-24.1 + \\ 71x_1)) + x_3(48724.4 + \\ x_1(-20269.3 + x_1(253.3 + 35.5x_1)))\end{array} \end{pmatrix}$$

By looking at above controllability matrix, it is evident that no row or column are linearly dependent upon each other. Hence, the final controllability matrix J_c is full rank and it can be concluded that the considered mathematical model is controllable.

The drug development is a costly and laborious process and needs improvements in the accuracy too. Now due to available computing power, the *in silico* methods are quite useful and can cost-effectively improve the overall development process. The problem discussed in the previous chapter can be modeled in the control systems paradigm, where the input to the system is the concentration of the drug Nutlin and the relevant output is the p53 protein. It can be rightfully assumed that for a cancerous cell p53 level should be relatively high and the Mdm2 level should be reasonably low, which constitutes the control problem to be addressed in the subsequent chapter.

3.4 Summary

This chapter presented the selected control-oriented mathematical model for the p53 pathway, along with the parameters and their definitions. To incorporate the *in vivo* effects of the drug Nutlin, a PBK model is presented. Lastly, the controllability analysis is performed, which ensures that the current system is controllable. For the design of a control system, multiple formats are used, mainly categorized as linear and non-linear control design. Every scheme has its merits and demerits depending upon the structure of the system and controller. Linear techniques can be applied to nonlinear systems after linearizing the model. However, linear control techniques perform better only in the vicinity of an equilibrium point. Owing to the fact that the current system is a complex nonlinear system so it is appropriate to use a non-linear control technique to achieve better results in the global sense. In the subsequent chapters, two state of the art nonlinear techniques are employed to design a control system for the selected p53 model, in order to obtain a desired constant level of the p53 protein.

Chapter 4

Lyapunov Based Control Design

Lyapunov theory, introduced by the Russian mathematician Alexandr Mikhailovich Lyapunov in late 19^{th} century, has proven to be a most useful approach in studying the stability of nonlinear systems. Lyapunov's direct method is a mathematical tool to analyze the stability of an equilibrium point. The method is based upon the fact that if the total energy of a system continuously dissipates, then the system should eventually settle down on an equilibrium point.

In system analysis, we assume that some kind of control function is already designed. However, in some problems, it is desired to find a control law for the given plant. For an autonomous system

$$\dot{x} = f(x, u), \tag{4.1}$$

where $x \in \mathbb{R}^n$ is the state vector and control input $u \in \mathbb{R}^m$, consider a candidate control Lyapunov function (CLF) $V(x)$, having the time derivative as $\dot{V}(x) < -W(x) \in \mathbb{R}^+$. The aim of the feedback control design is to find a control law $\big(u = \alpha(x)\big)$ that makes this candidate a real Lyapunov function. The control law u is chosen such that it ensures that the close loop system's equilibrium point $x = 0$ is globally asymptotically stable [83, 84]. The control design for the p53 pathway based on Lyapunov's Direct Method is discussed in the subsequent section.

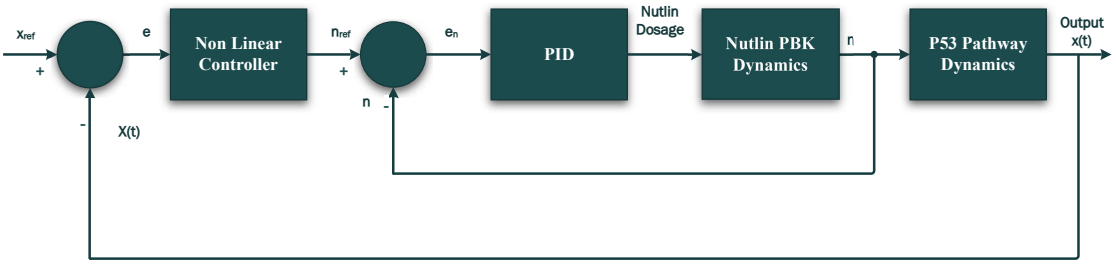

FIGURE 4.1: Block diagram of negative feedback control for Nutlin PBK dosage.

4.1 Lyapunov Based Control of p53 Pathway

For the production of a sustained p53 response, a two-loop negative feedback strategy shown in Figure 4.1, is employed. The outer loop comprises the main controller for the p53-MDM2 pathway. This nonlinear, Lyapunov based controller determines the required amount of Nutlin in order to revive p53 protein. This required amount of Nutlin is termed as a reference dosage or n_{ref}. Since our goal is to reduce MDM2 as much as possible, so as to give some space to p53 for growth. Physiologically, it implies that the reference dosage of Nutlin required is determined by the nonlinear controller with the use of actual concentrations or states of the system. This gives the reference Nutlin dosage which should be present in the cell.

However, to maintain reference dosage in the cell, a negative feedback inner loop is devised for the PBK dynamics of Nutlin. In the cascaded control arrangement, both the loops are running simultaneously, where the reference dosage is being generated by the outer loop and the inner loop tracks this reference dosage keeping in view the cellular dynamics of the drug. The inner loop should be fast as compared to the outer loop so that the reference value of the inner loop can be considered relatively constant. The proportional, integral, and derivative (PID) controller is a relatively simple and fast controller with ease of implementation, especially if it is implemented *in-vivo*, as discussed in Section 2.3.1. Hence, a PID controller is implemented in the inner loop to provide a dosage which is a function of the error between the reference dosage (generated by the outer loop control) and the Nutlin present in the cell.

4.1.1 Selection of Attractor Point

The model of p53 as given by (3.1) can be employed to determine the equilibrium point or an attractor point in the four-dimensional state space consisting of the concentrations of p53, Messenger RNA, MDM2, and p53-MDM2 complex. To determine an attractor point, equations in the model (3.1) are solved with their left-hand sides made zero. Suppose we represent the p53 system model (3.1) by a set of nonlinear differential equations

$$\dot{x} = f(x, u), \tag{4.2}$$

where f is a 4×1 nonlinear vector function, u is the control input and x is the 4×1 state vector. The equation 4.2 is numerically solved in MATLAB to find an equilibrium point x^*, that satisfies

$$0 = f(x^*, u^*). \tag{4.3}$$

Since it will be a system of four nonlinear equations, there will be more than one solution. We will go for an attractor or equilibrium point that fulfills the following conditions:

- The attractor point should be stable.
- It should consist of high p53 and low MDM2 concentration.

The stability of an attractor point can be determined by looking at the eigenvalues of the Jacobian of (3.1) with respect to states evaluated at the equilibrium point. If the real part of all eigenvalues is negative, then the equilibrium point is said to be asymptotically stable. The purpose of choosing an equilibrium point with

a higher concentration of p53 and a lower concentration of MDM2 is to aim for a healthy cell.

In the absence of any control input, the physical system has only one equilibrium point, i.e.,

$$x_0 = [17.6 \quad 15.5 \quad 18.3 \quad 90.7]^T. \tag{4.4}$$

This equilibrium point represents the steady-state of the cancerous cells. The eigenvalues of the system for the above equilibrium point are as follows: -198.58, -5.4500, and $-0.3200 \pm 1.1800i$, which clearly shows that the system is stable for this equilibrium point. However, in the presence of control input, there are various equilibrium points depending upon the value of the input.

Using above conditions, the following attractor is found suitable:

$$x^* = [64.0169 \quad 211.3598 \quad 4.9701 \quad 90.318]^T, \tag{4.5}$$

where $u^* = 197.1297$. The eigenvalues for this attractor point are found to be: -3.9756×10^4, -35.87,-7.82 and -0.60. It can be seen that all of the real eigenvalues are negative, hence, representing a stable system.

Once this equilibrium point is determined, then it would be desirable to drive the system (3.1) to this equilibrium point in order to revive p53. The subsequent sections further explain the procedure followed to design the control.

4.1.2 Control Design Procedure

In order to derive the system trajectories towards the equilibrium point (4.5), we need to determine how far is the system from this equilibrium point in the four-dimensional state space. From the system consisting of (3.1), the system states at

any given time t can be defined as

$$x(t) = [x_1 \quad x_2 \quad x_3 \quad x_4]^T. \tag{4.6}$$

The output of the closed loop system is complete state vector $x(t)$, which is fed back to the nonlinear controller. In order to make the model-based control design possible, the following assumptions are considered for the p53 model.

1. All of the state variables are assumed to be measurable,
2. The inter-cellular concentration of Nutlin is available.

4.1.2.1 Outer-loop Design

The difference between actual state vector $x(t)$ and the desired state vector x_{des} is the error to be minimized. Here, x_{des} is equal to the attractor point x^*, defined previously in (4.5). The control objective is to derive the system trajectories to this desired equilibrium point from arbitrary initial trajectories, i.e.

$$e = x(t) - x_{des}, \tag{4.7}$$

Substituting $x(t)$ and x_{des} (from (4.6) and (4.5)) into (4.7) gives

$$e = \begin{bmatrix} e_1 \\ e_2 \\ e_3 \\ e_4 \end{bmatrix} = \begin{bmatrix} x_1 - 64.0169 \\ x_2 - 211.3598 \\ x_3 - 4.9701 \\ x_4 - 90.318 \end{bmatrix}.$$

This e belongs to $\mathbb{R}^4$, taken as a measure of the cell on how far it is from p53 revival. Ideally, we would like this measure to be driven to zero so that the p53 in the cell gets active. This driving of the cell will be achieved by the recommended dosage of Nutlin in the cell termed as n_{ref}. The mechanism for the computation of this variable is elaborated next.

The half of square of the Euclidean norm can be taken as Lyapunov candidate function:

$$E = \frac{1}{2} e^T e. \tag{4.8}$$

Using Lyapunov theory, it is known that the system (3.1) will reach the desired equilibrium i.e., x_{des}, if the derivative of E is negative. The derivative of E can be figured as

$$\dot{E} = e^T \dot{e}, \tag{4.9}$$

which comes out to be

$$\begin{aligned} \dot{E} &= e_1 \dot{x_1} + e_2 \dot{x_2} + e_3 \dot{x_3} + e_4 \dot{x_4} \\ &= e_1(\sigma_p - \alpha x_1 - k_f x_1 x_3 + k_b x_4 + \gamma x_4) + e_2(k_t x_1^2 - \beta x_2) + \\ &\quad e_3(k_{tl} x_2 - k_f x_1 x_3 + k_b x_4 + \delta x_4 - \gamma x_3 - k_m u x_3) + \\ &\quad e_4(k_f x_1 x_3 - k_b x_4 - \delta x_4 - \gamma x_4) \end{aligned} \tag{4.10}$$

For $\dot{E}$ to be negative definite, the reference dosage or the control is chosen as;

$$n_{ref} = \frac{k_1 {e_1}^2 + k_2 {e_2}^2 + k_3 {e_3}^2 + k_4 {e_4}^2 + \varrho}{x_3 \, k_m \, e_3 + k\epsilon}, \tag{4.11}$$

where $k_i \in \mathbb{R}$ and ϱ is given as,

$$\begin{aligned} \varrho &= \sigma_p \, e_1 + k_{tl} \, e_3 \, x_2 - \alpha \, e_1 \, x_1 + \big(- kf \ (e_1 + e_3) \, x_1 - \gamma \, e_3 \big) x_3 + \\ &\quad \big((\delta + kb) \, e_3 + e_1 \ (\gamma + kb) \big) x_4 + \ (k_t x_1^2 - \beta x_2) \, e_2 - \\ &\quad \big(\gamma \, x_4 - (\delta + kb) \, x_4 - kf \, x_1 \, x_3 \big) \, e_4. \end{aligned}$$

This choice of n_{ref} makes $\dot{E} < 0$, which confirms the error convergence to zero.

The expression of the control input n_{ref} in (4.11), is the function of state errors defined in (4.7). It is assumed that the system is away from its desired state initially, so that the denominator does not become zero. Moreover, a term $k\epsilon$ is

added to the denominator of (4.11). where ϵ is a very small number i.e $|\epsilon| \to 0$ used in the simulations to avoid singularity, which can come due to the error e_3 in the denominator of (4.11). Very small error e_3 along with the ϵ makes the denominator of (4.11) too small, in turn making n_{ref} huge. To avoid this problem, the coefficient $k \in \mathbb{R}^+$ can be tuned during the *in silico* trials. If we had any performance issues, then we could have used exponential stability argument to determine n_{ref}.

Owing to the presence of e_3 in the expression for n_{ref}, the system can be taken arbitrarily close to the desired point, i.e in a ball of small radius around the equilibrium point. Once the system is in the ball then the control is made equal to u^* to make it go to the equilibrium point.

4.1.2.2 Inner-loop Design

To maintain n_{ref} in the cell, a negative feedback loop is devised for the PBK dynamics of Nutlin, defined previously by Equations (3.8) and (3.7). The dosage given to the patient should be a function of the error which comprises of the difference between the desired Nutlin concentration and the actual Nutlin concentration present in the cell, as determined by the PBK dynamics stated in (3.8). The error is defined as

$$e_n = n_{ref} - n, \tag{4.12}$$

where n_{ref} is the command generated by the outer loop controller and n is the actual amount of Nutlin present in the cell. On this error, a PID controller is tuned, so that the error goes to a very small value in minimum time. The mathematical expression for the control input (Nutlin dosage D), derived from a PID controller implemented in parallel form is given as:

$$D = K_p e_n + K_i \int e_n dt + K_d \frac{d}{dt} e_n, \tag{4.13}$$

where K_p, K_i and K_d are the proportional, integral and derivative gains of PID controller respectively. The control variable D is composed of three individual

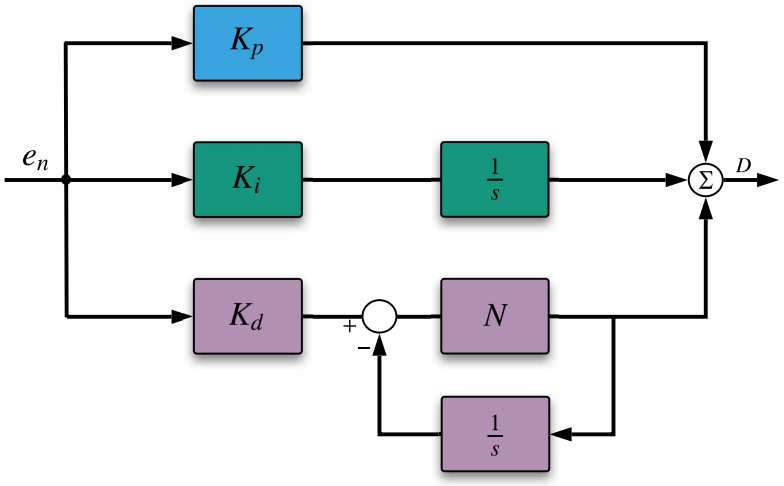

FIGURE 4.2: Structure of PID control with derivative filter for the p53 system

terms: the proportional term (proportional to the error), the integral term (proportional to the integral of the error) and derivative term (proportional to the derivative of the error). The controller in (4.13) can be represented in transfer function form as:

$$C(s) = K_p + \frac{K_i}{s} + K_d\ s. \tag{4.14}$$

The proportional control strives to reduce the error e_n, but mere proportional control is always left with a constant steady-state error. Increasing the proportional gain further increases the oscillations and overshoot of the response. The integral action makes sure that the output is in good agreement with the set-point (n_{ref}) in steady-state. The Proportional Integral (PI) control is used to minimize the error between n_{ref} and n, the objective is to achieve a zero steady-state error. Increasing the integral gain makes the response faster, but also introduces oscillations in the response. The purpose of the derivative control is to improve the overall stability of the inner closed loop. The derivative control term is used to get a smooth response (by minimizing the oscillations) and to speed up the response of the inner loop.

The addition of the derivative term makes the controller transfer function proper. Due to that, any high-frequency signal component in the reference causes the control input to be unreasonably large. Therefore, the controller in (4.14) can

not be implemented in practice. The problem highlighted above can be solved by filtering the derivative action by a first-order low pass filter [85]. The modified structure of the controller (shown in Figure 4.2) can be represented by the following transfer function:

$$C(s) = K_p + \frac{K_i}{s} + K_d \frac{N\,s}{s+N}, \tag{4.15}$$

where N is the filter coefficient, which sets the location of the pole in the derivative filter. The coefficient N should be selected such that it filters out the high-frequency components in the reference, without affecting the dominant dynamics of the controller. The subsequent section illustrates the obtained simulation results for the discussed control strategy.

4.1.3 Results and Discussions

The effectiveness of the proposed control scheme is evaluated by the closed loop simulation tests shown in Figs. 4.3(a) to 4.3(d). The initial value of states is chosen to be $x_0 = [x_{10} \quad x_{20} \quad x_{30} \quad x_{40}]^T = [17 \quad 300 \quad 8 \quad 115]^T$, which represents the cancerous state of a cell [27]. The desired state values, representing an operating point for a healthy cell are defined in (4.5). The design coefficient for the outer loop k, is selected as

$$k = 80, \tag{4.16}$$

and the following set of design parameters are chosen for the inner loop PID controller (by trial and error approach),

$$K_p = 68.3,\ K_i = 34.5,\ K_d = 22.1,\ N = 15.3, \tag{4.17}$$

such that the desired performance specifications are met. It is evident from the simulation results that the concentrations of all the state variables are reaching their desired equilibrium values successfully. The steady state error for all the

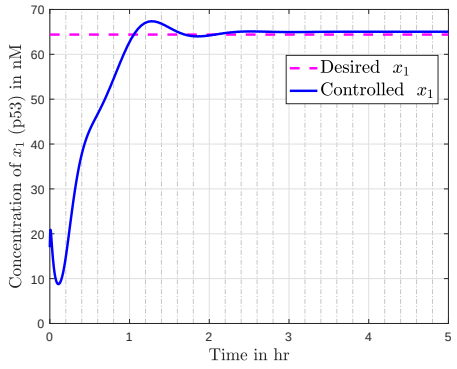

(a) Concentration level of p53, sustained to the required level by the action of Nutlin

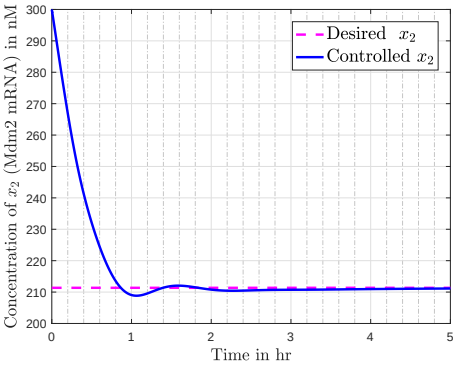

(b) The MDM2 mRNA concentration

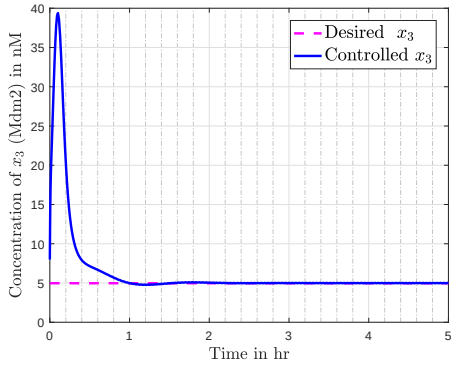

(c) The MDM2 concentration, reduced to a minimal level by the action of Nutlin

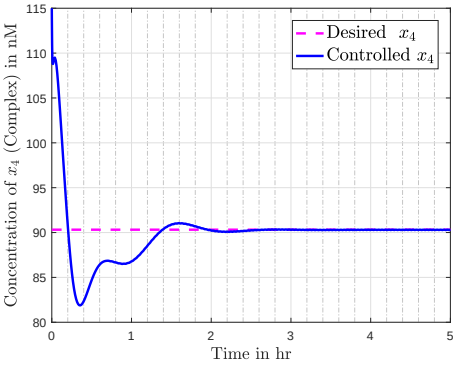

(d) Concentration of the p53-MDM2 Complex

FIGURE 4.3: Comparison of desired and obtained concentrations of the p53 pathway system states

state variables is less than 0.5%, except for x_1, which maintains the steady state value within 1.5% error, nonetheless satisfying the desired design criteria. The convergence time for all the state variables is within two hours, which is reasonable for a slow process like the one we are dealing with. However, this may be further reduced by tuning the gain of controllers as per therapeutic requirement.

The control effort presented in Figure 4.4 drags x_0 to x_{des}. Figure 4.4 also presents a comparison between reference Nutlin n_{ref}, generated by the Lyapunov controller and the actual Nutlin within a cell n, produced by the inner loop PID controller. Keeping in view the PBK dynamics of the drug, the PID controller ensures that the Nutlin inside the cell successfully tracks the reference dosage, as can be seen in Figure 4.4. After passing the initial bump, Nutlin remains around 200 mg/kg which is in accordance with the experimental results conducted by [82, 86, 87],

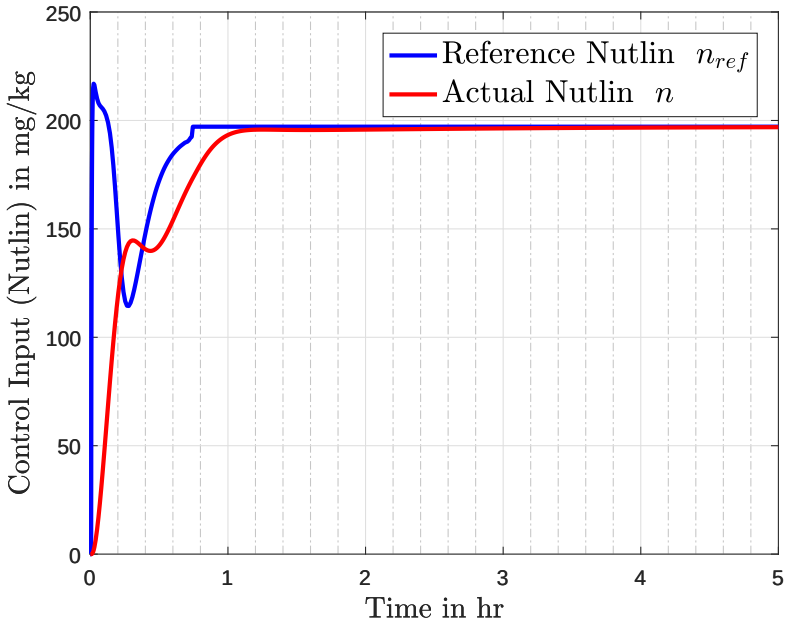

FIGURE 4.4: Comparison of reference Nutlin n_{ref}, generated by Lyapunov controller and actual Nutlin within a cell n, provided by PID controller

where they used intravenous and oral drug delivery in the range of 10 to 400 mg/kg in a various range of intervals. A small downward bump in Nutlin dosage can be seen initially, but after the state x_3 is in the vicinity of x_{3des}, i.e., $||e_3|| < 1$, u takes on the equilibrium input value u^* thereafter.

The control input for the Nutlin PBK dynamics in the inner loop is presented in Figure 4.5. The initial high value is due to the fast inner loop control action. Nevertheless, this can be reduced as per requirements by tuning the PID gains accordingly.

In order to test the robustness performance of the controller, the system is subjected to a vanishing input disturbance ζ (discussed later in Section 5.5). The simulation results are presented in Figure 4.6. By looking at these results, it is evident that states do not stay at the desired level when the system is subjected to disturbance. It show that the current controller does not perform well in case of disturbances. This technique lacks the capability to handle inaccuracies in the model and external disturbances, which are inevitable in the physical systems. Hence, we require a controller that effectively handles the uncertainties.

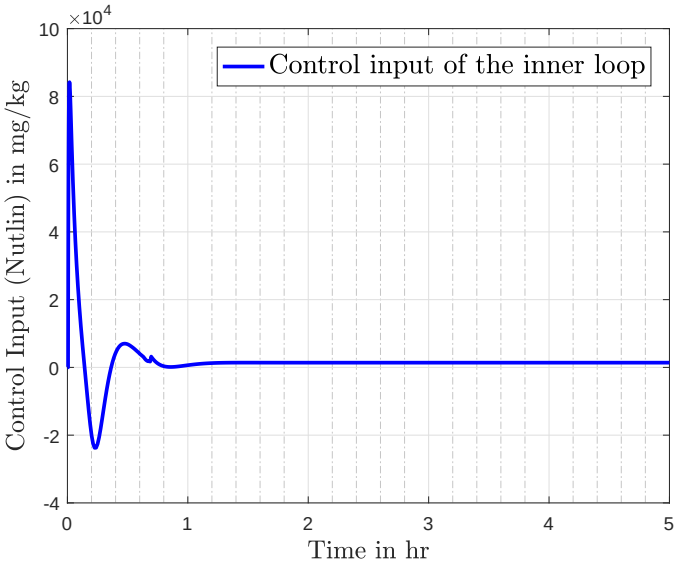

FIGURE 4.5: Control input provided by PID controller to the PBK dynamics

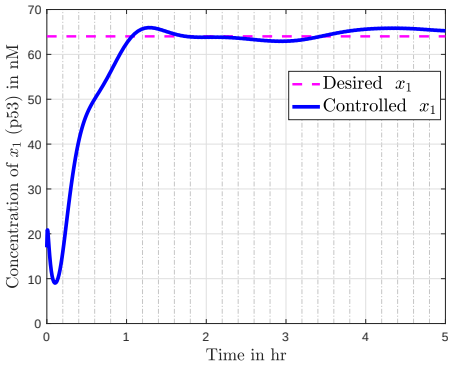

(a) Concentration level of p53

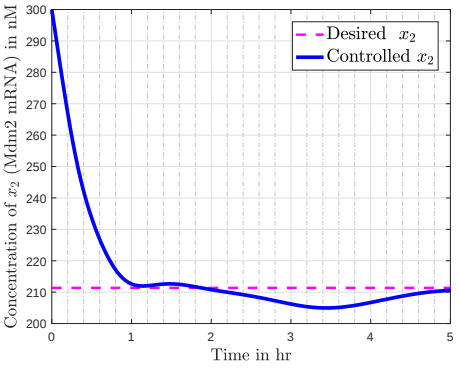

(b) The MDM2 mRNA concentration

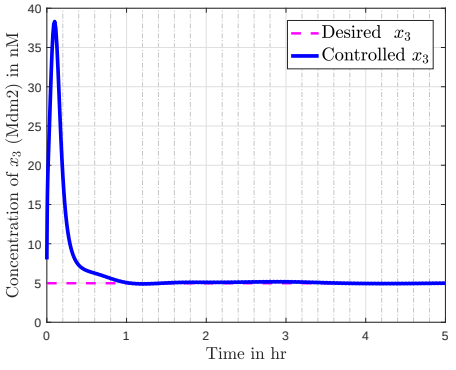

(c) The MDM2 concentration

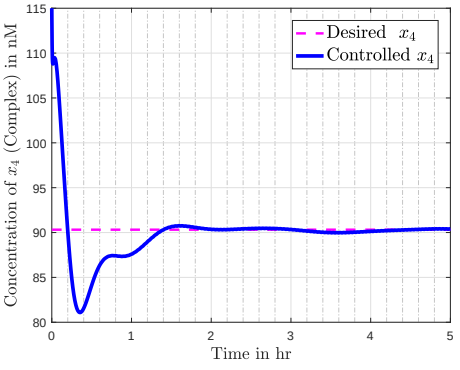

(d) Concentration of the p53-MDM2 Complex

FIGURE 4.6: Robustness performance of the controller for disturbance ζ

Moreover, the above-mentioned technique is based on certain assumptions. Therein, all the state variables and the input drug are considered to be measurable, which is not the case in actual scenarios. Despite the fact that the measurement techniques have largely improved, achieving real-time measurement of the drug concentration inside the cell remains a challenge. Another limitation of this approach is the dependency on the equilibrium point. According to the literature, the required amount of p53 in healthy cells is way more than depicted by the equilibrium point. There is essentially a trade-off between choosing an equilibrium point and having the desired amount of p53 in the cell.

4.2 Summary

In this chapter, the integrated model is used to achieve a drug dosage strategy for the reactivation of wild-type p53. The problem is defined in the control system paradigm where a two-loop feedback control strategy is employed to drag the system trajectories to the attractor point. The outer loop comprises a Lyapunov based nonlinear controller, which determines the required amount of Nutlin i.e the reference dosage. In order to maintain the reference dosage inside the cell, a PID based inner loop controller is devised for the PBK dynamics of Nutlin. The simulation results show that the trajectories are successfully moved to the desired point asymptotically.

The assumptions and limitations of the discussed technique demand for a sophisticated control strategy, which accounts for all the physical issues. Hence, the next chapter presents a sliding mode control based robust technique for the p53 pathway controller design.

Chapter 5

Sliding Mode Controller-Observer Design

The limited control over the selection of the equilibrium point makes it difficult to target for a specific amount of p53 concentration. In the following control strategies, the dependency on the equilibrium point, faced by the previous technique, is removed. The control problem is focused upon directly targeting the level of p53 protein. Furthermore, the issues mentioned for Lyapunov control in the previous chapter demand a more sophisticated control strategy, which is capable of delivering the required performance characteristics, keeping in view all the practical considerations. In the subsequent sections, two variants of a state of the art control technique, Sliding Mode Control (SMC), are employed to design a feedback control system for the p53 pathway. The main issues accompanied by SMC, i.e. chattering and discontinuous control input are handled by employing a modified algorithm based on the theory of dynamic sliding mode control (DSMC). The robustness of the proposed scheme is accessed by introducing parametric uncertainties, measurement noise, and an input disturbance. Moreover, a quantitative comparison is also made between the DSMC and the conventional SMC. The subsequent section presents the basic theory of the SMC technique, which serves as the basis for the SMC based control design for the p53 pathway system.

5.1 Sliding Mode Control

The theory of variable structure control (VSC) was first proposed by Emelyanov and his co-researchers in the early 1950's [88]. The switching control law designed by VSC showed fruitful results in comparison to the existing feedback techniques at that time. Over the years, the sliding mode control (SMC) has proven to be a preferred choice of control design for nonlinear systems operating under the uncertainty conditions. The major advantages include insensitivity to parameter variations and disturbances, which eliminates the need for exact modeling. The discontinuous control action can be easily implemented through pulse width modulation (PWM) switching devices [89, 90]. Owing to these attractive properties, SMC has proven to be a favorable choice in the wide range of engineering applications including electric drives, robotics, ground, and air vehicles and process control.

The basic idea of the SMC is to specify a function of the system states, and design a controller to regulate this function to zero, which in turn will make the system to behave in accordance with the selected parameters. This function is termed as the switching manifold (in the literature it is also called a switching surface, sliding surface or hyperplane). The controller strives to bring the system dynamics to this manifold with the help of a discontinuous control law [89].

The SMC is established in two phases, known as "Reaching phase" and "Sliding phase" [91]. In the reaching phase, the discontinuous control law drives the system dynamics towards the predefined sliding surface. When the system reaches on the sliding surface, the structure of the feedback loop is adaptively altered and the same control law slides the system states towards an equilibrium point along the manifold, this phase is known as "sliding phase" [89]. During the sliding phase, the constrained motion of the SMC is termed as "sliding mode". If some n-dimensional system has m-dimensional control input, then the system in sliding mode evolves with $n - m$ states. This order reduction provides invariance to parametric variations and external disturbances. Besides, the complexity of the system is also reduced, due to the decoupling of system motion into independent

components with lower dimension. The subsequent section includes the design strategy of SMC.

5.1.1 Sliding Mode Control Design Procedure

Consider a nonlinear control affine system

$$\dot{x} = f(x,t) + B(x,t)u \tag{5.1}$$

where $x \in \mathbb{R}^n$ is the system states vector, $f \in \mathbb{R}^n$ is a nonlinear function of the states, $B \in \mathbb{R}^{n\times m}$ is the input matrix and $u \in \mathbb{R}^m$ is the input vector. A set of switching surfaces S is defined as

$$S = \{x \in \mathbb{R}^n : s(x) = [s_1(x), \ldots, s_m(x)]^T\} \tag{5.2}$$

then the traditional SMC design procedure can be partitioned into sub problems of lower dimensions.

5.1.1.1 Switching Surface Design

The switching surface is designed, by keeping in view the desired close loop dynamical properties of the system. The "sliding mode", which is the "motion of the system as it slides along the surface" [92] is defined by

$$s(x) = Gx = 0, \tag{5.3}$$

where G is an $m \times n$ matrix of gradients of sliding variables i.e. $G = \frac{\partial s}{\partial x}$.

Sliding surface design is usually application-specific, e.g. in robotics, the sliding surface is generally $S = Cx$, where C is the gain matrix and x is the state vector. It can also be designed as an error surface e.g. $S = r - y$, where r is the reference

value and y is the controlled output. Moreover, for the systems in canonical form, the surface is chosen as a Hurwitz polynomial, where the surface is a linear function of state variables.

5.1.1.2 Existence of Sliding Mode

This step ensures that the system states converges on the switching surface in finite time. Once the system has acquired the sliding motion, the designed controller should be capable to keep the system in sliding motion in the presence of modeling inaccuracies and external disturbances. This is ensured by setting a condition on the control law known as " reachability condition". General approach is to perform stability analysis in presence of uncertainties. Consider a quadratic type candidate Lyapunov function

$$V(x) = \frac{1}{2}\, s^T(x)\, s(x), \tag{5.4}$$

then the first order time derivative becomes

$$\dot{V}(x) = \frac{1}{2}\, \dot{s}^T(x)\, s(x). \tag{5.5}$$

The switching surface is made attractive if the controller ensures the reachability condition i.e.

$$\dot{s}^T(x)\, s(x) < 0. \tag{5.6}$$

The above condition guarantees the asymptotic convergence of system states to the sliding manifold. However, if the finite time convergence is required, reachability condition is modified to the so-called η-reachability condition [93]

$$\dot{s}^T(x)\, s(x) \leq -\eta\, |s(x)|, \tag{5.7}$$

where η is a positive constant, which ensures that $\dot{V}$ remains negative definite. The inequality in (5.7) guarantees that sliding mode is enforced after a finite time

interval t_s [94], defined by

$$t_s \leq \frac{2\sqrt{V(0)}}{\eta}. \tag{5.8}$$

Hence, the control u, that satisfies the condition in (5.7) will drive the sliding variable $s(x)$ to zero in finite time defined by t_s, and will strive to keep it that way thereafter.

Generally the control law is selected as

$$u = u_{eq} + u_d, \tag{5.9}$$

where u_{eq} is the equivalent control term, taken as a function of system states, found by solving $\dot{s} = G\,f + G\,B\,u_{eq} = 0$, such that it cancels out all the known terms in expression of $\dot{s}$, implying that

$$u_{eq}(x) = -\big[G(x)\,B(x)\big]^{-1}\,G(x)\,f(x). \tag{5.10}$$

Moreover, u_d in (5.9) is the discontinuous term, usually taken as $u_d = -Msign(s)$, where $M \in \mathbb{R}^+$. The discontinuous term ensures finite time convergence to the chosen sliding surface, in presence uncertainties. Moreover, sliding mode is insensitive to external disturbances if it satisfies the so-called "matching condition". The matching condition is satisfied if the disturbance acts exactly in the input channel, or we can say that the disturbance is in the range space of input matrix B.

5.2 Sliding Mode Control of p53 Pathway

The SMC, due to its inherent properties like robustness against model imperfections and order reduction, has been widely used for a variety of nonlinear systems. It tries to bring the system dynamics to a manifold, known as switching surface. This predefined manifold is achieved with the help of a discontinuous control law

[89]. The sliding surface is independent of the modeling uncertainties and disturbances, hence provides the robustness property. In contrast to the Lyapunov based control, which offers asymptotic convergence of the error dynamics, the SMC, due to the inclusion of a discontinuous switching term, ensures finite-time convergence towards the sliding manifold. The next sections illustrate the SMC based, control design procedure for the p53 pathway system.

5.2.1 Problem Formulation

It is desired to design such a control system that maintains the level of the p53 protein at a desired level i.e x_{1d}. The control problem has to be solved in the presence of modeling inaccuracies, measurement noise, and external disturbances. The variation in certain model parameters and a matched input disturbance ζ is included in the model. Therefore the control problem can be rephrased as to achieve a desired constant level of x_1, i.e $x_1 \rightarrow x_{1d}$, in the presence of parametric uncertainties, measurement noise and the input disturbance ζ, while utilizing minimum control input. The maximum allowed control input (drug dosage) is $400mg/kg$. Due to the fact that all state measurements are unavailable, the control design becomes more challenging.

5.2.2 Outline of the Design Procedure

A generic procedure to design an SMC based control system is outlined below;

1. The sliding variable s is selected, such that the establishment of sliding mode leads to the desired properties. In an arbitrary finite dimensional system having n state variables, i.e. $x \in \mathbb{R}^n$, sliding mode is established when $s(x)$ and $\dot{s}(x)$ have opposite signs.

2. A discontinuous control is selected to enforce the sliding mode, i.e. such that $s(x)$ and $\dot{s}(x)$ have opposite signs.

3. Analysis of stability of the zero dynamics.

The complete schematic for the feedback control systems is depicted in Figure 5.1. The controller computes the control input u, depending upon the difference between x_1 and x_{1d}. The measurement time for the available states is quite small as compared to the characteristics time for the proteins, therefore the dynamics of sensors are ignored. Moreover, the actuator dynamics are also not considered.

5.2.3 Selection of the Sliding Variable

The design procedure for the selection of sliding variable s consists of two steps: First the variable x_3 is handled as a fictitious control, represented by a state function x_{3f}, defined by

$$x_{3_f} = \frac{1}{k_f x_1}\Big(\sigma_p - \alpha x_1 + (k_b + \gamma)x_4 + k(x_1 - x_{1d})\Big), \tag{5.11}$$

substituting $x_3 = x_{3f}$ in (3.1), yields

$$\dot{x_1} = -k(x_1 - x_{1d}), \tag{5.12}$$

The solution of (5.12) is given as

$$x_1(t) = x_{1d} + \big(x_1(0) - x_{1d}\big)e^{-kt}. \tag{5.13}$$

For a positive value of k, $x_1 \to x_{1d}$ asymptotically.

The second step employs selection of the real control u such that

$$x_3 = x_{3_f}. \tag{5.14}$$

Therefore, the sliding surface is chosen to be the error between x_3 and x_{3_f} i.e,

$$s = x_3 - x_{3_f}, \tag{5.15}$$

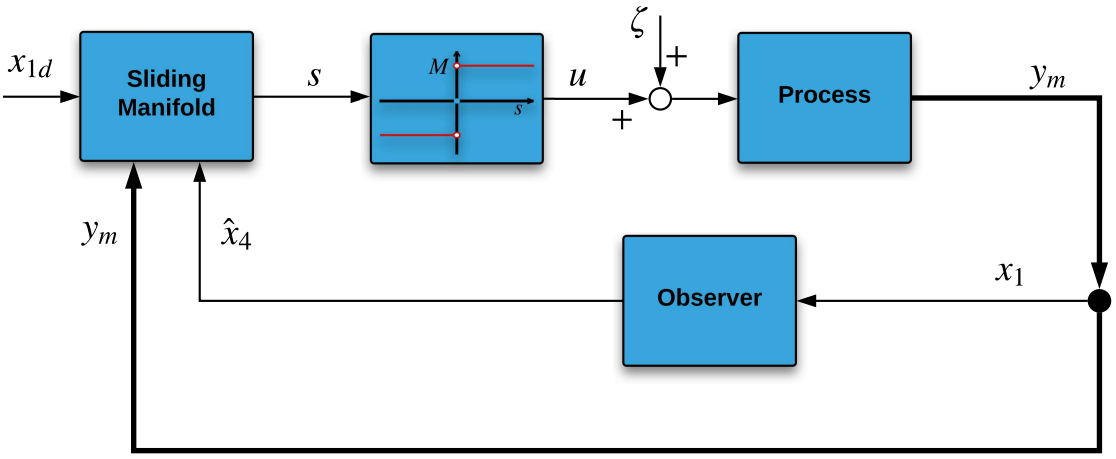

FIGURE 5.1: Sliding mode control implementation scheme-I

and the control input is chosen to be a discontinuous function

$$u = Msign(s), \qquad M > 0. \tag{5.16}$$

The problem in (5.14) is solved should sliding mode occur on $s = 0$.

5.2.4 Existence of Sliding Mode

The existence of sliding mode can be analyzed by taking a positive definite Lyapunov function

$$V = \frac{1}{2}s^2 > 0. \tag{5.17}$$

The time derivative of the Lyapunov function in (5.17) is found to be

$$\dot{V} = s\dot{s}. \tag{5.18}$$

The original system includes parameter variations and external disturbance. To find stability of the original system we consider the time derivative of the perturbed sliding variable i.e., $\dot{s} = \dot{x_3} - \dot{x_{3_f}}$. The expressions $\dot{x_3}$ and $\dot{x_{3_f}}$ can be found from (3.2) and (5.11), respectively.

Consequently (5.18) takes the following form

$$\begin{aligned}\dot{V} &= s\Big(\theta(x,t)+\upsilon(x,t)-k_m x_3 M sign(s)+k_m x_3\zeta\Big),\\ &= s\ -k_m x_3 M|s|+\theta(x,t)+s\,\upsilon(x,t)+s\,k_m x_3\zeta,\\ &\leq -M\bar{x}_3 k_m|s|+|s|\Theta+|s|\Upsilon+|s|\bar{x}_3 k_m\zeta_0,\\ &\leq -|s|\big(M\bar{x}_3 k_m-\Theta-\Upsilon-\bar{x}_3 k_m\zeta_0\big). \end{aligned} \tag{5.19}$$

Where $||\theta(x,t)|| \leq \Theta \in \mathbb{R}^+$ contains the nominal model parameters and $||\upsilon(x,t)|| \leq \Upsilon \in \mathbb{R}^+$ accommodates the parametric uncertainties. The mathematical expressions for θ and Υ are given as

$$\begin{aligned}\theta(x,t) &= \big(k_{tl}x_2-k_f x_1 x_3+(k_b+\delta)x_4-\gamma x_3\big)-\\ &\quad\left(\frac{1}{x_1^2}\big((k_b+\gamma)(x_1\dot{x}_4-x_4\dot{x}_1)-(\sigma_p-kx_{1d})\dot{x}_1\big)\right),\\ \Upsilon(x,t) &= \frac{1}{x_1^2}\Big(\Delta\gamma(x_1\dot{x}_4-x_4\dot{x}_1)-\\ &\quad(\sigma_p-kx_{1d})(\Delta\gamma x_4-\Delta k_f x_1 x_3)\Big).\end{aligned}$$

It is pertinent to mention that x_3 always satisfies the condition $x_3 > \bar{x}_3 > 0$. If the condition $M \geq (\tau+\Theta+\Upsilon+\bar{x}_3 k_m\zeta_0)/(\bar{x}_3 k_m)$ holds, where $\tau \in \mathbb{R}^+$, then time derivative of Lyapunov function becomes

$$\dot{V} \leq -\tau\sqrt{2V}, \tag{5.20}$$

The inequality in (5.20) guarantees that sliding mode($s=0$) is enforced after a finite time interval t_s [94], characterized by

$$t_s \leq \frac{\sqrt{2Vs(0)}}{\tau}. \tag{5.21}$$

After the establishment of sliding mode, $x_3 = x_{3f}$ and eventually $x_1 = x_{1d}$. Hence, the control (5.16), satisfying condition in (5.20) will drive the sliding variable s to zero in finite time, and will strive to keep it that way thereafter.

5.2.5 Stability of the Zero Dynamics

It is mandatory to check stability of zero dynamics after sliding mode has been established. The relative degree r of sliding variable is equal to 1, as u appears in $\dot{s}$. Therefore the system exhibits zero dynamics involving states x_2, x_3 and x_4. Under sliding mode, $s = 0 \Rightarrow x_3 = x_{3f}$, and $x_1 = x_{1d}$. Now the zero dynamics is governed by

$$\begin{aligned} \dot{x_2} &= k_t\, x_{1d}^2 - \beta\, x_2, && (5.22) \\ \dot{x_4} &= k_f\, x_{1d}\, x_{3f} - (k_b + \delta + \gamma)\, x_4, \\ &= k_f x_{1d}\Big(\frac{1}{k_f x_{1d}}\big(\sigma_p - \alpha x_{1d} + (k_b + \gamma)x_4\big)\Big) - (k_b + \delta + \gamma)x_4, \\ &= (\sigma_p - \alpha\, x_{1d}) - \gamma\, x_4. && (5.23) \end{aligned}$$

Equations (5.22) and (5.23) are first order linear differential equations, therefore, the boundedness of zero dynamics is observed analytically for x_2 and x_4. The solutions of the ODEs are given by

$$\begin{aligned} x_2(t) &= \Big(x_2(0) - \Theta_z\Big)e^{-\beta t} + \Theta_z, && (5.24) \\ x_4(t) &= \Big(x_4(0) - \xi\Big)\, e^{-\gamma t} + \xi, && (5.25) \end{aligned}$$

where Θ_z, $\xi \in \mathbb{R}^+$ are given by

$$\begin{aligned} \Theta_z &= \frac{k_t\, x_{1d}^2}{\beta}, \\ \xi &= \frac{\sigma_p - \alpha\, x_{1d}}{\gamma}. \end{aligned}$$

It is obvious from (5.24) and (5.26), that x_2 and x_4 are bounded.

The control law (5.16) directly depends upon variables x_1, x_3 and x_4. The measurements of only x_1 and x_3 are available, hence there is a need to design an observer to estimate the unknown state x_4. The discussion regarding state observer will be presented in Section 5.2.6. Figure 5.1 illustrates the overall implementation scheme

of the sliding mode controller in conjunction with the reduced-order sliding mode observer.

It is worth mentioning that we don't need x_2 in the control explicitly, but to enforce sliding mode, x_2 must be available. Sliding mode existence condition is based on inequality (5.19), therefore it is sufficient to know an upper estimate x_{2max} only. It demonstrates the robustness of sliding mode with respect to unknown state x_2.

5.2.6 Sliding Mode Observer

The state estimation using sliding modes has been conducted for several years. A sliding mode observer (SMO) is based upon the same design theory and reasoning as the sliding mode controllers. An SMO guarantees finite time convergence by the introduction of the sliding mode through a discontinuous output injection term. This injection term induces the sliding mode on the known output error variables. Subsequently, the remaining observer states converge to the actual states according to the equivalent value of the injection in sliding mode [95, 96].

As ideal sliding mode does not exist in practice, hence the trajectories undergo chattering around the manifold. In sliding mode, the discontinuous input can be considered as a combination of an equivalent control term (average value of the discontinuous control) and a high-frequency switching term. When the discontinuous input is passed through a low pass filter, for which the cutoff frequency (f_c) holds the following properties:

1. f_c is less than that of the switching frequency,
2. f_c is greater than the maximum frequency of the system dynamics,

then the high-frequency component is eliminated and remaining is the equivalent control term which is a continuous state function [97]. In other words, the filter should have a sufficiently small time constant (T_c), which allows for the slow components of the motion (equivalent control component) to pass, and should be large enough to block high-frequency components.

Implementation of the control discussed in Section 5.2 requires variable x_4, which can be found by using a reduced order state observer. The observer eliminates the need to estimate the state variables which are readily available. The control input u (5.16) is a function of states x_1, x_3 and x_4. The unknown state variable x_4 can be estimated by enforcing sliding mode on the error term $\tilde{x}_1$, equal to the difference between its real value x_1 and the estimate $\hat{x}_1$. The SMO equation is defined in terms of the time derivative of $\hat{x}_1$, taken as

$$\dot{\hat{x}}_1 = \sigma_p - \alpha x_1 - k_f x_1 x_3 + \mu sign(\tilde{x}_1), \tag{5.26}$$

where

$$\tilde{x}_1 = x_1 - \hat{x}_1, \tag{5.27}$$

The error dynamics of the SMO is obtained by computing the time derivative of $\tilde{x}_1$, given by

$$\begin{aligned} \dot{\tilde{x}}_1 &= \dot{x}_1 - \dot{\hat{x}}_1, \\ &= (k_b + \gamma)x_4 - \mu sign(\tilde{x}_1). \end{aligned} \tag{5.28}$$

The sliding mode with $\tilde{x}_1 = 0$ is established in finite time, if $\mu > |(k_b + \gamma)x_{4_{max}}|$. In the perspective of SMO, the $sign(\tilde{x}_1)$ term is the input, which enforces the sliding mode. The equivalent value of this term can be found after replacing $\tilde{x}_1 = \dot{\tilde{x}}_1 = 0$ in (5.28). Then sliding mode equation is defined by equivalent control [90]

$$\Big(\mu sign(\tilde{x}_1)\Big)_{eq} = (k_b + \gamma)x_4, \tag{5.29}$$

which can be obtained by a low pass filter, having the signal $\mu sign(\tilde{x}_1)$ as its input and z as its output. The transfer function of the first order low pass filter can be presented as;

$$z = \frac{\mu sign(\tilde{x}_1)}{\tau s + 1},$$

which can be written as;

$$\tau\dot{z} + z \;=\; \mu sign(\tilde{x}_1),$$

hence, the output of the filter is the equivalent control part, under the following ideal condition;

$$\lim_{z\to 0} z \;=\; \Big(\mu sign(\tilde{x}_1)\Big)_{eq}.$$

Eventually x_4 can be obtained as

$$x_4 \;=\; \frac{z}{(k_b+\gamma)}. \tag{5.30}$$

Figure 5.1 illustrates the overall implementation scheme of the SMC in conjunction with the reduced-order SMO.

Although the discontinuous control u in (5.16) provides robustness against modeling uncertainties, but the modeling imperfections can result in an unwanted high-frequency motion, called chattering. In the subsequent section, this issue is further discussed and a modification in the existing technique is proposed to suppress the chattering.

5.2.7 The Chattering Problem

In an ideal sliding mode, the control oscillates with infinite frequency and the states reach at $s = 0$ in a finite time. Whereas, ideal systems do not exist in practice, therefore, in the real sliding mode, the trajectories merely reach the vicinity of $s = 0$ and undergo vibrations with finite frequency, usually referred to as the "chattering phenomenon", depicted in Figure 5.2. During this high-frequency motion, the system is unable to maintain its trajectories on the switching manifold, rather they cross it. The chattering is mainly caused by the imperfections in

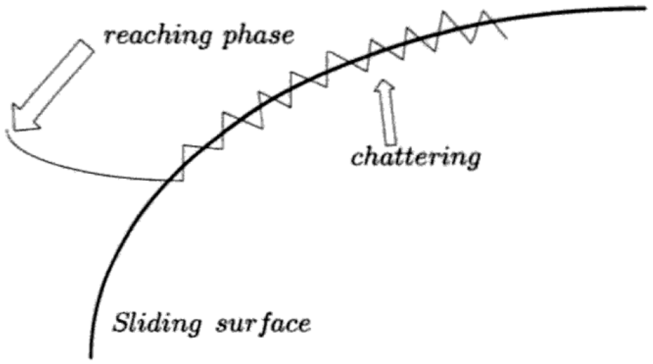

FIGURE 5.2: The chattering phenomenon [92].

switching devices and inherent delays. This involves fast switching of the discontinuous control implementation, which may excite the unmodeled dynamics. The chattering also leads to high wear and tear of the mechanical components being used as actuators for the plant. Moreover, chattering may lead to lower control accuracy.

In many practical control systems, it is desired to avoid the chattering phenomenon by rather providing a continuous/smooth control signal. The requirement of smoothness in control input and the limitations in actuators for biological control processes limit the application of discontinuous SMC. The inherent properties associated with the SMC (i.e., robustness and parameter invariance) can still be exploited by modifying the discontinuous controller. Therefore, many procedures have been evolved in order to reduce or eliminate the chattering, see for example [98]. However, there is generally a trade-off between the chattering reduction and the robustness properties of SMC. Keeping that in mind, many variants of SMC are introduced, one of them is the dynamic sliding mode control (DSMC). In the subsequent section, we discuss the modified control strategy in order to obtain a continuous and smooth control input.

5.3 Dynamic Sliding Mode Control

The smoothness of the control law is an important requirement for controller realization *in silico* due to the physical nature of the biological actuators. Moreover,

overshooting and instantaneous error correction by SMC is typically not applicable in fairly slow biological systems. The requirement of smoothness in control input has limited the application of discontinuous SMC in biological control. The inherent properties associated with the SMC (i.e., robustness and parameter invariance) can still be exploited by shifting the discontinuous *sign* function in the time derivative of the control input. Accordingly, a continuous control input can be acquired and the chattering phenomenon can be sufficiently reduced [99]. The design procedure for DSMC is elaborated in the subsequent section.

5.3.1 Control Design Methodology

Consider a nonlinear system as

$$\begin{aligned} \dot{x}_i &= x_{i+1}, \qquad i = 1, 2, 3, \ldots, n-1, \\ \dot{x}_n &= f(x) + g(x)u + d(t), \\ y &= x_i. \end{aligned} \tag{5.31}$$

Where $x \in \mathbb{R}^n$ is the states vector, y is the output, $f(x)$ and $g(x)$ are some known smooth functions, and $d(t)$ is an uncertainty with $|d(t)| \leq D_0$, $|\dot{d}(t)| \leq D$. The tracking error and the switching function are respectively defined as

$$e = y - y_r, \tag{5.32}$$

$$s = \alpha e + \dot{e}, \tag{5.33}$$

where y_d is the desired output and $\alpha \in \mathbb{R}^+$. The sliding motion i.e. $s = \dot{s} = 0$ is governed by $\dot{e} = -\alpha\, e$. The positive values of the control parameter α guarantees that $e \to 0$ when $t \to \infty$, moreover, the rate of convergence is also governed by choice of c. Subsequently, the time derivative of the switching surface becomes

$$\dot{s} = \alpha\dot{e} + \ddot{e} = f(x) + g(x)u + d(t) + \ddot{y}_d + \alpha\dot{e} \tag{5.34}$$

The desired trajectory tracking for the output is achieved with the choice of sliding function proposed in (5.33). A new dynamic sliding manifold σ is defined in terms of the sliding manifold s. i.e.

$$\sigma = \dot{s} + \lambda s, \tag{5.35}$$

which can be considered as a filtered version of s. Here, the gain $\lambda \in \mathbb{R}^+$, ensures a vanishing tracking error i.e. $\sigma = 0 \implies \dot{s} = -\lambda s$, hence, $e \to 0$ and $\dot{e} \to 0$.

5.3.2 Stability Analysis

Consider a quadratic type candidate Lyapunov function of the form

$$V(\sigma) = \frac{1}{2}\sigma^2 > 0, \quad \forall \sigma \neq 0. \tag{5.36}$$

then the first order time derivative becomes

$$\dot{V}(\sigma) = \dot{\sigma}\sigma. \tag{5.37}$$

For asymptotic stability, the reaching condition must be satisfied, i.e., $\dot{V}(\sigma) < 0$, for $\sigma \neq 0$. Moreover, the finite time convergence of the sliding surface can be achieved if $\dot{V}$ satisfies η-reachability condition [93] i.e.,

$$\dot{V}(\sigma) = \dot{\sigma}\,\sigma \leq -\eta\,|\sigma|, \tag{5.38}$$

where η is a positive constant, which ensures that $\dot{V}(\sigma)$ remains negative definite. The inequality in (5.38) guarantees that sliding mode is enforced after a finite time interval t_s [94], defined by

$$t_s \leq \frac{2\sqrt{V(0)}}{\eta}. \tag{5.39}$$

Hence, the control u, that satisfies the condition in (5.38) will drive the sliding variable σ to zero in finite time defined by t_s, and will strive to keep it at sliding

surface thereafter. The corresponding control law can be selected in the form of derivative of input u i.e.,

$$\dot{u} = \nu = \eta sign(\sigma). \tag{5.40}$$

It is evident that the switching term only effects the first time derivative of the the control input. The injection of the input to the system is done after an integration, which leads to continuous and smooth control input, hence, the chattering phenomenon is suppressed.

5.4 DSMC Control Algorithm for p53 Pathway

As the control input cannot be discontinuous so the discontinuous *sign* function is shifted in the time derivative of the control input. The modified technique is inspired by dynamic sliding mode control (DSMC), which provides a continuous control input along with the inherent properties of SMC. A new sliding variable is proposed, which shifts the discontinuous function (5.16) into the first order time derivative of the control input. The desired trajectory tracking for the output is achieved with the choice of sliding function proposed in (5.15).

A new sliding manifold σ is defined in terms of the sliding manifold s. i.e.

$$\sigma \quad = \quad \dot{s} + \lambda s, \tag{5.41}$$

where s is given by (5.15), and $\dot{s}$ is defined by

$$\dot{s} \quad = \quad \theta(x,t) + \upsilon(x,t) - k_m x_3 M sign(s) - k_m x_3 \zeta. \tag{5.42}$$

The dynamics of the sliding mode ($\sigma = 0$) is governed by

$$\dot{s} + \lambda s = 0, \tag{5.43}$$

where $\lambda > 0$ defines convergence rate of s.

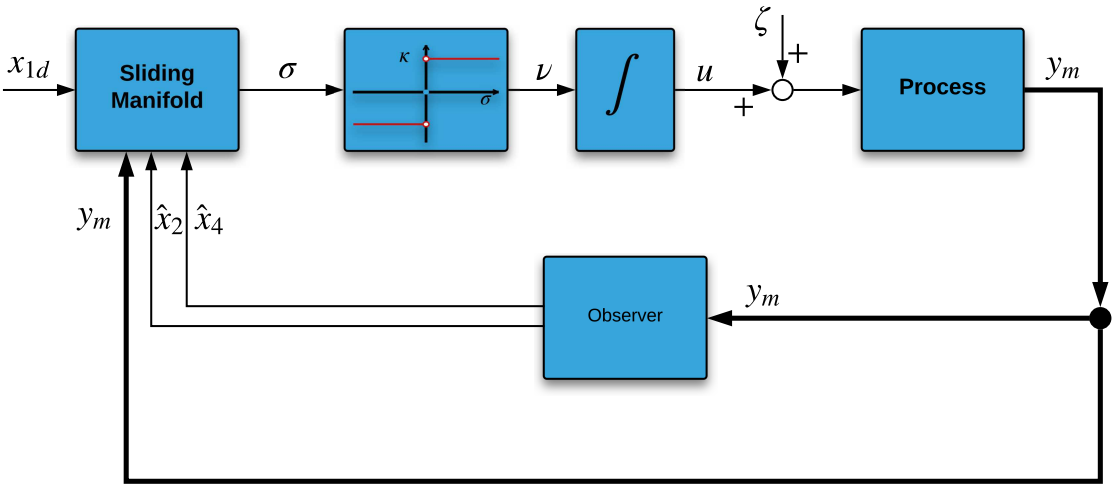

FIGURE 5.3: Control implementation scheme-II

The tracking error vanishes under the sliding mode i.e. $\sigma = 0 \implies s = 0$, then $x_3 = x_{3f}$, and $x_1 = x_{1d}$. This new sliding surface can be considered as a filtered version of s, with $\dot{u} = \nu$, where

$$\nu = \kappa sign(\sigma). \tag{5.44}$$

The complete implementation scheme with the modified controller is presented in Figure 5.3.

5.4.1 Existence of Sliding Mode

The existence of the sliding mode for the modified control design is also analyzed by taking a positive definite Lyapunov function

$$V(\sigma) = \frac{1}{2}\sigma^2 > 0, \tag{5.45}$$

The time derivative of the Lyapunov function (5.45) is computed as

$$\dot{V} = \sigma\dot{\sigma}. \tag{5.46}$$

By considering the parametric perturbations and the disturbance, the time derivative of sliding variable can be found from (3.2) and (5.41). Consequently (5.46) takes the following form

$$\begin{aligned}
\dot{V} &= \sigma\left(\Omega(x,t,u) - k_m\, x_3(\dot{u} - \dot{\zeta}) + \Psi(x,t)\right),\\
\dot{V} &= -\kappa\, k_m\, x_3 \sigma\, sign(\sigma) + \sigma\, \Omega(x,t,u) + \sigma\, k_m\, x_3 \dot{\zeta} + \sigma\, \Psi(x,t),\\
\dot{V} &\leq -\kappa\, k_m\, \bar{x}_3 |\sigma| + |\sigma|\, \Omega_0 + |\sigma|\, k_m \bar{x}_3 \psi_0 + |\sigma|\, \Psi_0,\\
\dot{V} &\leq -|\sigma|\big(\kappa\, k_m\, \bar{x}_3 - \Omega_0 - k_m\, \bar{x}_3 \psi_0 - \Psi_0\big).
\end{aligned} \tag{5.47}$$

Where the function $||\Omega(x,t,u)|| \leq \Omega_0 \in \mathbb{R}^+$ contains the nominal model parameters and is defined as

$$\begin{aligned}
\Omega(x,t,u) &= \frac{S_1 - S_2\, x_1\, \dot{x_1} - S_3\, {x_1}^2 - S_4\, {x_1}^2}{k_f\, {x_1}^3}\\
S_1 &= -N\, x_1(2\, k_t\, x_1\, \dot{x_1} - \beta\, x_2) + (O\, x_4 + 2\, k\, x_{1des} - 2\, \sigma)\, {\dot{x_1}}^2\\
S_2 &= O\, \dot{x_4} + {x_1}^2\, x_3\, {k_f}^2 + \lambda\, N\\
S_3 &= k_f\, x_1\, (P + \lambda\, Q) + \big(-k_f\, (\delta + k_b)\, x_1 + \lambda\, (\gamma + k_b)\big)\dot{x_4}\\
S_4 &= (\gamma + k_b)\left(k_f(x_1\, \dot{x_3} + \dot{x_1}\, x_3) - (k_b + \delta + \sigma)\dot{x_4}\right)
\end{aligned}$$

where,

$$\begin{aligned}
N &= k\, x_{1des} - (k_b + \gamma)\, x_4 - \sigma\\
O &= -2\, (\gamma + k_b)\\
P &= (k_m\, u + k_f\, x_1 + \gamma)\, \dot{x_3} - k_{tl}\, \dot{x_2}\\
Q &= k_f\, x_1 x_3 - (\delta + k_b)\, x_4 + (k_m\, u + \gamma)\, x_3 - k_{tl}\, x_2
\end{aligned}$$

and $||\Psi(x,t)|| \leq \Psi_0 \in \mathbb{R}^+$ accommodates the parametric uncertainties.

The sliding mode can be enforced and reachability condition ($\dot{V} \leq 0$) can be achieved by selecting a discontinuous controller gain $\kappa \geq (\epsilon + \Omega_0 - k_m\, \bar{x}_3 \psi_0 + \Psi_0)/(k_m\, \bar{x}_3)$, where $\epsilon \in \mathbb{R}^+$.

The time derivative of V becomes

$$\dot{V} \leq -\sqrt{2V}\epsilon, \tag{5.48}$$

and the system trajectories will converge to the desired state within finite time t_s, defined by

$$t_s \leq \frac{\sqrt{2V\sigma(0)}}{\epsilon}. \tag{5.49}$$

The new sliding variable σ (5.41), associated with the DSMC, requires the states x_2 and x_4. The estimation of the x_4 has been discussed in Section 5.2.6, whereas, the reconstruction of x_2 is discussed in the subsequent section.

5.4.2 Sliding Mode Observer

Figure 5.3 represents the complete implementation scheme for the modified controller accompanied by the observer. The estimation of x_2 is carried out in a similar way as the reconstruction of x_4 has been performed. Here, the sliding mode is enforced in the manifold $\tilde{x}_3 = x_3 - \hat{x}_3$. The structure of the reduced order SMO is

$$\dot{\hat{x}}_3 = (k_b + \delta)\, x_4 - k_f x_1 x_3 - (\gamma + k_m u)x_3 + \vartheta sign(\tilde{x}_3). \tag{5.50}$$

It is worth mentioning that x_4 is used instead of $\hat{x}_4$ (estimated in Section 5.2.6) in (5.50). By selecting a suitable discontinuous gain μ, it has been ensured that x_4 is already estimated during the estimation of x_2. From (5.26) it can be seen that the system trajectories reach the sliding manifold $\tilde{x}_1 = 0$ in finite time ts_1, which is inversely proportional to the discontinuous gain μ [94]. Afterwards, x_4 is estimated by simply applying a low pass filter, as in (5.30). Similarly, the system trajectories in (5.50) reach the sliding manifold $\tilde{x}_3 = 0$ in finite time ts_2, depending upon the discontinuous gain ϑ. The discontinuous gain $\mu >> \vartheta \implies ts_1 << ts_2$, hence,

the sliding manifold $\tilde{x}_1 = 0$ is achieved much faster than the manifold $\tilde{x}_3 = 0$. Consequently, during the estimation of the x_2, the state x_4 is already estimated. Now, the error dynamics of the SMO is obtained by computing the time derivative of $\tilde{x}_3$, which is given by

$$\begin{aligned} \dot{\tilde{x}}_3 &= \dot{x_3} - \dot{\hat{x}}_3, \\ &= k_{tl}x_2 - \vartheta sign(\tilde{x}_3). \end{aligned} \tag{5.51}$$

The sliding mode is established if $\vartheta > k_{tl}||x_2||$, and the sliding mode equation is defined in terms of the equivalent control

$$\Big(\vartheta sign(\tilde{x}_3)\Big)_{eq} = k_{tl}x_2,$$

which can be obtained by employing a low pass filter, characterized by

$$\begin{aligned} \tau\dot{z}_2 + z_2 &= \vartheta sign(\tilde{x}_3), \\ \lim_{z_2 \to 0} z_2 &= \Big(\vartheta sign(\tilde{x}_3)\Big)_{eq}. \end{aligned} \tag{5.52}$$

Consequently, x_2 is determined as

$$x_2 = \frac{z_2}{k_{tl}}. \tag{5.53}$$

It is worth mentioning that there is no need to estimate x_2 if $\dot{s}$ is obtained by a differentiator.

5.5 Results and Discussions

In this section, a thorough simulation analysis for the sliding mode controller and observer pair is described for the regulation of p53 protein. Moreover, a comparison between the conventional SMC and DSMC techniques is also presented. It is worth mentioning that for a fair comparison between both techniques, the discontinuous gains (M and κ) are kept identical. Furthermore, the design parameter λ in the

case of DSMC is chosen such that the s in (5.43) converges in minimum time. For simulations of SMC and DSMC, the design parameters are selected as

$$M = 90,\ \kappa = 10,\ \lambda = 100.$$

Moreover, the design parameters for SMO are chosen as

$$\mu = 2000,\ \vartheta = 50.$$

The challenges faced while implementation of these feedback control techniques for biological systems are catered by a rigorous simulation analysis in presence of the practical issues.

A major challenge while developing computational models for complex biological systems is the existence of multiple free parameters. The dynamic behavior of the model is often highly dependent upon these parameters. Although high accuracy methods for discovering interactions are well developed, accurate methods for measurement of parameters are still limited [100]. Traditionally these parameters are estimated using regression techniques, by optimizing the consensus between available data and the model. The parameters estimated using *in-vitro* measurements can lead towards inaccuracies due to differences in *in-vitro* and *in-vivo* conditions. Moreover, the amount of measured data is usually limited due to expensive and time-consuming techniques. Consequently, these approaches often yield parametric uncertainties. For the p53 model discussed in [27], most of the parameters mentioned in Table 3.1 are constrained however, the parameters k_f, δ and γ can vary in accordance with the the environmental conditions, application of different stresses, and due to cell-cell variability. In order to study the robustness property of the sliding mode control for the p53 pathway, 20% parametric uncertainties are introduced in the nominal parameters. The uncertain parameters are listed in Table 5.1. It is worth mentioning that the controller and estimator contain the nominal system parameters.

A matched input disturbance ζ is also considered to test robustness. Here, ζ

is the disturbance, faced by cellular structure due to intrinsic noise, unwanted interference from neighboring pathways, undesirable signals from neighboring cells and environmental stresses [101]. All the above effects are lumped together to form a single disturbance, which indicates the loss in the amount of the drug Nutlin. Due to the fact that the exact function of disturbance is unknown, a hypothetical profile is assumed. This profile follows the time profile of a typical drug concentration in the human body (in the blood) following an oral delivery [102]. The time profile for the vanishing disturbance is shown in Figure 5.4. Moreover, the effect of measurement noise has also been incorporated. It is assumed that both the measurements from the sensors i.e., x_1 and x_3 are noisy, and the average error in each measurement is 1%. In this regard, an additive white Gaussian noise (AWGN) with zero mean and a variance of 1×10^{-4} is added in each measurement of the p53 plant. The robustness of the proposed control scheme is assessed by introducing parametric uncertainties, external disturbance and sensor noise simultaneously.

According to different studies conducted on cancerous cells in literature, it is well noted that in normal healthy cells concentration of p53 (x_1) is around 400 nanomoles (nM). In cancerous cells, p53 is prohibited to raise its level so it remains in a lower concentration state. In the simulations x_1 is initialized for a case of cancerous cell i.e $17nM$ [27], and desired concentration of p53 (x_{1d}) is set to 400 nM in the controller. It is also evident from the literature that sustained p53 concentration is possible only if MDM2 concentration is kept low. The designed controller strategy ensures a sustained high level of p53 (Figure 5.5) and lower concentration of MDM2 (Figure 5.6). It is evident from Figure 5.5 that an excellent tracking behavior of the output (p53) is obtained, level of the p53 protein rises quickly after application of controller and maintains its desired value at steady

TABLE 5.1: Parameters subjected to variations

Parameter	Nominal Value	Actual Value	Unit
γ	0.2	0.24	hr^{-1}
δ	11	13.2	hr^{-1}
k_f	5.1428	6.168	$nM^{-1}hr^{-1}$

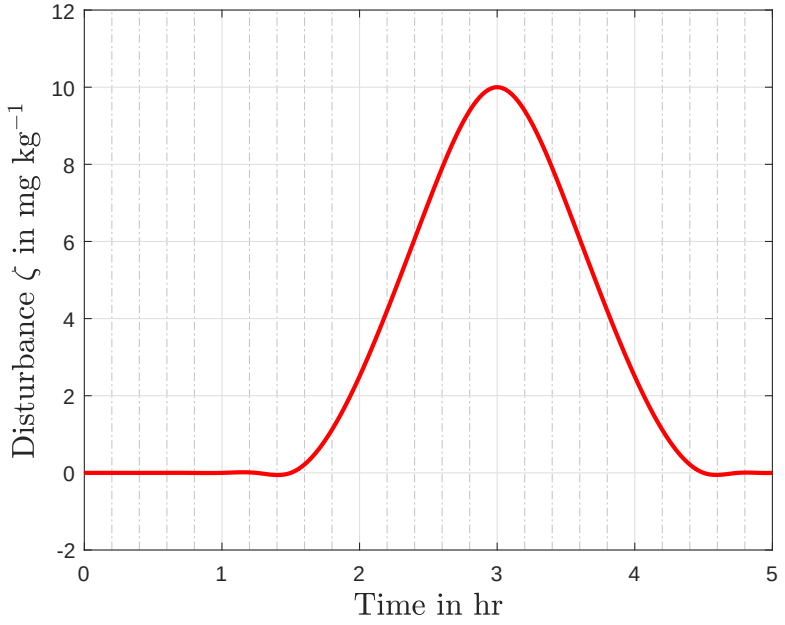

FIGURE 5.4: Time profile of the disturbance

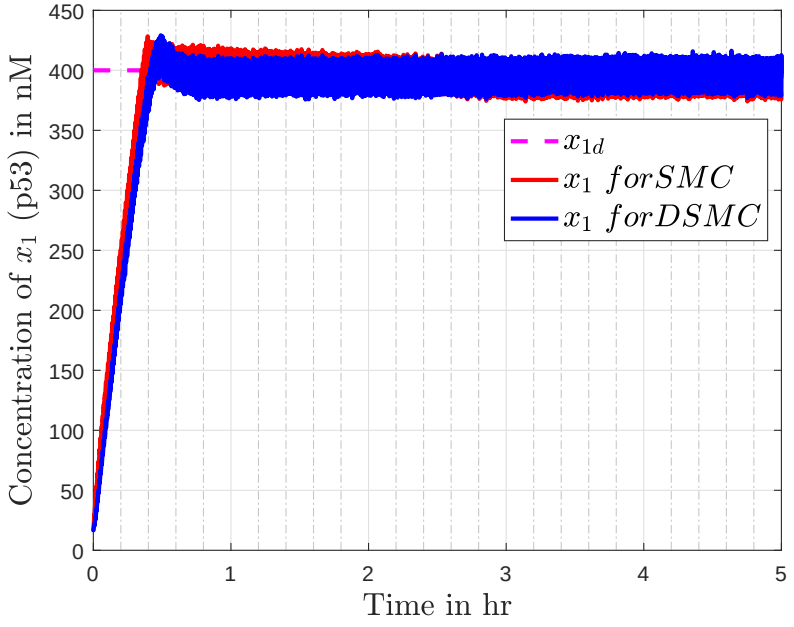

FIGURE 5.5: Output of the p53 pathway for both controllers

state. The results show that by the action of the chemotherapy drug Nutlin, MDM2 is blocked to interact with p53. Therefore, the p53 protein is able to raise its concentration to the desired level.

Figure 5.5 compares the simulation results for x_1, obtained from both SMC and

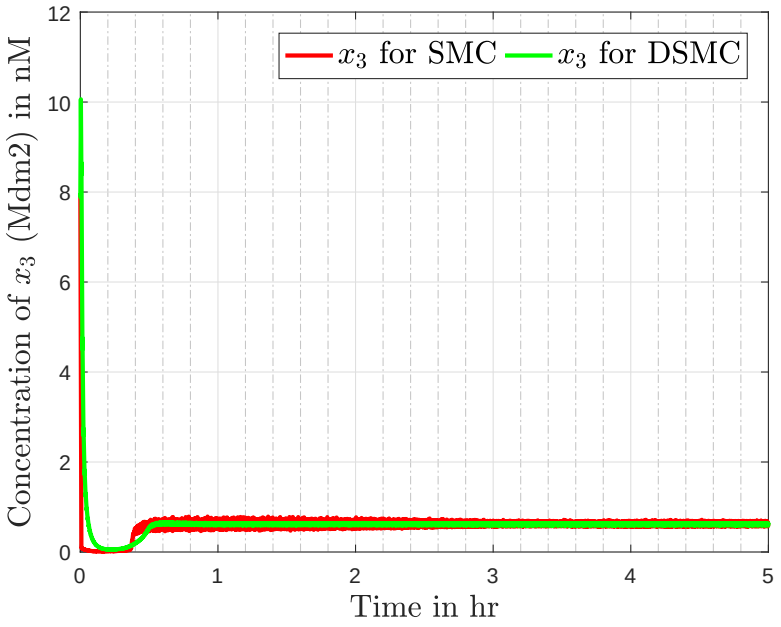

FIGURE 5.6: Concentration of MDM2 for both controller

DSMC. As can be seen in Figure, x_1 reaches the desired value in 45 minutes for SMC, whereas, it takes 60 minutes to reach for DSMC. It is worth mentioning that these results are far superior as compared to the results obtained through Lyapunov based technique, presented in Chapter 4, Figure 4.3. Where the settling time for p53 was about 2 hours.

Figure 5.6 represents the concentration of MDM2, and compare the simulation results obtained by SMC and DSMC. It is observed that MDM2 is quite smooth in the case of DSMC as compared to the SMC, due to the effect of continuous control. The continuous control introduces a small overshoot in the output and slightly increases the settling time, but that all comes with the advantage of chattering reduction in the system. The corresponding tracking error ($e = x_1 - x_{1d}$) in the case of SMC and DSMC is depicted in Figure 5.7.

The control action by the ideal sliding mode is not suitable for real-time applications due to excessive chattering. One solution is to approximate the *sign* function with a saturation function, named as "the boundary layer solution". The idea is to replace the discontinuous switching action with a continuous function

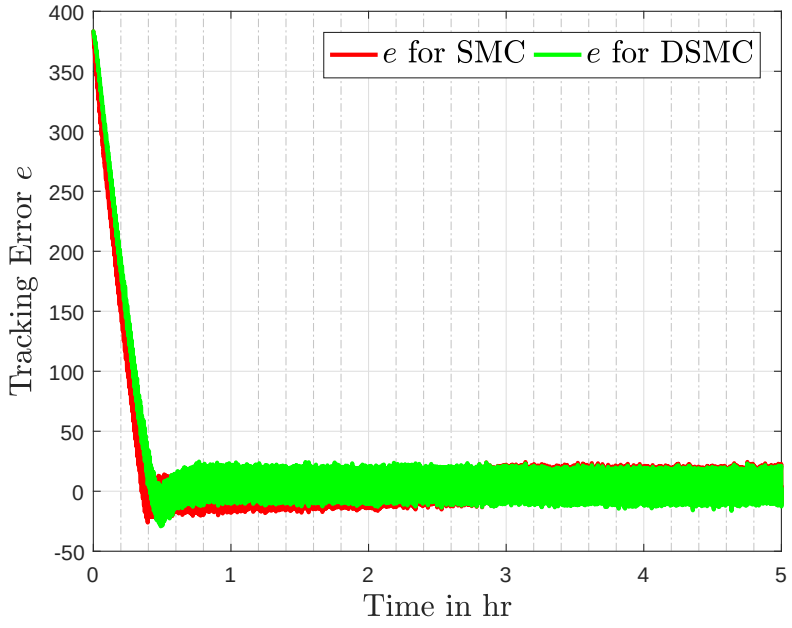

FIGURE 5.7: Tracking Error e for SMC and DSMC

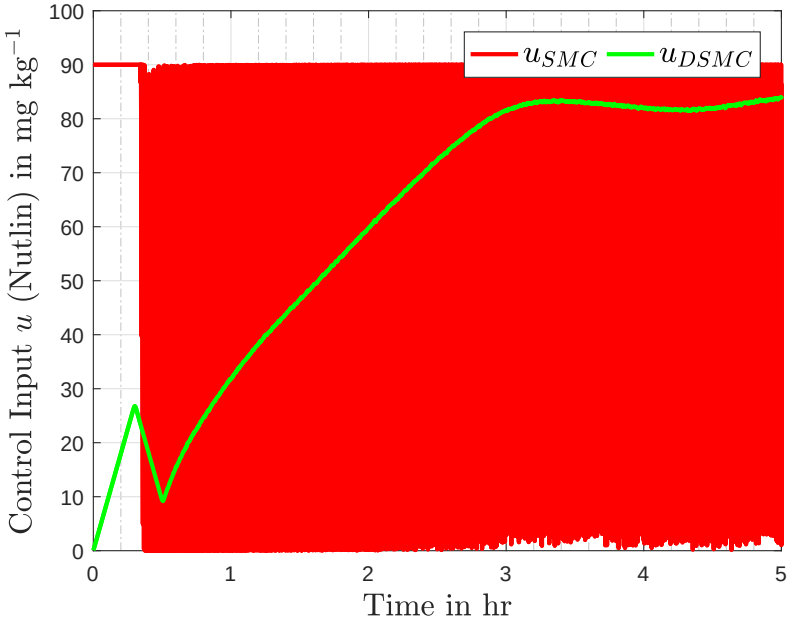

FIGURE 5.8: Control Input (Nutlin) comparison for both controllers

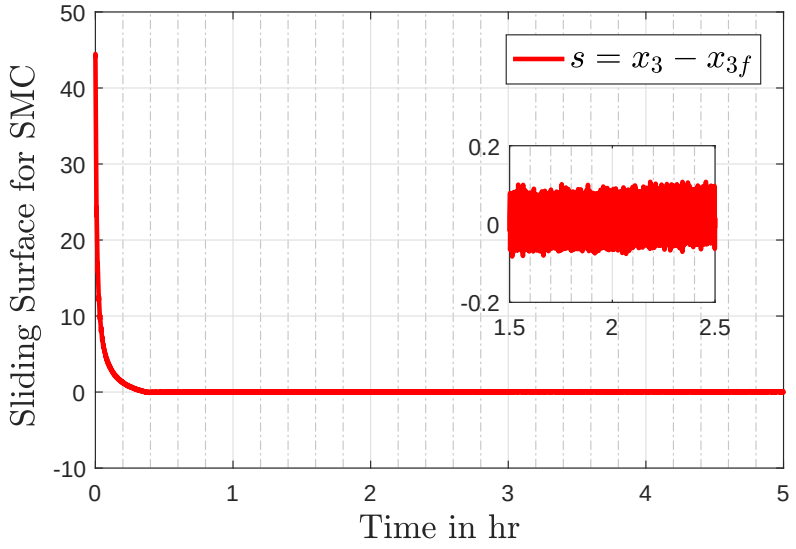

FIGURE 5.9: Sliding Surface in case of SMC

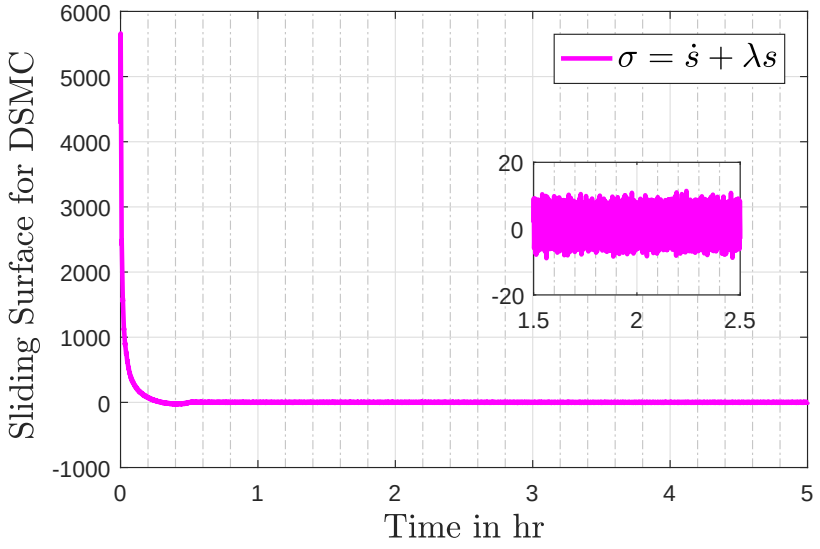

FIGURE 5.10: Sliding Surface in case of DSMC

i.e., $tanh(s/w)$, where w defines the width of the boundary. After the replacement, the system trajectories are confined to the vicinity of the sliding surface rather exactly at $s = 0$, as was the case in ideal sliding mode. The major problem with this approach is that it is not guaranteed that the trajectories converge to zero. Hence, it can be said that the robustness of the SMC is compromised. This issue can be resolved by taking a very small width of the layer, which will retain the robustness performance of the controller as well as a pure discontinuous input can be avoided. for the SMC, we have chosen the width of the boundary layer as

$w = 0.02$.

Figure 5.8 compares the discontinuous control input generated by first-order SMC and the control input provided by the modified control, which is smooth as compared to its counterpart. The smoothness of input is attributed to the use of the discontinuous term in first-order time derivative of the control input. It can be observed that the control effort remains under 90 mg/kg for SMC and 85 mg/kg for DSMC, which is in accordance with the upper bound i.e 400 mg/kg, which is obtained by carrying out experiments by the authors in [82]. One of the design objectives in controlled dosage administration is to reduce the amount of total administered drug. By looking at the above drug profiles and the profile generated by the Lyapunov based control in Figure 4.4 (which remains around 200 mg/kg), it can be easily concluded that the control effort is much reduced in the case of the sliding mode techniques.

The sliding variables s and σ, for the conventional SMC and the DSMC, are shown in Figures 5.9 and 5.10 respectively. In the reaching phase ($s \neq 0$), the controller drags x_3 towards x_{3f} and during the sliding motion ($s = 0$), the design of s keeps the tracking error e zero, consequently the output x_1 attains its desired value x_{1d}. The chattering phenomenon can also be seen in the zoomed version of Figures 5.9 and 5.10.

A quantitative analysis is also carried out to evaluate and compare the performance of DSMC with the conventional SMC. The performance criteria to measure the error i.e. root-mean-square error (RMSE), is computed by

$$RMSE = \sqrt{\frac{1}{N_s}\sum_{i=1}^{N_s} e^2(i)}, \tag{5.54}$$

where N_s is the number of total time samples. Since the aim of the model-based control design is to track a desired level of p53 protein, the error function in RMSE is expressed as

$$e(i) = x_1(i) - x_{1d}(i). \tag{5.55}$$

TABLE 5.2: $RMSE$ and P_{avg} of different controllers

Controller	$RMSE\ (nM)$	$P_{avg}\ (mg/kg)^2$
SMC	56.3273	6.030×10^3
DSMC	62.9805	4.286×10^3

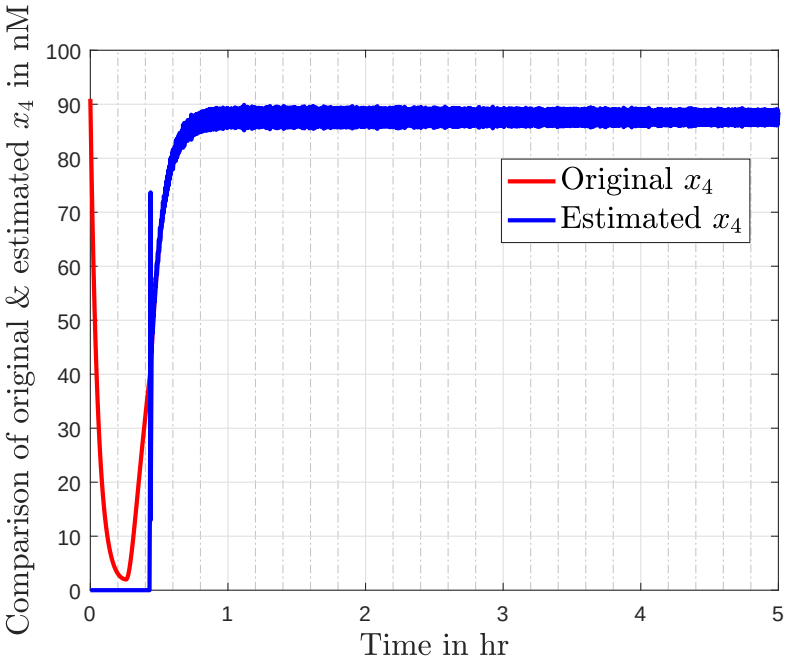

FIGURE 5.11: Reconstruction of state x_4 in case of control scheme I

Furthermore, the average power of the both control signals, defined by

$$P_{avg} = \frac{1}{N_s} \sum_{i=1}^{N_s} u^2(i) \tag{5.56}$$

evaluates the control effort efficiency. The $RMSE$ and P_{avg} for both the controllers are given in Table 5.2. The comparison shows that conventional SMC has slightly better tracking performance than DSMC, but that comes at the cost of higher control energy consumption and discontinuous control input.

In order to study the estimation performance of the observer, it is required to initialize plant and observer using different initial conditions. Figure 5.11 depicts comparison of original state (x_4) with the estimated one ($\hat{x}_4$) in case of control scheme I (Conventional SMC). It can be noted that after an initial deviation, $\hat{x}_4$ coincides with the original state for all future time. Due to the high-frequency

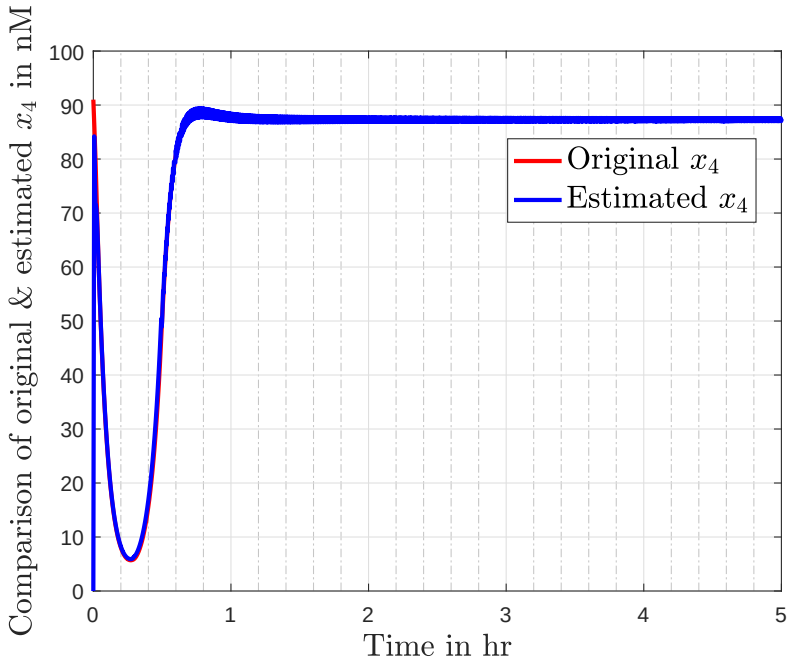

FIGURE 5.12: Reconstruction of state x_4 in case of control scheme II

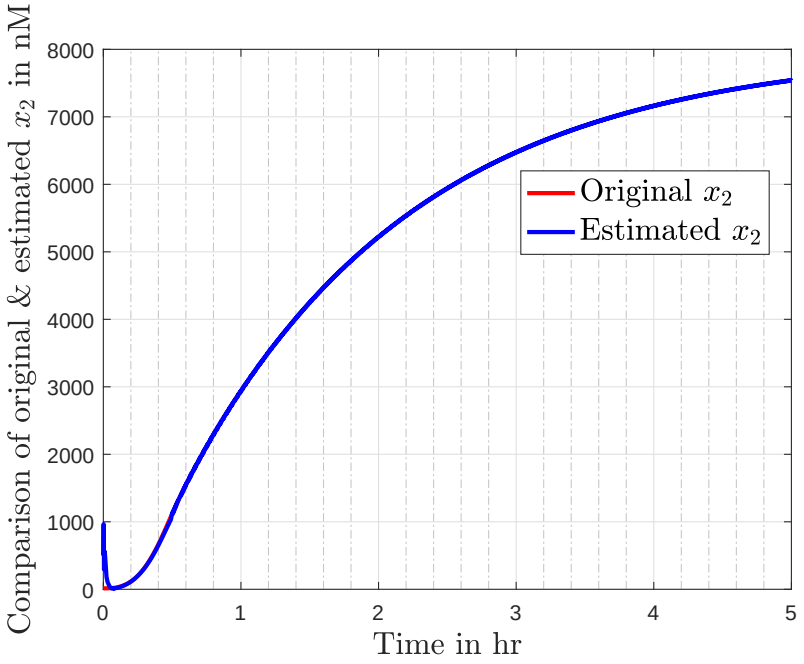

FIGURE 5.13: Reconstruction of state x_2

oscillations in control input, a large chattering is visible in the MDM2 protein (Figure 5.6) as well as in the estimate of x_4 (Figure 5.11).

Figure 5.12 represents the comparison of the original state (x_4) with the estimated state ($\hat{x}_4$) in the case of the control scheme II (DSMC). The chattering reduction in

control input and states enhances the reconstruction performance of the observer, as can be seen in the estimate of x_4 in Figure 5.12. After a negligible initial deviation, the estimate converges to the original value quickly and remains intact for all future time. Figure 5.13 depicts comparison of original state (x_2) with the estimated one ($\hat{x}_2$) in case of the modified observer for control scheme II (DSMC). It is evident that the estimate converges to the original estimates in a finite time and stays alongside afterward.

5.6 Summary

This chapter has addressed a sliding mode control (SMC) based robust non-linear technique for the drug dosage design of the control-oriented p53 model. In the control problem, the drug Nutlin is considered as the control input to revive p53 protein to the desired concentration level. Simulation tests are performed to evaluate the effectiveness of the control scheme, which shows promising results but with the issue of undesirable high-frequency chattering. Hence, another variant of SMC i.e. dynamic sliding mode control (DSMC) is also designed to reduce chattering and obtain a smooth control signal. The modified control leads to a decent trajectory tracking while guaranteeing smooth control actions. Furthermore, to make the model-based control design possible, the unknown states of the system are estimated using equivalent control based, reduced-order sliding mode observer (SMO). The robustness of the proposed scheme is accessed by introducing parametric uncertainties, measurement noise, and an input disturbance. The effectiveness of the proposed control scheme is witnessed by performing *in-silico* trials, which show that the SMC based techniques successfully maintain the desired concentration levels in the presence of uncertainties. Moreover, a quantitative comparison is also made between the DSMC and the conventional SMC, which shows that the DSMC consumes lesser control energy for similar tracking performance.

Chapter 6

Conclusion and Future Work

In this chapter, a summary of the research work carried out is presented. Moreover, some future research avenues are explored to further enhance the performance of the proposed scheme.

6.1 Conclusion

In recent years the p53 pathway has gained a lot of importance, equally among scientists and biologists, due to its possible role as a drug target for cancer. The current research work demonstrates a system-oriented framework for devising a dosage design strategy for the p53 pathway. In the current research, a novel drug dosage design is accomplished for obtaining the desired level of p53 concentration. To accomplish this task, two control strategies have been devised. The first strategy is based on Lyapunov control and the second strategy is based on the theory of sliding mode control.

In the first strategy, a control-oriented mathematical model is considered with the addition of PBK dynamics for small molecule drug Nutlin. The integrated model is used to achieve a drug dosage strategy for reactivation of wild-type p53. The problem is defined in the control system paradigm where two loop feedback control strategy is employed to produce a sustained response of p53. The outer loop

comprises of the p53-Mdm2 pathway and its nonlinear controller. The nonlinear controller determines the required amount of Nutlin i.e reference dosage. However, to maintain reference dosage in the cell, a negative feedback inner loop is devised for the PBK dynamics of Nutlin. The PID control provides a dosage which is a function of the error between the reference and the Nutlin present in the cell. It is shown by *in-silico* trials that sustained response of p53 can be achieved by proper drug administration. The obtained dosage remains within suitable limits.

In the second control strategy, an SMC based robust nonlinear technique is presented for the re-activation of wild-type p53 protein. The small molecules based drug Nutlin is considered as the control input to revive p53 protein to the desired concentration level. Simulation tests are performed to evaluate the effectiveness of the control scheme, which shows promising results but with the issue of undesirable high-frequency chattering. For smooth control actions and chattering reduction, a modified control technique based on the theory of dynamic sliding mode is presented. The modified control leads to decent trajectory tracking while guaranteeing smooth control actions.

For the estimation of the unmeasured system states, a reduced-order sliding mode observer is employed. The robustness of the proposed scheme is accessed by introducing parametric uncertainties, measurement noise, and an input disturbance. Moreover, quantitative analysis for the conventional SMC and DSMC is performed by considering the root mean square error ($RMSE$) of the output and the average power (P_{avg}) of the control input. The comparison reveals that the conventional SMC gives slightly better tracking performance than DSMC, but that comes at the cost of higher control energy consumption and a discontinuous control input.

Hence, it can be concluded that the required p53 response can be achieved by proper administration of Nutlin dosage. Feedback control being a generic approach can be applied to other similar pathways as well to obtain required therapeutic drug dosage. Moreover, the proposed control method can complement existing chemotherapy treatments and can become a valuable asset in targeted cell therapy.

6.2 Future Work

A number of potential avenues can be explored in the future, based upon the contributions and results of the current study. The following are some of the proposed future directions.

1. The efficacy of the proposed control scheme with the support of biological data is highly desirable. We encourage experimental biologists to apply discussed methods (in the light of discussed implementation schemes) to test the potential of the proposed scheme.

2. According to the established theories, p53 responds in two ways, either performing oscillatory behavior or maintaining its constant concentration. The current study targets the sustained behavior, and successfully demonstrate that by blocking the p53-MDM2 complex we can achieve a sustained response of p53. However, the mere application of the Nutlin through feedback controller is not sufficient to obtain the oscillatory response, as dissociation of the p53-Mdm2 complex is required. Hence, an alternate scheme can be proposed to obtain the oscillatory response.

3. The mathematical model can be improved to account for cell-cell variability and a comprehensive study can be performed to include the effect of cross-talk between related pathways.

4. Living organisms have the ability to develop resistance against any foreign intrusion due to their inherent biological robustness. Through their adaptation property, the robust biological systems have the ability to cope with environmental changes. Moreover, with the passage of time systems develop a relative insensitivity to some kinetic parameters, providing structural stability. The robustness is also enforced by the redundancy in the system, acquired through functioning at different independent levels. Therefore, we can account for this issue as well while designing drugs.

5. In this research, we have focused on mono-therapy to obtain the desired results. It can be extended to combination therapy in future work to achieve higher response rates and to better cope with drug resistance problems. Moreover, combinational strategies can be explored to target both the wild-type and mutant p53 at the same time.

6. The proposed estimator scheme is based upon the equivalent control method, hence the robustness against uncertainties is not guaranteed. Although the accompanied robust SMC is capable to cater for small estimation errors, but larger magnitudes of disturbance may cause degradation in the performance. Hence, a robust estimator strategy can be adopted in the future.

7. In the current research, a hypothetical profile is assumed for the external disturbance. However, a disturbance estimator can be constructed to better cope with the effects of the disturbance.

Bibliography

[1] American Cancer Society, "Cancer facts & figures 2019," pp. 2–6, 2019.

[2] A. J. Levine, "p53, the cellular gatekeeper for growth and division," *cell*, vol. 88, no. 3, pp. 323–331, 1997.

[3] J. G. Teodoro, S. K. Evans, and M. R. Green, "Inhibition of tumor angiogenesis by p53: a new role for the guardian of the genome," *Journal of molecular medicine*, vol. 85, no. 11, pp. 1175–1186, 2007.

[4] C. J. Brown, S. Lain, C. S. Verma, A. R. Fersht, and D. P. Lane, "Awakening guardian angels: drugging the p53 pathway," *Nature Reviews Cancer*, vol. 9, no. 12, pp. 862–873, 2009.

[5] A. J. Levine and M. Oren, "The first 30 years of p53: growing ever more complex," *Nature Reviews Cancer*, vol. 9, no. 10, pp. 749–758, 2009.

[6] S. A. Goffin, "Targeting the p53/mdm2 protein-protein interaction," Ph.D. dissertation, University of East Anglia, 2016.

[7] M. Oren, "Decision making by p53: life, death and cancer," *Cell Death & Differentiation*, vol. 10, no. 4, pp. 431–442, 2003.

[8] J.-C. Bourdon, "p53 family isoforms," *Current pharmaceutical biotechnology*, vol. 8, no. 6, pp. 332–336, 2007.

[9] T. G. Graeber, J. F. Peterson, M. Tsai, K. Monica, A. Fornace, and A. J. Giaccia, "Hypoxia induces accumulation of p53 protein, but activation of a g1-phase checkpoint by low-oxygen conditions is independent of p53 status," *Molecular and cellular biology*, vol. 14, no. 9, pp. 6264–6277, 1994.

[10] A. Villunger, E. M. Michalak, L. Coultas, F. Müllauer, G. Böck, M. J. Ausserlechner, J. M. Adams, and A. Strasser, "p53-and drug-induced apoptotic responses mediated by bh3-only proteins puma and noxa," *Science*, vol. 302, no. 5647, pp. 1036–1038, 2003.

[11] J. Momand, D. Jung, S. Wilczynski, and J. Niland, "The mdm2 gene amplification database," *Nucleic acids research*, vol. 26, no. 15, pp. 3453–3459, 1998.

[12] U. M. Moll and O. Petrenko, "The mdm2-p53 interaction," *Molecular cancer research*, vol. 1, no. 14, pp. 1001–1008, 2003.

[13] T. Sun and J. Cui, "Dynamics of p53 in response to dna damage: Mathematical modeling and perspective," *Progress in Biophysics and Molecular Biology*, vol. 119, pp. 175–182, 2015.

[14] R. Zhao, K. Gish, M. Murphy, Y. Yin, D. Notterman, W. H. Hoffman, E. Tom, D. H. Mack, and A. J. Levine, "Analysis of p53-regulated gene expression patterns using oligonucleotide arrays." *Genes Dev.*, vol. 14, pp. 981–993, 2000.

[15] S. Wang, Y. Zhao, A. Aguilar, D. Bernard, and C.-Y. Yang, "Targeting the mdm2–p53 protein–protein interaction for new cancer therapy: progress and challenges," *Cold Spring Harbor perspectives in medicine*, pp. 262–269, 2017.

[16] G. L. Bond, W. Hu, and A. J. Levine, "Mdm2 is a central node in the p53 pathway: 12 years and counting," *Current cancer drug targets*, vol. 5, no. 1, pp. 3–8, 2005.

[17] S. Fang, J. P. Jensen, R. L. Ludwig, K. H. Vousden, and A. M. Weissman, "Mdm2 is a ring finger-dependent ubiquitin protein ligase for itself and p53," *Journal of Biological Chemistry*, vol. 275, no. 12, pp. 8945–8951, 2000.

[18] A. Burgess, K. M. Chia, S. Haupt, D. Thomas, Y. Haupt, and E. Lim, "Clinical overview of mdm2/x-targeted therapies," *Frontiers in oncology*, vol. 6, pp. 10–17, 2016.

[19] D. Spiegelberg, A. C. Mortensen, S. Lundsten, C. J. Brown, D. P. Lane, and M. Nestor, "The mdm2/mdmx-p53 antagonist pm2 radiosensitizes wild-type p53 tumors," *Cancer research*, vol. 78, no. 17, pp. 5084–5093, 2018.

[20] S. Shangary and S. Wang, "Small-molecule inhibitors of the mdm2-p53 protein-protein interaction to reactivate p53 function: a novel approach for cancer therapy," *Annual review of pharmacology and toxicology*, vol. 49, pp. 223–241, 2009.

[21] S. He, G. Dong, S. Wu, K. Fang, Z. Miao, W. Wang, and C. Sheng, "Small molecules simultaneously inhibiting p53-murine double minute 2 (mdm2) interaction and histone deacetylases (hdacs): Discovery of novel multitargeting antitumor agents," *Journal of medicinal chemistry*, vol. 61, no. 16, pp. 7245–7260, 2018.

[22] P. H. Kussie, S. Gorina, V. Marechal, B. Elenbaas, J. Moreau, A. J. Levine, and N. P. Pavletich, "Structure of the mdm2 oncoprotein bound to the p53 tumor suppressor transactivation domain," *Science*, vol. 274, no. 5289, pp. 948–953, 1996.

[23] L. T. Vassilev, B. T. Vu, B. Graves, D. Carvajal, F. Podlaski, Z. Filipovic, N. Kong, U. Kammlott, C. Lukacs, C. Klein *et al.*, "In vivo activation of the p53 pathway by small-molecule antagonists of mdm2," *Science*, vol. 303, no. 5659, pp. 844–848, 2004.

[24] K. Puszynski, A. Gandolfi, and A. d'Onofrio, "The pharmacodynamics of the p53-mdm2 targeting drug nutlin: The role of gene-switching noise," *PLOS Comput Biol*, vol. 10, no. 12, pp. 391–404, 2014.

[25] D. S. M. Steven M. Paul and Christopher, "How to improve r & d productivity: the pharmaceutical industry's grand challenge," *Nature*, vol. 9, pp. 203–214, 2010.

[26] G. B. Leenders and J. A. Tuszynski, "Stochastic and deterministic models of cellular p53 regulation," *Frontiers in oncology*, vol. 3, pp. 64–69, 2013.

[27] A. Hunziker, M. H. Jensen, and S. Krishna, "Stress-specific response of the p53-mdm2 feedback loop," *BMC systems biology*, vol. 4, no. 1, pp. 94–99, 2010.

[28] H. Kitano, "Systems biology: a brief overview," *Science*, vol. 295, no. 5560, pp. 1662–1664, 2002.

[29] T. Sun and J. Cui, "Dynamics of p53 in response to dna damage: Mathematical modeling and perspective," *Progress in biophysics and molecular biology*, vol. 119, no. 2, pp. 175–182, 2015.

[30] R. L. Bar-Or, R. Maya, L. A. Segel, U. Alon, A. J. Levine, and M. Oren, "Generation of oscillations by the p53-mdm2 feedback loop: a theoretical and experimental study," *Proceedings of the National Academy of Sciences*, vol. 97, no. 21, pp. 11 250–11 255, 2000.

[31] G. Lahav, N. Rosenfeld, A. Sigal, N. Geva-Zatorsky, A. J. Levine, M. B. Elowitz, and U. Alon, "Dynamics of the p53-mdm2 feedback loop in individual cells," *Nature genetics*, vol. 36, no. 2, pp. 147–150, 2004.

[32] J. E. Purvis, K. W. Karhohs, C. Mock, E. Batchelor, A. Loewer, and G. Lahav, "p53 dynamics control cell fate," *Science*, vol. 336, no. 6087, pp. 1440–1444, 2012.

[33] J. J. Tyson, K. C. Chen, and B. Novak, "Sniffers, buzzers, toggles and blinkers: dynamics of regulatory and signaling pathways in the cell," *Current opinion in cell biology*, vol. 15, no. 2, pp. 221–231, 2003.

[34] J. E. Purvis, K. W. Karhohs, C. Mock, E. Batchelor, A. Loewer, and G. Lahav, "p53 dynamics control cell fate," *Science*, vol. 336, no. 6087, pp. 1440–1444, 2012.

[35] E. Batchelor and A. Loewer, "Recent progress and open challenges in modeling p53 dynamics in single cells," *Current opinion in systems biology*, vol. 3, pp. 54–59, 2017.

[36] N. Geva-Zatorsky, N. Rosenfeld, S. Itzkovitz, R. Milo, A. Sigal, E. Dekel, T. Yarnitzky, Y. Liron, P. Polak, G. Lahav *et al.*, "Oscillations and variability in the p53 system," *Molecular systems biology*, vol. 2, no. 1, pp. 1250–1255, 2006.

[37] G. Lahav, N. Rosenfeld, A. Sigal, N. Geva-Zatorsky, A. J. Levine, M. B. Elowitz, and U. Alon, "Dynamics of the p53-mdm2 feedback loop in individual cells," *Nature genetics*, vol. 36, no. 2, pp. 147–150, 2004.

[38] L. Ma, J. Wagner, J. J. Rice, W. Hu, A. J. Levine, and G. A. Stolovitzky, "A plausible model for the digital response of p53 to dna damage," *Proceedings of the National Academy of Sciences of the United States of America*, vol. 102, no. 40, pp. 14 266–14 271, 2005.

[39] A. Ciliberto, B. Novák, and J. J. Tyson, "Steady states and oscillations in the p53/mdm2 network," *Cell cycle*, vol. 4, no. 3, pp. 488–493, 2005.

[40] N. Geva-Zatorsky, N. Rosenfeld, S. Itzkovitz, R. Milo, A. Sigal, E. Dekel, T. Yarnitzky, Y. Liron, P. Polak, G. Lahav *et al.*, "Oscillations and variability in the p53 system," *Molecular systems biology*, vol. 2, no. 1, pp. 1250–1255, 2006.

[41] X. Cai and Z.-M. Yuan, "Stochastic modeling and simulation of the p53-mdm2/mdmx loop," *Journal of Computational Biology*, vol. 16, no. 7, pp. 917–933, 2009.

[42] G. Tiana, M. Jensen, and K. Sneppen, "Time delay as a key to apoptosis induction in the p53 network," *The European Physical Journal B-Condensed Matter and Complex Systems*, vol. 29, no. 1, pp. 135–140, 2002.

[43] K. Puszyński, B. Hat, and T. Lipniacki, "Oscillations and bistability in the stochastic model of p53 regulation," *Journal of Theoretical Biology*, vol. 254, no. 2, pp. 452–465, 2008.

[44] G. A. Giridharan and M. Skliar, "Nonlinear controller for ventricular assist devices," *Artificial organs*, vol. 26, no. 11, pp. 980–984, 2002.

[45] A. Sievert, C. Wiesener, A. Arndt, W. Drewelow, and O. Simanski, "Control of an extracorporeal heart assist device," in *Control Applications (CCA), 2012 IEEE International Conference on*. IEEE, 2012, pp. 63–68.

[46] M. Bakouri, "Evaluation of an advanced model reference sliding mode control method for cardiac assist device using a numerical model," *IET systems biology*, vol. 12, no. 2, pp. 68–72, 2018.

[47] M. Shahin and S. Maka, "Pi controller based closed loop drug delivery for the long term blood pressure regulation," in *2012 Annual IEEE India Conference (INDICON)*. IEEE, 2012, pp. 998–1002.

[48] H. Delavari, H. Heydarinejad, and D. Baleanu, "Adaptive fractional-order blood glucose regulator based on high-order sliding mode observer," *IET Systems Biology*, vol. 13, no. 2, pp. 43–54, 2018.

[49] M. Aliyari, M. Teshnehlab *et al.*, "A new approach in drug delivery control in anesthesia," in *Systems Man and Cybernetics (SMC), 2010 IEEE International Conference on*. IEEE, 2010, pp. 2064–2068.

[50] H.-H. Lin, C. Beck, and M. Bloom, "Multivariable lpv control of anesthesia delivery during surgery," in *American Control Conference, 2008*. IEEE, 2008, pp. 825–831.

[51] R. S. Peña and A. Ghersin, "Lpv control of glucose for diabetes type i," in *2010 Annual International Conference of the IEEE Engineering in Medicine and Biology*. IEEE, 2010, pp. 680–683.

[52] K. Rouhollahi, M. E. Andani, J. A. Marnanii, and S. M. Karbassi, "Rehabilitation of the parkinson's tremor by using robust adaptive sliding mode controller: a simulation study," *IET Systems Biology*, vol. 13, no. 2, pp. 92–99, 2019.

[53] S. S. Ge, Z. Tian, and T. H. Lee, "Nonlinear control of a dynamic model of hiv-1," *IEEE transactions on biomedical engineering*, vol. 52, no. 3, pp. 353–361, 2005.

[54] M. K. Bera, P. Kumar, and R. K. Biswas, "Robust control of hiv infection by antiretroviral therapy: a super-twisting sliding mode control approach," *IET systems biology*, vol. 13, no. 3, pp. 120–128, 2019.

[55] J. J. Westman, "Cancer treatment and control," in *42nd IEEE International Conference on Decision and Control (IEEE Cat. No.03CH37475)*, vol. 3, Dec 2003, pp. 3030–3035 Vol.3.

[56] L. G. De Pillis and A. Radunskaya, "A mathematical tumor model with immune resistance and drug therapy: an optimal control approach," *Computational and Mathematical Methods in Medicine*, vol. 3, no. 2, pp. 79–100, 2001.

[57] L. G. De Pilliss and A. Radunskaya, "The dynamics of an optimally controlled tumor model: A case study," *Mathematical and computer modelling*, vol. 37, no. 11, pp. 1221–1244, 2003.

[58] M. Itik, M. U. Salamci, and S. P. Banks, "Optimal control of drug therapy in cancer treatment," *Nonlinear Analysis: Theory, Methods & Applications*, vol. 71, no. 12, pp. 1473–1486, 2009.

[59] M. Itiik, M. U. Salamci, and S. P. Banks, "Sdre optimal control of drug administration in cancer treatment," *Turkish Journal of Electrical Engineering & Computer Sciences*, vol. 18, no. 5, pp. 715–730, 2010.

[60] Y. Batmani and H. Khaloozadeh, "Optimal chemotherapy in cancer treatment: state dependent riccati equation control and extended kalman filter," *Optimal Control Applications and Methods*, vol. 34, no. 5, pp. 562–577, 2013.

[61] N. Babaei and M. U. Salamci, "Personalized drug administration for cancer treatment using model reference adaptive control," *Journal of theoretical biology*, vol. 371, pp. 24–44, 2015.

[62] M. Haseeb, S. Azam, A. Bhatti, R. Azam, M. Ullah, and S. Fazal, "On p53 revival using system oriented drug dosage design," *Journal of theoretical biology*, vol. 415, pp. 53–57, 2017.

[63] G. G. Rigatos, "Non-linear feedback control of the p53 protein–mdm2 inhibitor system using the derivative-free non-linear kalman filter," *IET systems biology*, vol. 10, no. 3, pp. 94–106, 2016.

[64] F. Menolascina, G. Fiore, E. Orabona, L. De Stefano, M. Ferry, J. Hasty, M. di Bernardo, and D. di Bernardo, "In-vivo real-time control of protein expression from endogenous and synthetic gene networks," *PLoS computational biology*, vol. 10, no. 5, pp. 625–634, 2014.

[65] J. Uhlendorf, A. Miermont, T. Delaveau, G. Charvin, F. Fages, S. Bottani, G. Batt, and P. Hersen, "Long-term model predictive control of gene expression at the population and single-cell levels," *Proceedings of the National Academy of Sciences*, vol. 109, no. 35, pp. 14 271–14 276, 2012.

[66] A. Milias-Argeitis, S. Summers, J. Stewart-Ornstein, I. Zuleta, D. Pincus, H. El-Samad, M. Khammash, and J. Lygeros, "In silico feedback for in vivo regulation of a gene expression circuit," *Nature biotechnology*, vol. 29, no. 12, pp. 1114–1116, 2011.

[67] G. Yan, D. Xing, S. Tan, and Q. Chen, "Rapid and sensitive immunomagnetic-electrochemiluminescent detection of p53 antibodies in human serum," *Journal of immunological methods*, vol. 288, no. 1, pp. 47–54, 2004.

[68] A. L. Slusarczyk, A. Lin, and R. Weiss, "Foundations for the design and implementation of synthetic genetic circuits," *Nature reviews. Genetics*, vol. 13, no. 6, pp. 406–412, 2012.

[69] D. Endy, "Foundations for engineering biology," *Nature*, vol. 438, no. 7067, pp. 449–460, 2005.

[70] T. P. Prescott and A. Papachristodoulou, "Synthetic biology: A control engineering perspective," in *Control Conference (ECC), 2014 European.* IEEE, 2014, pp. 1182–1186.

[71] A. W. Harris, J. A. Dolan, C. L. Kelly, J. Anderson, and A. Papachristodoulou, "Designing genetic feedback controllers," *IEEE transactions on biomedical circuits and systems*, vol. 9, no. 4, pp. 475–484, 2015.

[72] C. J. Myers, *Engineering Genetic Circuits.* Chapman and Hall, 2010, pp. 211-212.

[73] J. A. Brophy and C. A. Voigt, "Principles of genetic circuit design," *Nature methods*, vol. 11, no. 5, pp. 508–520, 2014.

[74] J. A. Stapleton, K. Endo, Y. Fujita, K. Hayashi, M. Takinoue, H. Saito, and T. Inoue, "Feedback control of protein expression in mammalian cells by tunable synthetic translational inhibition," *ACS synthetic biology*, vol. 1, no. 3, pp. 83–88, 2011.

[75] R. J. Bloom, S. M. Winkler, and C. D. Smolke, "Synthetic feedback control using an rnai-based gene-regulatory device," *Journal of biological engineering*, vol. 9, no. 1, pp. 5–12, 2015.

[76] C. Briat, A. Gupta, and M. Khammash, "Antithetic integral feedback ensures robust perfect adaptation in noisy biomolecular networks," *Cell systems*, vol. 2, no. 1, pp. 15–26, 2016.

[77] R. Sawlekar, F. Montefusco, V. V. Kulkarni, and D. G. Bates, "Implementing nonlinear feedback controllers using dna strand displacement reactions," *IEEE transactions on nanobioscience*, vol. 15, no. 5, pp. 443–454, 2016.

[78] J. A. Barboza, T. Iwakuma, T. Terzian, A. K. El-Naggar, and G. Lozano, "Mdm2 and mdm4 loss regulates distinct p53 activities," *Molecular Cancer Research*, vol. 6, no. 6, pp. 947–954, 2008.

[79] A. Hsing, D. V. Faller, and C. Vaziri, "Dna-damaging aryl hydrocarbons induce mdm2 expression via p53-independent post-transcriptional mechanisms," *Journal of Biological Chemistry*, vol. 275, no. 34, pp. 26 024–26 031, 2000.

[80] O. Schon, A. Friedler, M. Bycroft, S. M. Freund, and A. R. Fersht, "Molecular mechanism of the interaction between mdm2 and p53," *Journal of molecular biology*, vol. 323, no. 3, pp. 491–501, 2002.

[81] C. J. Proctor and D. A. Gray, "Explaining oscillations and variability in the p53-mdm2 system," *BMC systems biology*, vol. 2, no. 1, pp. 75–81, 2008.

[82] F. Zhang, M. Tagen, S. Throm, J. Mallari, L. Miller, R. K. Guy, M. A. Dyer, R. T. Williams, M. F. Roussel, K. Nemeth *et al.*, "Whole-body physiologically based pharmacokinetic model for nutlin-3a in mice after intravenous and oral administration," *Drug Metabolism and Disposition*, vol. 39, no. 1, pp. 15–21, 2011.

[83] J.-J. E. Slotine, W. Li *et al.*, *Applied nonlinear control*. Prentice hall Englewood Cliffs, NJ, 1991, vol. 199, no. 1, pp. 220-235.

[84] R. Freeman and P. V. Kokotovic, *Robust nonlinear control design: state-space and Lyapunov techniques*. Springer Science & Business Media, 2008, pp. 325-330.

[85] A. Visioli, *Practical PID control*. Springer Science & Business Media, London, 2006, pp. 3-8.

[86] K. Kojima, M. Konopleva, T. McQueen, S. O'Brien, W. Plunkett, and M. Andreeff, "Mdm2 inhibitor nutlin-3a induces p53-mediated apoptosis by transcription-dependent and transcription-independent mechanisms and may overcome atm-mediated resistance to fludarabine in chronic lymphocytic leukemia," *Blood*, vol. 108, no. 3, pp. 993–1000, 2006.

[87] M. Michaelis, F. Rothweiler, D. Klassert, A. von Deimling, K. Weber, B. Fehse, B. Kammerer, H. W. Doerr, and J. Cinatl, "Reversal of p-glycoprotein–mediated multidrug resistance by the murine double minute 2 antagonist nutlin-3," *Cancer research*, vol. 69, no. 2, pp. 416–421, 2009.

[88] U. Itkis, *Control systems of variable structure*. Halsted Press, Sydney, 1976, pp. 125-130.

[89] J. Guldner, V. Utkin, and J. Shi, *Sliding mode control in electromechanical systems.* Taylor & Francis, 1999, vol. 5, no. 3, pp. 22-25.

[90] V. Utkin, *Sliding modes in control and optimization, ser. Communications and control engineering series.* Berlin: Springer Verlag, 1992, pp. 52-53.

[91] A. Levant, "Sliding order and sliding accuracy in sliding mode control," *International journal of control*, vol. 58, no. 6, pp. 1247–1263, 1993.

[92] W. Perruquetti and J. P. Barbot, *Sliding mode control in engineering.* M. Dekker, 2002, vol. 11, pp. 35-40.

[93] A. Fossard and T. Floquet, "Introduction: an overview of classical sliding mode control," in *Sliding mode control in engineering.* CRC Press, 2002, pp. 22–49.

[94] C. Edwards and S. Spurgeon, *Sliding mode control: theory and applications.* CRC Press, Taylor & Francis group, Florida, 1998, vol. 7, pp. 52-53.

[95] S. V. Drakunov, "Sliding-mode observers based on equivalent control method," in *Decision and Control, 1992., Proceedings of the 31st IEEE Conference on.* IEEE, 1992, pp. 2368–2369.

[96] S. Drakunov and V. Utkin, "Sliding mode observers. tutorial," in *Decision and Control, 1995., Proceedings of the 34th IEEE Conference on*, vol. 4. IEEE, 1995, pp. 3376–3378.

[97] I. Haskara, "On sliding mode observers via equivalent control approach," *International Journal of control*, vol. 71, no. 6, pp. 1051–1067, 1998.

[98] H. Lee and V. I. Utkin, "Chattering suppression methods in sliding mode control systems," *Annual reviews in control*, vol. 31, no. 2, pp. 179–188, 2007.

[99] H. Sira-Ramirez, "On the dynamical sliding mode control of nonlinear systems," *International journal of control*, vol. 57, no. 5, pp. 1039–1061, 1993.

[100] R. N. Gutenkunst, J. J. Waterfall, F. P. Casey, K. S. Brown, C. R. Myers, and J. P. Sethna, "Universally sloppy parameter sensitivities in systems biology models," *PLoS computational biology*, vol. 3, no. 10, pp. 189–201, 2007.

[101] F. J. Doyle III, "Robust control in biology: From genes to cells to systems," *IFAC Proceedings Volumes*, vol. 41, no. 2, pp. 3470–3479, 2008.

[102] S. A. Qureshi, "In vitro-in vivo correlation (ivivc) and determining drug concentrations in blood from dissolution testing–a simple and practical approach," *The Open Drug Delivery Journal*, vol. 4, no. 1, pp. 171–180, 2010.

[103] Z. Zi, "Mathematical modeling and kinetic analysis of cellular signaling pathways," Master's thesis, Humboldt-Universitt zu Berlin, Germany, 2008.

[104] H. El-Samad and M. Khammash, "Modelling and analysis of gene regulatory network using feedback control theory," *International Journal of Systems Science*, vol. 41, no. 1, pp. 17–33, 2010.

Appendix A

Mathematical Modeling of Biological Systems

A cell is a basic building block of tissues, organs, and an entire organism. Living organisms have evolved to protect their inner environment by constraining certain variables within the limit. This phenomenon is known as homeostasis, which can be achieved by coordinated physiological processes known as regulatory networks, employing complex nonlinear interactions of genes and proteins. The subsequent section investigates the mathematical modeling in the context of cell signaling in biological systems.

A.1 Modeling Preliminaries

A pathway or regulating networks can be described as the combination of biochemical reactions. If we denote chemical species by capital letter e.g. X_i, the pathway can be described by following mathematical scheme

$$K_1 X_1 + K_2 X_2 + \cdots + K_n X_n \xrightarrow{k_1} \ldots, \tag{A.1}$$

where $K_i \in \mathbb{R}^+$ is the stoichiometric coefficient associated with a reactant species X_i, and $k_i \in \mathbb{R}^+$ is the rate constant which determines the speed of a reaction. The

+ sign represents a combination of different species and the right arrow represents a transformation.

The modeling technique for the signaling pathway depends on properties of the system under consideration and requirement for any specific questions to be answered by the model. Although there are various modeling methods, broadly characterized as deterministic and stochastic, we will focus on the most widespread deterministic method: ordinary differential equations (ODEs). The ODEs describe the time evolution of molecular species in their concentration levels. Consider a system having n states, it can be represented by ODEs as;

$$\frac{dx_i}{dt} = f_i(x_1, x_2, \ldots\ldots, x_n), \tag{A.2}$$

where, f_i is a nonlinear function consisting of rate equations, based upon the reaction kinetics. The variable x_i represents the concentration of i^{th} protein or protein complex. In a molecular regulatory network, for a time varying chemical species x having concentration [x], the ODE is constituted by subtracting the sum of the reaction rates consuming x, from the sum of the reaction rates producing x, i.e.

$$\frac{d[x]}{dt} = \sum f_{production} - \sum f_{consumption}. \tag{A.3}$$

Usually, the species in any regulatory network maintains themselves at steady state to achieve homeostasis. At the steady state, $\frac{d[x]}{dt} = 0$, hence the total rate of formation and removal are balanced i.e. $\sum f_{production} = \sum f_{consumption}$. There are various modeling mechanisms for the reaction kinetics, including Law of Mass Action, Michaelis Menten kinetics and Hill equation. In this research, we will focus our attention to the Law of Mass Action based ODE formulation. According to the Law of Mass Action, "the rate of a reaction is proportional to the product of the concentrations of the reacting substances". It takes into account the fact that the speed of any reaction is proportional to the probability of collision of the reactants.

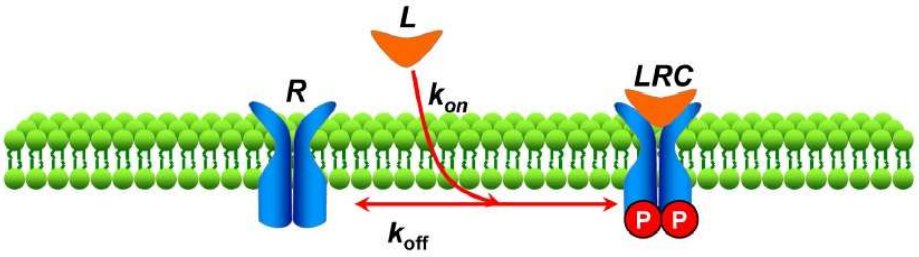

FIGURE A.1: A Ligand-Receptor interaction [103]

The ligand-receptor interaction shown in Figure A.1 is a basic phenomenon in the signaling networks. As every drug is initially a ligand that effectively binds with its target site. Therefore, ligand-receptor interaction can be taken as an example to demonstrate the interaction of the drug Nutlin to the protein MDM2. Furthermore, It can illustrate the ODE modeling by the Law of Mass Action. When the extracellular ligand (L) binds to the receptor (R) on the cell membrane, a ligand-receptor complex (LRC) is formed, with a kinetic rate constant k_{on}. Similarly, the dissociation of the complex can also take place with the rate constant k_{off}.

The ligand-receptor process is schematically represented as

$$\mathrm{L} + \mathrm{R} \underset{k_{off}}{\overset{k_{on}}{\rightleftharpoons}} \mathrm{LRC}, \tag{A.4}$$

where, the double sided arrows represent a reversible reaction. Traditionally, a [ ] symbol denotes the concentration of the components, however, for simplicity we will denote the concentrations with the lowercase letters i.e., $l = [L]$, $r = [R]$, and $lrc = [LRC]$. Subsequently, the concentration change over time is represented by the differential equations for the ligand, receptor and the complex:

$$\begin{aligned} \frac{d\,l}{dt} &= k_{off}\,lrc - k_{on}\,l\,r, \\ \frac{d\,r}{dt} &= k_{off}\,lrc - k_{on}\,l\,r, \\ \frac{d\,lrc}{dt} &= k_{on}\,l\,r - k_{off}\,lrc. \end{aligned} \tag{A.5}$$

Where, $k's$ are constants of proportionality in the application of the Law of Mass

Action. Here, k_{on} and k_{off} are forward and backward rate constants respectively. For example the first equation for l, describes that the concentration l is constituted by the production rate proportional to lrc and the removal rate proportional to $l\,r$. Here, the '+' sign represents the production and the negative sign represents a removal of the substance. The model presented in (A.5), is a starting point in the analysis of the biological systems *in silico*. In the subsequent section, we explore a complicated mechanism of the signaling pathways: feedback loops. These loops play a significant role in defining the possible behavior of the pathways.

A.2 Feedback Loops in Regulatory Networks

Feedback loops play a significant role in attaining the stability of biological organisms. They occur when a protein is involved in auto-regulation, i.e when it represses or down-regulates its own activity, either directly or indirectly. The dynamic behavior of a regulatory network is determined by, whether it is constituted of positive or negative feedback loops. The diversity in dynamic behaviors includes homeostasis, multi-stability, and stable oscillations. Subsequent paragraphs explain the role of feedback loops in generating these versatile dynamical behaviors [104].

1. "Homeostasis" or mono-stability is described as restoring equilibrium condition in presence of environmental disturbances. The auto-regulation is involved in achieving the homeostasis in biological mechanisms. It has been demonstrated that the negative feedback loop helps to attain stability by limiting the concentration range of certain network components.

2. "Mono-stability" is achieved when a system toggles between two discrete and distinct steady states. It has been shown that the positive feedback loops result in a multi-stable system. The positive feedback loops can be either in direct form: transcription factor is involved in activation of its own transcription or indirect form: two transcription factors mutually repress each other.

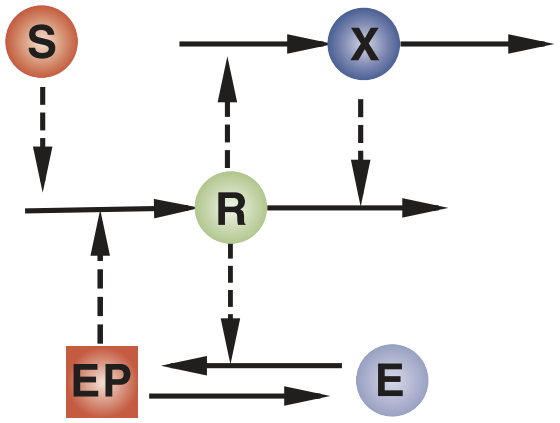

FIGURE A.2: Gene regulatory network containing both the positive and negative feedback loops.

3. "Oscillations" are the periodic patterns expressed by the concentration of a protein. Usually, oscillations are the outcome of the interaction of both the positive and negative feedback loops, although in some cases negative feedback loop alone is seen to be sufficient to cause oscillatory behaviors. The positive feedback causes bi-stability and the negative feedback shifts between these stable system states alternatively, leading to oscillations in system response.

Figure A.2 presents a gene network containing both the positive and negative feedback loops. The protein R enhances the production of X, but in turn, X inhibits and degrades the R, hence forming a negative feedback loop. On the other hand, R promotes the conversion of E to EP, which activates R, hence forming a positive feedback loop. Whenever the protein R rises its level, X inhibits it, at the same time E promotes it, hence the phenomenon of oscillation takes place. Tyson et al. in [33], performed simulations through a mathematical model and demonstrated that this combination of positive and negative feedback loop generates an oscillatory response.